



HAL
open science

Chlorides, other Halides, and Pseudo-Halides as Additives for the Fabrication of Efficient and Stable Perovskite Solar Cells

Fei Cheng, Jie Zhang, Thierry Pauporté

► **To cite this version:**

Fei Cheng, Jie Zhang, Thierry Pauporté. Chlorides, other Halides, and Pseudo-Halides as Additives for the Fabrication of Efficient and Stable Perovskite Solar Cells. *ChemSusChem*, 2021, 14 (18), pp.3665-3692. 10.1002/cssc.202101089 . hal-03367802

HAL Id: hal-03367802

<https://hal.science/hal-03367802v1>

Submitted on 6 Oct 2021

HAL is a multi-disciplinary open access archive for the deposit and dissemination of scientific research documents, whether they are published or not. The documents may come from teaching and research institutions in France or abroad, or from public or private research centers.

L'archive ouverte pluridisciplinaire **HAL**, est destinée au dépôt et à la diffusion de documents scientifiques de niveau recherche, publiés ou non, émanant des établissements d'enseignement et de recherche français ou étrangers, des laboratoires publics ou privés.

Cite this paper as: F. Cheng, J. Zhu, Th. Pauporté, Chlorides, other Halides and Pseudohalides as Additives for the Fabrication of Efficient and Stable Perovskite Solar Cells. ChemSusChem 14 (2021) 3665–3692. DOI: 10.1002/cssc.202101089

Chlorides, other Halides and Pseudo-halides as Additives for the Fabrication of Efficient and Stable Perovskite Solar Cells

Fei Cheng,^[a] Jie Zhang*^[b] and Thierry Pauporté*^[a]

[b] Dr J. Zhang

The Key Lab of Fuel Cell Technology of Guangdong Province, Guangdong, School of Chemistry and Chemical Engineering, South China University of Technology, Guangzhou, 510640, China.

E-mail : cejzhang@scut.edu.cn;

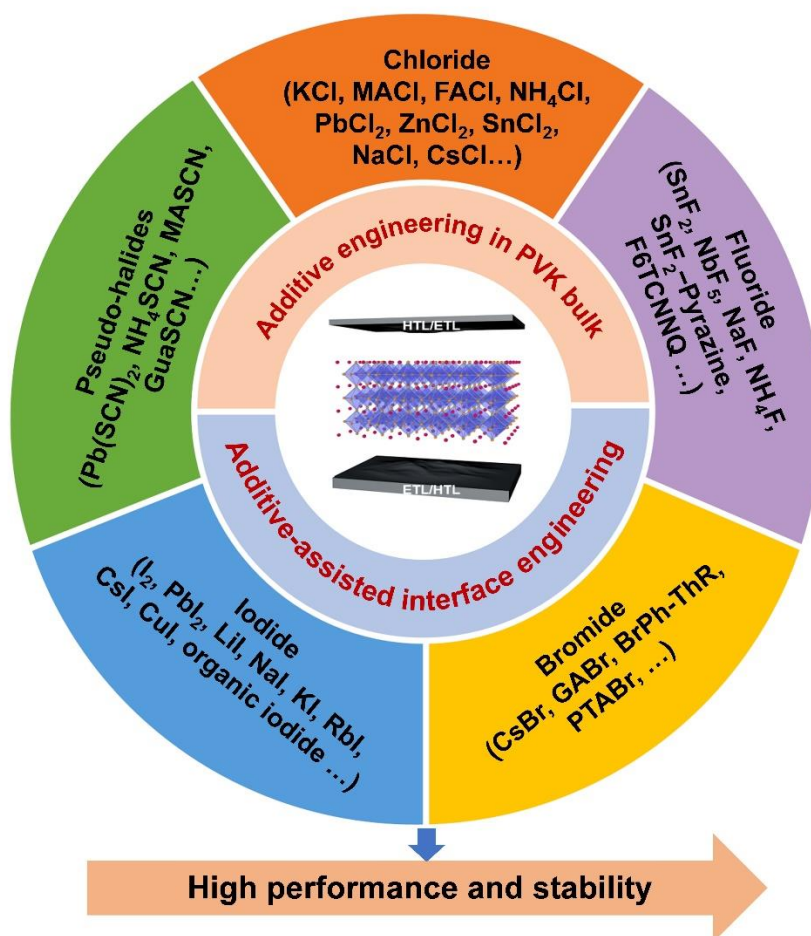
[a] F. Cheng and Prof. T. Pauporté

Chimie ParisTech, PSL Research University, CNRS, Institut de Recherche de Chimie Paris (IRCP), UMR8247, 11 rue P. et M. Curie, F-75005 Paris, France.

E-mail : thierry.pauporte@chimieparistech.psl.eu;

www.pauportegroup.com

**Authors for the correspondence*



Abstract

Perovskite solar cells (PSCs) are attracting a tremendous attention from the scientific community due to their excellent power conversion efficiency, low cost and great promise for the future of solar energy. The best PSCs have already achieved a certified power conversion efficiency (PCE) of 25.5% after an unprecedented rapid performance rise. However, high requirement with respect to large area, high efficiency devices and stability are still the challenges. Major efforts, especially for achieving a high degree of chemical control, have been made to reach these targets. The use of halide additive has been playing a critical role in improving the efficiency and stability. The present paper reviews the important breakthroughs in PSC technologies made by using halide additives, especially chloride, and pseudo-halide additives for the preparation of the perovskite layers, other layers and interfaces of the devices. These additives help perovskite (PVK) crystallization and layer morphology control, grain boundary reduction, bulk and interface defects passivation and so on. Normally, these halide

Cite this paper as: F. Cheng, J. Zhu, Th. Pauporté, Chlorides, other Halides and Pseudohalides as Additives for the Fabrication of Efficient and Stable Perovskite Solar Cells. ChemSusChem 14 (2021) 3665–3692. DOI: 10.1002/cssc.202101089

additives play different roles depending on their categories and their location. Herein, we review recent progresses made due to additives employment in every possible layer of PSCs. We develop chloride, other halides and pseudohalides as additives in PVK films, halide additives in carrier transport layers and at PVK-contact interfaces. Finally, an outlook of halide additive engineering in PSC progress is given.

Keywords: Perovskite solar cell; Halide additives; Chloride additives; Pseudo-Halide additives; High efficiency; High stability.

Abstract.....	2
1. Introduction	5
2. Chloride additives for PVK films	7
2.1 Inorganic chloride additives.....	8
2.2 Organic chlorides additives	10
2.3 Mechanism of chloride additives action on the growth of PVK films.....	16
2.4 Measurement of the residual chloride in the layers	18
2.5 Other applications of chloride additives	19
2.5.1 Fabricate lead-less PSC	19
2.5.2 Fabrication of 2D/3D dimensional PVKs.	21
3. Other halides and pseudo-halides additives for PVK films	25
3.1 Halogen acids additives for PVK films	25
3.2 Fluoride additives for PVK films.....	27
3.3 Bromide additives for PVK films	29
3.4 Iodide additives for PVK films	31
3.4.1 Iodide ions additive.....	31
3.4.2 Excess amount of PbI_2 and other inorganic iodide additives	32
3.5 Pseudo-halides additives for PVK films	34
4. Halides at the interfaces of PSCs.....	40
4.1 Introduction of halogen atoms at the ETL/PVK interface	40
4.2 Halides at the ETL/PVK interface	40
4.3 PVK layer surface engineering	44
4.3.1 Hydrophobic organo-halogen at the surface of PVK.....	44
4.3.2 Passivation of PVK defects and near surface film modification.....	46
4.4 HTL surface engineering	48
References:	50

1. Introduction

The use of halide perovskites (PVKs) in all solid-state solar cells appeared less than a decade ago and has revolutionized the field of photovoltaics (PV).^[1-6] PVKs are highly flexible semiconductors with many advantages for this application such as high light absorption coefficient,^[7] high charge carrier mobility,^[8] long charge carrier diffusion length^[9] and a bandgap tunable over a large energy range.^[10] PVK thin films can be prepared from precursor solutions at mild temperature ($\leq 160^\circ\text{C}$) on either insulating or conducting substrates.^[11-14]

Perovskite solar cells (PSCs) can be considered as a competitor of silicon solar cells as well as a complementary technology in the case of multijunction solar cells.^[15, 16] A typical hybrid metal halide PVK has a three-dimensional structure (3D) with a chemical formula of ABX_3 , where A is an organic or inorganic cation, such as FA^+ (formamidinium), MA^+ (methylammonium) or Cs^+ (cesium), B is a metal cation, such as Pb^{2+} or Sn^{2+} , and X is an halogen anion, such as I^- or Br^- .^[17, 18] In PSCs, the PVK thin film is only several hundred nanometers thick and is contacted on both sides by semiconductor selective contact layers. An electron transporting layer (ETL) ensures the photogenerated electron collection and transport.^[19, 20] While, on the other side, holes are collected and transported by a hole transporting layer (HTL).^[21, 22] Depending on the position and structure of these layers, three different typical PSC architectures are distinguished : direct mesoporous, direct planar and inverted planar as schematically presented in Fig. 1A.^[23] According to NREL, the certified power conversion efficiency (PCE) for a PVK cell achieves a present 25.5 % value,^[24] which is superior to any other thin film technology and approaches the record for Si single crystal technologies. However, according to the recalculated Shockley-Queisser limit,^[25, 26] for AM 1.5G (1000.4 W m^{-2}) and a temperature of 298.15 K, a highest theoretical PCE of 32.91% (short-circuit photocurrent density (J_{sc}) = 32.88 mA cm^{-2} , open circuit voltage V_{oc} = 1.122 V, and fill factor (FF) = 89.3%) can be expected for a single junction PSC with a bandgap (E_g) of 1.4 eV. It indicates that PSC technology still presents space for performance improvement. Finding a light absorbing PVK material with the optimal E_g , improving the lifetime and diffusion length of carriers, as well as reducing the recombination due to traps states at the interfaces, grain boundaries and in the bulk are of utmost importance to maximize the performance of PSCs. Comparing the parameter of certified efficiency in 2019 by KRICT/MIT and in 2018 by ISCAS, the improvement of PCE from 23.3% to 25.2% is owed to the improvement of the fill factor,^[27] which is mainly limited by the carriers transport times.^[28] Huang et al.^[29] reported that

Cite this paper as: F. Cheng, J. Zhu, Th. Pauporté, Chlorides, other Halides and Pseudohalides as Additives for the Fabrication of Efficient and Stable Perovskite Solar Cells. ChemSusChem 14 (2021) 3665–3692. DOI: 10.1002/cssc.202101089

FAPbI₃-based PSCs could achieve an efficiency of 28.4 % with the trap density of thin film being reduced to its single crystal value. Besides, long-term stability is also a challenge for the commercialization and broad diffusion of PSCs.^[30,31] Thus, much efforts have focused on fabricating highly oriented crystal films, increasing grain size, reducing traps, increasing heat, humidity, illumination stability and so on.^[32-36] Among all the improvement methods, the employment of halide and pseudohalide additives for the preparation of various layers and treatments of interfaces is of major interest. The analysis of the web of science database reveals that the percentage of papers in which halide and pseudohalide additives are used in PSC is increasing (Fig. 1B). We can cite as recent examples You and co-workers^[37] who got a certified PCE of 23.32% via a post-treatment by phenylethylammonium iodide (PEAI) and Kim and co-workers^[38] who achieved a certified PCE of 23.48% using MAI as an additive and treating the PVK layer surface by PEA. More impressively, Seok et al.^[39] got a PCE of 25.17 % and improved the device heat stability by relaxing the lattice strain of FAPbI₃ via cooperating methylenediamine dihydrochloride (MDACl₂) and cesium iodide (CsI) into the PVK precursor.

These additives consist in salts composed of a large organic or inorganic cation combined to a halide anion: F⁻, Cl⁻, Br⁻, I⁻ or a pseudo halide such as SCN⁻ (Fig. 1C). These additives can be added into the PVK precursor solution, in the carrier transport material precursor solution or employed at the PVK-selective contact (ETL or HTL) interface. Finally, it is important to note that most of these additives will be fully or partly removed upon the post-annealing treatment of the layers. They will help the crystal to grow, the defect passivation, the stabilization of the structure, the improvement of interfaces and so on. Park et al.^[40] comprehensively worked on the effect of different halide additives on FAPbI₃ films growth by introducing AX (A=FA, MA, Cs, Rb, NH₄, X=Cl, Br, I) into PVK precursor, giving a sight of synergy effect of different halide species with FAPbI₃. Liu et al.^[41] compared the additives of PbCl₂, PbBr₂ and MAI in MAPbI₃. Researchers commonly focus on one or two kinds of halide additive in the specific PVK without a large view on the topic.^[42-45] It thus appears important to review on how these varied halide additives cooperate with different PVK materials and different PVK solar cell layers in various PSC structures. In this perspective, we summarize the recent progresses on species of halide additives in halide PVK solar cells and their function such as the morphology adjusting, phase stabilizing, energy-level adjusting, trap state passivation and hysteresis elimination. A deep understanding of the relationship between halide/pseudohalide additive and the improved properties of PVK solar cell is presented. We have attached a special attention to the chloride and pseudohalide ones. First, in Section 2, we develop the employment of chloride additives for the preparation of PVK layers. Section 3 is dedicated to other halide and

Cite this paper as: F. Cheng, J. Zhu, Th. Pauporté, Chlorides, other Halides and Pseudohalides as Additives for the Fabrication of Efficient and Stable Perovskite Solar Cells. ChemSusChem 14 (2021) 3665–3692. DOI: 10.1002/cssc.202101089

pseudohalide additives employed for PVK films synthesis. Section 4 reports on the use of halide additives in the carrier transport layers and interfaces of PSC. Finally, we provide a conclusion and an outlook of halide additive engineering in PSC progress.

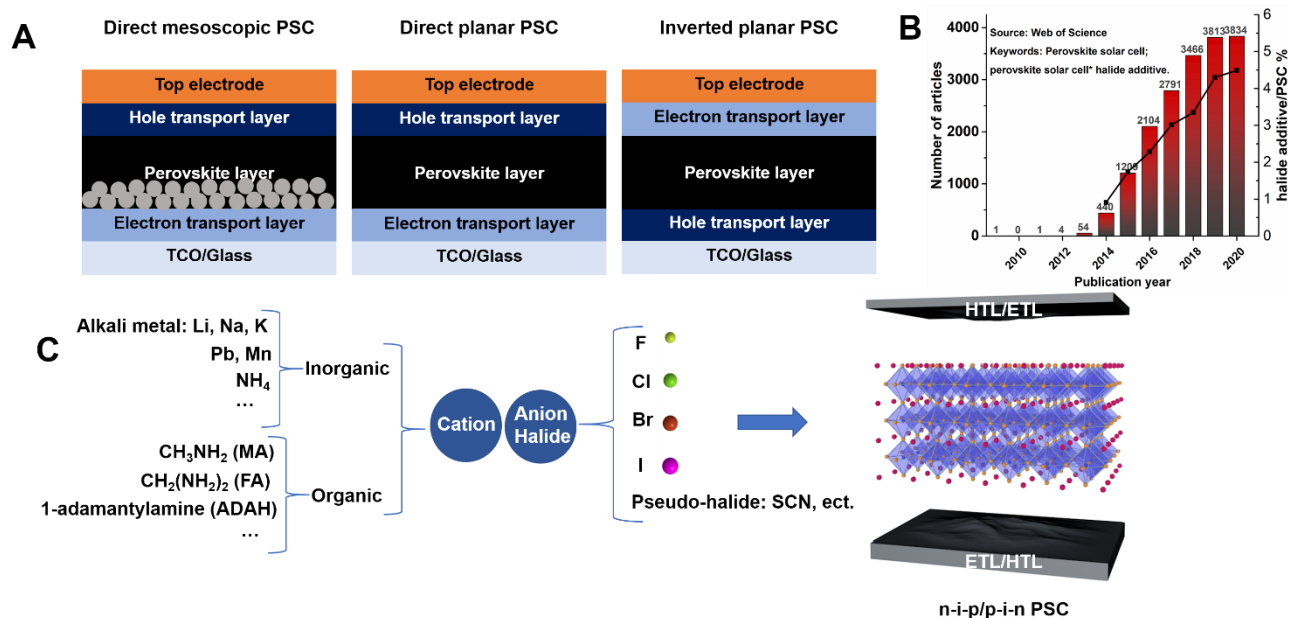


Fig. 1 (A) Schematic of the different PSC structures: direct mesoscopic, direct planar and inverted planar. (B) Halide additive research activities seen from the number of papers on PVK solar cell published each year. (C) Structure of this review, the additive species introduced into PSC.

2. Chloride additives for PVK films

A first breakthrough in PVK solar cell research field was achieved in 2012 with the first fabrication of all-solid-state devices.^[46] At the early age of PSC science, the possibility of playing on non-stoichiometry and of using added halide compound in the precursor solution attracted the curiosity of scientists. Snaith et al.^[47] combined an excess of methylammonium iodide (MAI) with a non-iodide lead source PbCl₂ in a 3:1 MAI:PbCl₂ molar ratio, to deposit high-quality films into mesoporous alumina. The PCE of 12.3 % was attributed to the efficient transport of carriers with minimal recombination losses in MAPbI₃(Cl). Zhang et al.^[48] latterly verified whether Cl or excess MA⁺ was responsible for the enhanced diffusion length by fabricating a typical 1:1 PbI₂:MAI and comparing it with the non-stoichiometric PbCl₂:3MAI system. The higher optoelectronic property in the presence of PbCl₂ was explained by the easy removal of the MAI by-product upon the final annealing step at 100°C. They concluded that Cl is the key for high performance. Then after, a lot of research efforts

Cite this paper as: F. Cheng, J. Zhu, Th. Pauporté, Chlorides, other Halides and Pseudohalides as Additives for the Fabrication of Efficient and Stable Perovskite Solar Cells. ChemSusChem 14 (2021) 3665–3692. DOI: 10.1002/cssc.202101089

focused on the employment of a large variety of either organic or inorganic chloride salts as additives to fabricate better performance PSCs. Most recently, Xu et al.^[49] fabricated a two-terminal monolithic tandem cell with a triple-halide alloys PVK as top cell and achieved a PCE of 27% with an area of 1 square centimeter. Cl from MAPbCl₃ additive was detected throughout the film and was incorporated into the PVK lattice. Chloride, among all the halogens, is the most promising element for PSC performance improvement.

2.1 Inorganic chloride additives

In inorganic chloride additives, the cation includes alkali metal (K⁺, Na⁺, Li⁺),^[50] Pb²⁺, Mn²⁺^[44] and ammonia species NH₄⁺.^[50] Normally, inorganic chloride additives present in the PVK precursor solution increase the grain size as well as enhance the grain orientation and finally often increase the PCE of the device.

Following the pioneering research by Snaith et al. in 2012^[51] and 2013^[47], the effects of metal chloride additives, especially PbCl₂, were investigated in many further studies. Wang et al.^[52] reported an improved PSC performance by incorporating PbCl₂ into the PVK precursor, forming a Lewis acid-base adduct. They showed that 2.5 mol% of PbCl₂ increases the grain size, charge carrier lifetime and electron-hole collection efficiency in MAPbI₃ PSCs. As a result, they achieved an average efficiency of 18.1 %. Cao et al.^[53] studied the effect of PbCl₂ in a two-step method formation of MAPbI₃(Cl), different concentrations of PbCl₂ (0%, 5 mol%, 10mol%) were introduced into PbI₂/DMF solution. The mean grain size of MAPbI₃ increased from 223 nm to 353 nm when 5 mol% PbCl₂ was introduced. The diffraction peak intensity ratios of I₍₁₁₀₎/I₍₃₁₀₎ and I₍₂₂₀₎/I₍₃₁₀₎ were introduced to quantify the effects of chloride incorporation on grain orientation. The values of I₍₁₁₀₎/I₍₃₁₀₎ and I₍₂₂₀₎/I₍₃₁₀₎ increased to 15.13 and 6.49, respectively, when 5 mol% PbCl₂ was introduced, compared to 3.15 and 1.70 for the pristine film. It indicated a better preferred (110) grain orientation. The fast photoluminescence (PL) decay time and slow PL decay time of the 5 mol% PbCl₂ modified device were 0.43 ns and 40.81 ns, respectively (compared to the 3.47 ns and 39.08 ns without PbCl₂). Finally, the device reached a maximum PCE of 17.05%.

The influence of alkali metal halides (KCl, NaCl, LiCl) as additives on the performance of PVK solar cells has been studied in a large extent. 0.75 wt.% KCl, 1 wt.% NaCl and 0.25 wt.% LiCl were introduced into PbI₂/salt mixture.^[54] The detailed parameters of the measured photovoltaic performances are gathered in Table 1. The best dosage for each alkali metal halide was given, among them, KCl at 0.75 wt.% got the best PCE. By x-ray diffraction (XRD) measurement, the average crystallite size was estimated using the Scherrer relationship:

$$D = 0.89\lambda/\beta \cos\theta \quad (1)$$

Cite this paper as: F. Cheng, J. Zhu, Th. Pauporté, Chlorides, other Halides and Pseudohalides as Additives for the Fabrication of Efficient and Stable Perovskite Solar Cells. ChemSusChem 14 (2021) 3665–3692. DOI: 10.1002/cssc.202101089

D is the crystallite size, λ is the wavelength of the X-rays, β is the full width at half maximum (FWHM) of the diffraction peak, and θ is the diffraction angle. The crystallite sizes of the PVKs prepared with 0.75 wt.% KCl, 1 wt.% NaCl, and 0.25 wt.% LiCl were 468 ± 50 nm, 384 ± 40 nm, and 422 ± 40 nm, respectively. The intensity of crystallinity and crystallite size (Fig. 2A, 2B) of the PVK film gave a glimpse of the reason why 0.75 wt.% of KCl got the best efficiency. Zheng et al. have clearly shown that K^+ from KCl suppresses iodide mobility in PVK and linked it to J - V curve hysteresis cancellation.^[50]

Table 1. Photovoltaic performance parameters of devices prepared with various salt additives. (from Ref^[54] with permission from The Royal Society of Chemistry, copyright 2013)

Salt	V_{oc} (V)	J_{sc} (mA cm^{-2})	FF (%)	PCE (%)
0.75% KC	1.04	19.42	74.67	15.08 ^a (14.12) ^b
1% NaCl	0.96	17.59	75.62	12.77 ^a (12.14) ^b
0.25% LiCl	0.91	15.97	68.67	9.98 ^a (9.35) ^b
Without salt	0.9	15.88	76.31	11.4 ^a (10.86) ^b

^a Best device performance. ^b Average performance from 10 devices.

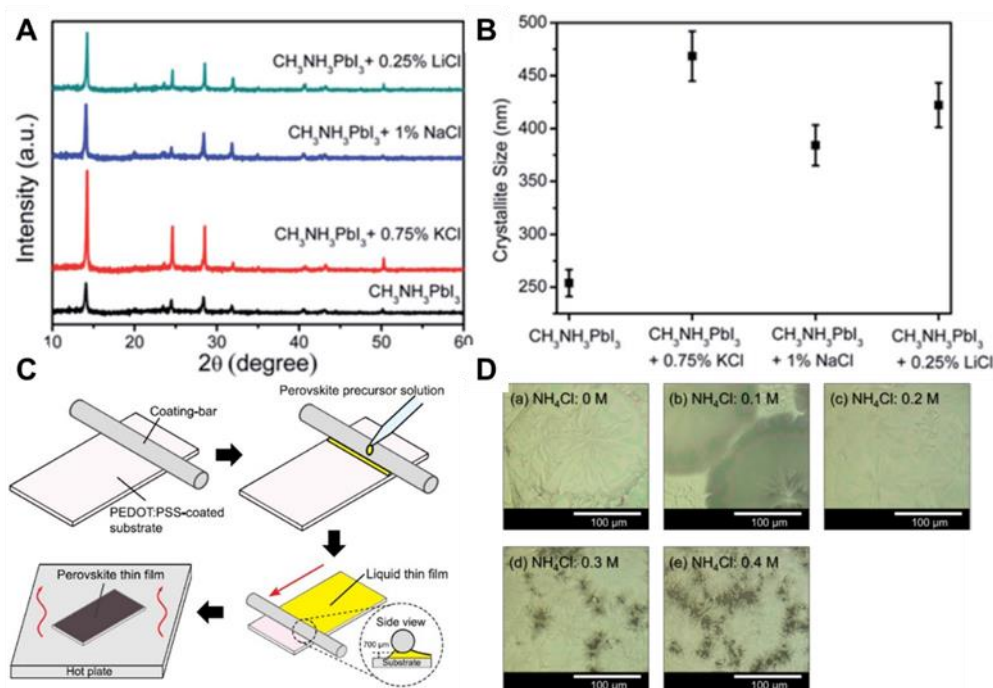


Fig. 2 (A) XRD patterns and (B) crystallite sizes in PVK thin films prepared without and with KCl, NaCl, and LiCl salt additives.^[54] with permission from The Royal Society of Chemistry, copyright 2013; (C) Schematic

Cite this paper as: F. Cheng, J. Zhu, Th. Pauporté, Chlorides, other Halides and Pseudohalides as Additives for the Fabrication of Efficient and Stable Perovskite Solar Cells.

ChemSusChem 14 (2021) 3665–3692. DOI: 10.1002/cssc.202101089

diagram of the fabrication process of PVK thin film by bar-coating; (D) Microscope images of MAPbI₃ thin films fabricated by bar-coating with various concentrations of NH₄Cl.^[55] with permission from Elsevier, copyright 2013.

Fujii et al.^[55] introduced NH₄Cl additive into the MAPbI₃ precursor solution. By a bar-coating process (Fig. 2C) they obtained a highly (100)-oriented and uniform thin film of MAPbI₃ with large grains, giving a reference for industrial mass-production. As shown in Fig. 2D the homogeneous and large grains were obtained for 0.2 M NH₄Cl additive. The solar cell utilizing the MAPbI₃ thin film prepared with 0.2 M NH₄Cl demonstrated a hysteresis-free behavior and achieved a PCE of 12.5% with J_{sc} of 20.6 mA cm⁻², V_{oc} of 0.83 V, and FF of 0.73 in the forward scan. Zong et al.^[56] added NH₄Cl with a molar ratio value of 0.8 to PbI₂ into the PVK precursor solution to adjust the kinetics of crystallization and growth of the active layer and it resulted in high-quality MAPbI₃ film formation. The diffraction peak intensity of the (110) face was enhanced and the FWHM reached a minimum value with an additive ratio of 0.8. It proved an increase of the crystallinity by NH₄Cl. Combined with a hydrophobic carbon electrode, the final device got a PCE of 9.89% with a V_{oc} of 878.9 mV, J_{sc} of 22.38 mA cm⁻², FF of 0.503. Under the condition of ambient air, the PSCs maintained 96% of the initial efficiency after 576 h due to the triple mesoporous scaffold^[36] and PVK material quality. Pauporté et al.^[50] demonstrated the benefit of employing NH₄Cl additive combined with KCl for the preparation of methylammonium-free bromide-free Cs_{0.1}FA_{0.9}PbI₃ perovskite layers. They showed that KCl favors the PbI₂ precursor solubilization and it resulted in pure perovskite phase. The crystal growth speed and direction were controlled by NH₄Cl which led to the formation of large crystal grains and well-crystallized layers. These authors used the glow-discharge optical emission spectroscopy (GD-OES) technique to directly visualize that potassium incorporated in the whole film blocks the iodide mobility by defect passivation. They clearly correlated the reduction (or suppression) of iodide mobility and the reduction (or suppression) of the $J-V$ curve hysteresis. Combined with the PVK surface treatment with n-propylammonium iodide (PAI), the cells reached at stabilized PCE of 21.1 %.

2.2 Organic chlorides additives

Organic chloride additives include a bigger-size cation, such as MA⁺, FA⁺ or 1-adamantylamine (ADAH), compared to inorganic ones. Due to the bulky size of the organic cation, the interionic space is large, thus, the

attractive electrostatic force is weaker. Because chloride ion is volatile, it results in an easy removal of the organic chloride additive during the PVK annealing post-treatment.

Choy et al.^[58] proposed that Cl⁻ additive can significantly increase the hole and electron diffusion lengths, in agreement with the previously mentioned research by Snaith^[47] in 2013. It also reduces the bulk trap-state density in PVK thin film. To investigate the role of chloride in different PSC devices architectures and thus provide a deeper understanding of its action mechanism, Burda et al.^[59] prepared varied ratios of MACl : MAI (0:1, 0.5:1, 1:1, and 2:1) PVK film on planar and mesoporous TiO₂/FTO substrates. They found by time-resolved photoluminescence (TRPL) spectroscopy (Table 2) that the interfacial electron injection rate from PVK to planar TiO₂ is accelerated with increasing Cl⁻ content. It explained the increased PCE in direct planar device using Cl⁻ as modifier. In contrast, Cl⁻ demonstrated no influence on electron injection into mesoporous TiO₂, suggesting that a reduction of interfacial charge recombination gives rise to the improved performance.

Table 2. Grain size, PL wavelength (λ_{PL}), PL FWHM, PL decay lifetimes (τ_{PL}), PL rate constants (k_{PL}), injection rate constants (k_{inj}), injection efficiencies (Φ_{inj}), and PCEs (η_f) of PVK films on planar or mesoporous TiO₂ coated FTO substrates.^[59] With permission from The Royal Society of Chemistry, copyright 2018.

Architecture	Sample	Grain size (nm)	λ_{PL} (nm)	FWHM (nm)	τ_{PL} (± 0.19 ns)	k_{PL} (s ⁻¹)	k_{inj} (s ⁻¹)	ϕ_{inj} (%)	η_f^a (%)
	x MACl for 1 MAI								
Planar	0 MACl	28	775	52	2.68	3.7×10^8	2.1×10^8	52	1.34
	0.5 MACl	39	778	49	2.27	4.4×10^8	2.7×10^8	59	9.5
	1 MACl	42	786	41	1.77	5.6×10^8	4.0×10^8	68	10.51
	2 MACl	46	784	47	0.98	1.0×10^9	8.5×10^8	83	10.85
Mesoporous	0 MACl	36	765	41	1.4	7.1×10^8	5.5×10^8	75	7.64
	0.5 MACl	22	754	54	1.05	9.5×10^8	7.9×10^8	81	9.12
	1 MACl	27	757	54	1.07	9.3×10^8	7.7×10^8	81	9.57
	2MACl	36	766	57	1.18	8.5×10^8	6.8×10^8	79	10.09

^a From ref.^[60-63]

2D PVKs are a class of two-dimensional quantum wells (QWs) compounds which include Dion-Jacobson (DJ) and Russlesden-Popper (RP) phases.^[60-63] By incorporating 10 mg mL⁻¹ MACl into (GA)(MA)_nPb_nI_{3n+1} (GA=guanidinium; n=3) DJ film precursor solution, Luo et al.^[40] got a champion stabilized PCE of 18.36% (with a stable J_{sc} of 20.86 mA.cm⁻²). In Luo's work, the grain size increased from ≈ 0.3 –1.0 μm up to >3 μm as shown in Fig. 3A, and then grain boundaries were reduced. FWHM decreased from 0.165° to 0.143°, indicating an increased crystallite size. The emission peak position of the bulk phase varied from 760 to 754 nm in the PL measurement, the blueshift was attributed to a trap density reduction, yielding lower nonradiative recombination

losses. The average lifetimes increased to 94.0 ns in TRPL measurements. The influence of additive concentration on the thickness distribution of QWs was also evaluated by femtosecond transient absorption (TA) spectroscopy. The additive enabled the formation of low- n QWs and a narrower thickness distribution of high- n QWs, leading to a gradient distribution of QW thickness. The carrier-populating time significantly decreased to 0.6–0.8 ps from 30 ps with the addition of 10 mg mL⁻¹ MAI, indicating that the additive enabled highly efficient electron transfer from low- n QWs to the bulk phase due to an optimized thickness distribution of the QWs (Fig. 3B), which is beneficial for charge transport/extraction in solar cells. Finally, the optimized solar cells without encapsulation had much better environmental stability, thermal stability, and illumination stability.

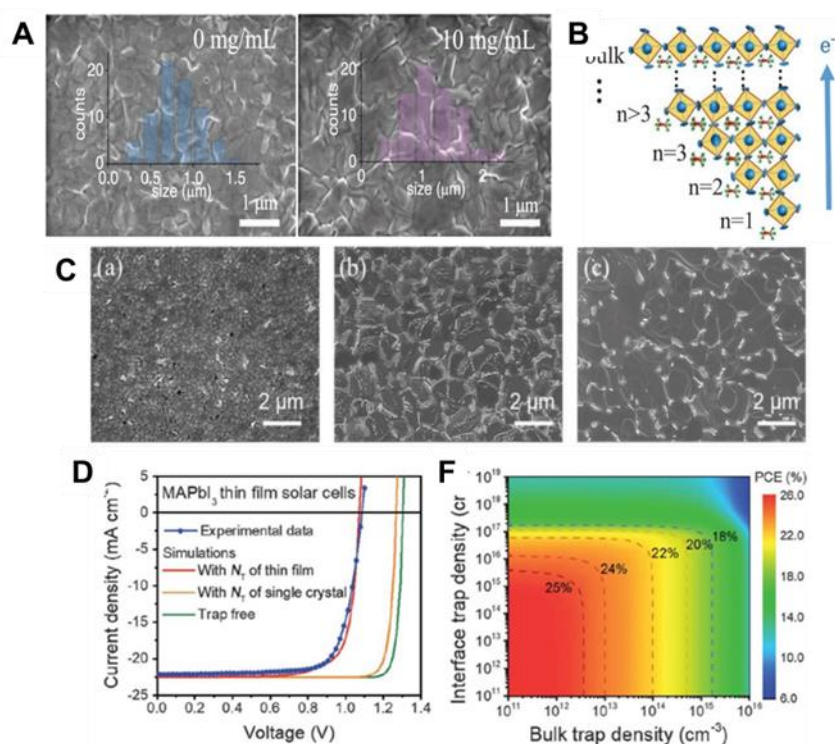


Fig. 3 (A) Top-view scanning electron microscopy (SEM) images and statistical chart of grain size of the 2D (GA)(MA)₃Pb₃I₁₀ films without and with 10 mg mL⁻¹ MAI additive. (B) Schematic thickness distribution of QWs and electron transfer from low- n to high- n QWs.^[64] with permission from Wiley-VCH, copyright 2019. (C) Effect of MAI and CNT-NH₂ additives on the morphologies of MA_{0.85}FA_{0.15}PbI₃ thin films. SEM images of a) MA_{0.85}FA_{0.15}PbI₃, b) MA_{0.85}FA_{0.15}PbI₃ (MAI), and c) MA_{0.85}FA_{0.15}PbI₃ (MAI)/CNT-NH₂ thin films.^[65] with permission from Wiley-VCH, copyright 2019. (D) Measured and simulated J - V curves of planar-structured solar cells based on MAPbI₃ polycrystalline thin films. The thin-film (single crystal) bulk and interface trap densities were adopted for the simulations. (E) Dependence of the PCE on MAPbI₃ thin-film bulk and interface trap densities. The dashed lines denote the contour lines of iso-PCE values.^[29] With permission from the American Association for the Advancement of Science, copyright 2020

Cite this paper as: F. Cheng, J. Zhu, Th. Pauporté, Chlorides, other Halides and Pseudohalides as Additives for the Fabrication of Efficient and Stable Perovskite Solar Cells. ChemSusChem 14 (2021) 3665–3692. DOI: 10.1002/cssc.202101089

In the work by Zhao et al.,^[65] 0.05 mg mL⁻¹ of amino-functionalized carbon nanotube (CNT-NH₂) and 0.21 M of MACl were employed to fabricate highly crystalline uniaxial-orientated PVK thin films with enhanced charge carrier transport. The MA_{0.85}FA_{0.15}PbI₃ (MACl) film showed enhanced crystallinity by XRD, and the peak intensity ratios of (110)/(310) and (220)/(310) became larger. It proved a preferred growth along the (110) and (220) crystallographic planes. The morphologies of modified film are shown in Fig. 3C. The average grain size reached > 1.5 μm by addition of MACl which was further enlarged to 2 μm with CNT-NH₂. The champion PSC device (FTO/c-TiO₂/SnO₂/PVK/Spiro-OMeTAD/Ag) achieved a PCE of 21.05% with a J_{sc} of 23.52 mA cm⁻², V_{oc} of 1.091 V, and FF of 0.82. The long-lasting charge carriers' lifetime in MA_{0.85}FA_{0.15}PbI₃ (MACl) films improved from 6.28 ns to 18.85 ns, compared with MA_{0.85}FA_{0.15}PbI₃, but decreased to 4.78 ns with CNT-NH₂. Such a decrease of PL lifetime is similar to the case of PVK films covered with charge transport (carrier- quencher) layers and indicated a promotion of charge-carrier transport by CNT-NH₂.

Normally, the defects at the film surface and grain boundaries of PVK cause deep traps. These traps act as recombination centers for charge carriers. Ni et al.^[29] studied the spatial and energetic distributions of trap states in halide PSC by Drive-level capacitance profiling (DLCP) method. They calculated that the trap density of the interfaces of polycrystalline PVK ranges between 9.0×10^{15} cm⁻³ and 2.0×10^{17} cm⁻³, which is 1 ~ 2 orders of magnitude the bulk value. For the polycrystalline MAPbI₃ fabricated solar cell discussed in their work, the authors calculated that decreasing the interface trap density from 1.0×10^{17} cm⁻³ to 2.0×10^{15} cm⁻³, would enhance the PCE to 25.4%, which is comparable to the PCE of 26.6% for trap-free MAPbI₃ thin film PVK solar cell (Fig. 3D and 3E).

Grätzel et al.^[66] fabricated planar PSCs with SnO₂/TiO₂ double layer oxide for an efficient electron extraction. They used MACl additive to aid the crystallization of the PVK film and get high quality large grains of PVK. The grain size enlarged to over 1 μm. Additionally, they treated the PVK film surface by iodine dissolved in isopropanol to passivate trap states. With Spiro-OMeTAD as HTL, the best PCE achieved 21.65% (J_{sc} of 23.2 mA cm⁻², a V_{oc} of 1193 mV, and FF of 78.2%). By using PTAA as hole transporting material (HTM), the device maintained 96%, 90%, and 85% of their initial PCE values after 500 h continuous light soaking at 20, 50, and 65 °C, respectively.

In a typical unstable PVK FAPbI₃, the main function of MACl additive is to stabilize the black α-phase since it is easily transformed into yellow non-PVK δ-phase at ambient environment. Kim et al.^[38] fabricated a high quality pure α-phase FAPbI₃ by employing 40 mol% of MACl as additive in the PVK precursor solution. The

Cite this paper as: F. Cheng, J. Zhu, Th. Pauporté, Chlorides, other Halides and Pseudohalides as Additives for the Fabrication of Efficient and Stable Perovskite Solar Cells. *ChemSusChem* 14 (2021) 3665–3692. DOI: 10.1002/cssc.202101089

mechanism of MACl effect on the formation of α -phase PVK was elucidated using DFT calculation. The formation energies revealed that Cl stabilizes the PVK structure thermodynamically. The projected density of states (PDOS) results revealed that Cl enhances the intensity of the p orbital of I at the HOMO state, then, the interactions of FA and I could be enhanced, thus improving the stability of FAPbI₃. Attractively, the device got a PCE of 24.02% (23.48% for the certified one) with improved surface morphology, crystallographic properties, optical absorption, and PL properties.

One of us and co-workers employed methylammonium chloride (MACl) as additive at 20 to 55 mol% of PbI₂ precursor for the growth of FA_{1-x}MA_xPbI₃ PVK layers.^[36, 67] The average grain size increased continuously with MACl with average values at 604 nm, 775 nm and 982 nm for 40 mol%, 48 mol% and 55 mol%, respectively. Monolithic PVK large grains were formed. Liquid-NMR was developed to analyze the photovoltaic layers. NMR peaks of MA, FA and of condensation products were identified and were reliably used to measure MA and FA content in films actually used in PSCs (Fig. 4A). x was quantified at 0.06 ± 0.01 for the pure α -phase films and was shown to correspond to the best entropic compound stabilization. The MACl excess was eliminated upon the annealing step. The best performance was achieved for 48 mol% MACl. It resulted in a stabilized PCE as high as 22.1%. These devices were also highly stable under solar irradiation and high moisture.

Kim et al.^[68] found that the addition of MACl into PVK precursor solution not only improves the crystallinity, but also increases the solubility of GeI₂ (Fig. 4B). The 3% MACl-assisted Ge doped Pb-hybrid PVK film show superior PL lifetime of 18846 ns, a PCE of 22.7%, and a great stability toward illumination and humidity. 80% of the initial device performance was maintained after 1 month in 30~40% of relative humidity (RH).

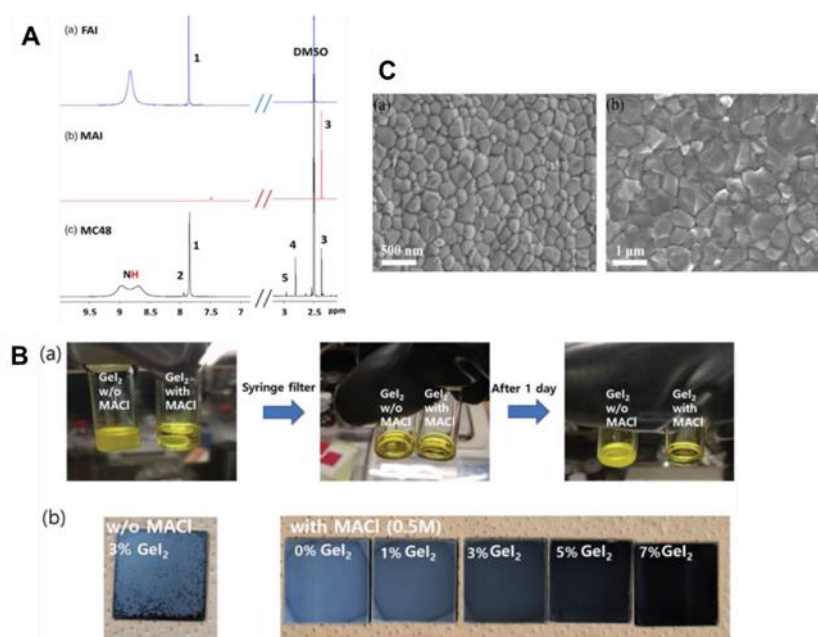


Fig. 4 (A) ¹H-NMR spectra of a) MAI, b) FAI, and c) FA_{0.94}MA_{0.06}PbI₃ layer with indexation. 1. NH=CHNH₃I; 2. CH₃NH₂CH=NHI; 3. CH₃NH₃I; 4. CH₃NH₂CH=NHI þ CH₃N=CHNH₂CH₃I; 5. CH₃N=CHNH₂CH₃I (N,N'-dimethyl FAI).^[36] with permission from Wiley-VCH, copyright 2020. (B) a) GeI₂-containing DMF/DMSO organic–inorganic PVK (3% GeI₂, FA_{0.83}MA_{0.17}Pb_{0.97}Ge_{0.03}(I_{0.9}Br_{0.1})₃) inks with and without MAI (0.5M). b) Pictures of PVK films of FA_{0.83}MA_{0.17}Ge_xPb_{1-x}(I_{0.9}Br_{0.1})₃ prepared without and with MAI additive and with various concentration of GeI₂ (x = 0-0.07).^[68] with permission from Wiley-VCH, copyright 2020. (C) Top-view SEM images of PVK films a) reference and b) with the FAI additive.^[69] with permission from Wiley-VCH, copyright 2021.

Formamidinium chloride (FACl) is another alternative for chloride source, with better solubility than MAI helping to get higher crystallinity. Suzuki et al.^[70] mixed various mol% of FACl into the MAI and PbCl₂ precursor solution. Using 10 mol% of FACl additive, energy dispersive X-ray spectroscopy (EDX) mapping gave the molar ratio of Cl in the halogen component with the sum of I and Cl which was slightly increased to be about 7.5%. The performance with the photovoltaic PCE was improved from 9.59 % to 13.75% with J_{sc} of 22.5 mA cm⁻², V_{oc} of 0.888 V, FF of 0.690. XRD patterns showed an increase of the (100) diffraction peak, a decrease of the FWHM and a peak shift due to a texturation of the layer, an increase of the crystal domain size and an enlargement of the d-spacing with addition of FACl at 10 mol%. Kong^[69] modified PVK bulk with FACl while another Cl additive, 1-adamantylamine hydrochloride (ADAHCl, 3 mg.mL⁻¹ in chlorobenzene, CB) was employed for the surface treatment. It formed a high-density SAM and passivated the surface (Fig. 4C). A longer carrier lifetime at 22.3 ns and reduced carrier recombination were found. Based on the double Cl modification, a SnO₂-based planar PSC was achieved with a PCE of 21.2%, low hysteresis, and high open circuit voltage of

Cite this paper as: F. Cheng, J. Zhu, Th. Pauporté, Chlorides, other Halides and Pseudohalides as Additives for the Fabrication of Efficient and Stable Perovskite Solar Cells. ChemSusChem 14 (2021) 3665–3692. DOI: 10.1002/cssc.202101089

1.152 V. 88% of initial PCE was retained after 700 h of aging under continuous illumination. Cl doping of MAPbI₃ is difficult to obtain due to the low formation energy and low boiling point of MAPbCl₃ at the origin of layer defects. A novel Cl containing additive, chloroformamidinium chloride (Cl-FACl)^[71], was presented as a “stabilizer” to restrain the removal of Cl avoiding the formation of defects in the layer. Gradually positive shift in XRD measurement indicated the shrinking of crystal lattice with the increase of smaller ions content doping, that is Cl and not Cl-FA. SEM showed that the grain size became larger with the concentration of Cl-FACl. The defects density based on the space charge limited current (SCLC) measurements and lifetime of TRPL decay measurements were calculated at $4.75 \times 10^{15} \text{ cm}^{-3}$ and 110.1 ns, respectively, for the Cl-FACl doped PVK films. It was much lower and longer than that of without Cl-FACl ($5.70 \times 10^{15} \text{ cm}^{-3}$ and 90.3 ns). For devices with 5 mol% Cl-FACl, a maximum PCE of 20.36% was achieved with lower hysteresis, 94% of their initial performance was retained after 600 minutes. Seok et al.^[72] stabilized the α -FAPbI₃ phase by doping with 3.8 mol% of methylenediammonium dichloride in replacement of MAPbBr₃ to get a methylammonium-free PSC. They achieved a certified PCEs of 23.7%. For the modified device, more than 90% of the initial efficiency was retained after 600 hours of operation at the maximum power point. Unencapsulated devices retained more than 90% of their initial PCE after annealing at 150°C in air for 20 hours.

2.3 Mechanism of chloride additives action on the growth of PVK films

Cl additives are mixed to the PVK precursor solution employed to prepare the films. Based on a coupled scanning transmission electron microscopy and energy-dispersive spectroscopy (STEM-EDS) measurements done by Dar et al.^[73] in 2014, and a combined *in-situ* X-ray diffraction and *ex-situ* TOF-SIMS chemical analysis study done by Yang et al.^[74] in 2016, Cl ions were proved to control the nucleation as well as the growth of MAPbI₃ without entering into the lattice. It rather resides at the grain boundaries after post-annealing because of its volatile property. Precisely, MACl controls the homogeneity of MAPbI₃ thin films by formation of intermediates with PbI₂ and reduction of the reaction rate between PbI₂ and MAI. The crystal growth rate is slowed-down and the crystals are more uniform. Consequently, the grains are larger, the film morphology is improved with less pinholes. It finally enhances the photovoltage property of the cell. To verify the function of MACl in the intermediate state, Dai et al.^[75] demonstrated a novel facile intermediate engineering. They dripped 20 mg.mL⁻¹ MACl onto the deposited FAI-MAI-PbI₂-DMSO intermediate film before the end of the second stage of spinning. They showed that this MACl treatment induces an ion exchange process in the FAI-MAI-

PbI₂-DMSO intermediate phase and transforms it into FAI-MAI-MACl-PbI₂-DMSO intermediate phase, further suppressing the crystal evolution rate and letting grains more time to evolve and self-embedding into the lattice network. As illustrated in Fig. 5A, 20 mg mL⁻¹ MACl modified film got a maximum grain size of 770 nm, and the lowest root-mean-square roughness of 11.6. Finally, the fabricated FTO/SnO₂/PVK/spiro-OMeTAD/Au achieved a PCE of 20.4%.

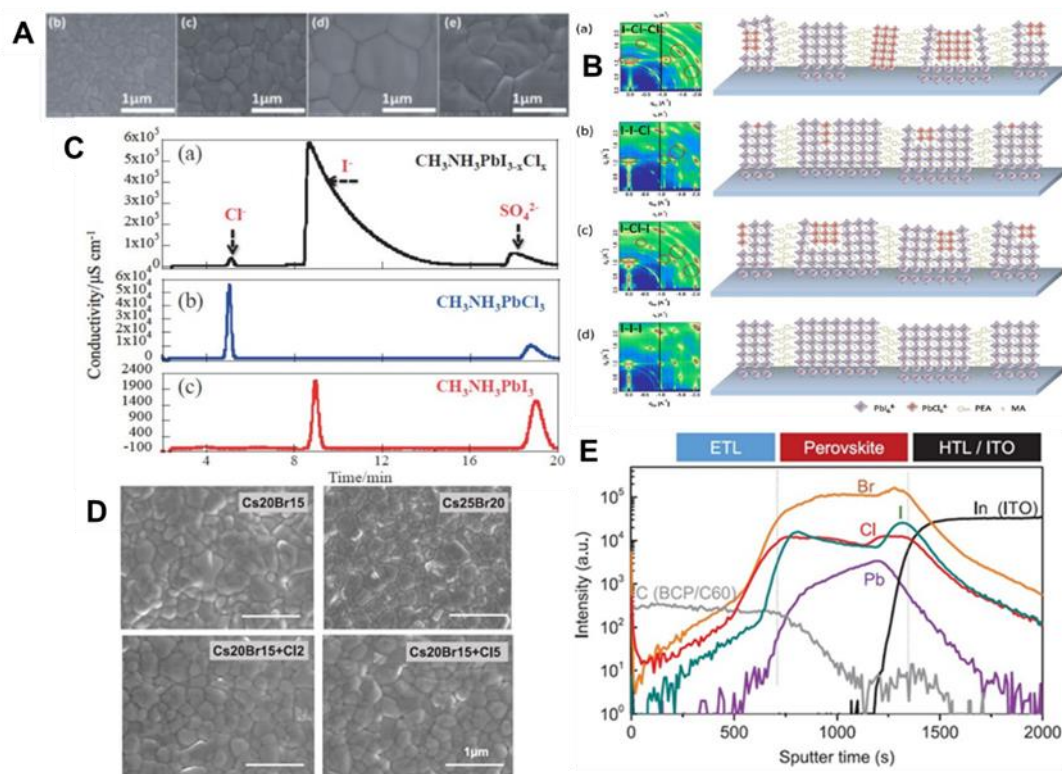


Fig. 5 (A) Surface SEM images of the films prepared with varied concentrations of MACl, (b) control film without-treatment, and films treated with c) MACl-10, d) MACl-20, e) MACl-30.^[75] with permission from the American Chemical Society, copyright 2020. (B) GIWAXS images and proposed crystal orientation for a) I-Cl-Cl, b) I-I-Cl, c) I-Cl-I and d) I-I-I LDRP PVK films. The characteristic peaks in chloride-containing systems are shown in red rings.^[76] with permission from Elsevier, copyright 2019 (C) Ion chromatography analysis of three different PVK solutions a) CH₃NH₃PbI_{3-x}Cl_x, b) CH₃NH₃PbCl₃, and c) CH₃NH₃PbI₃.^[77] With permission from the The Chemical Society of Japan, copyright 2015 (D) Top-view SEM images showing no evident difference in apparent grain size between triple-halide PVKs and double-halide control films; (E) TOF-SIMS depth profiles show the uniform distribution of halides throughout the entire film thickness of the triple-halide PVK (Cs₂₀Br₁₅+Cl₅).^[49] With permission from the American Association for the Advancement of Science, copyright 2020

The mechanism of optical and electronic properties improvement by Cl for low dimensional Ruddlesden-Popper (LD-RP) PVKs solar cell was also investigated. Devices with PbI₂+PEACl+MAI (I-Cl-I), PbI₂+PEAI+MACl (I-I-Cl), PbI₂+PEAI+MAI (I-I-I), PbI₂+PEACl+MACl (I-Cl-Cl) were fabricated.^[76] It was

Cite this paper as: F. Cheng, J. Zhu, Th. Pauporté, Chlorides, other Halides and Pseudohalides as Additives for the Fabrication of Efficient and Stable Perovskite Solar Cells. ChemSusChem 14 (2021) 3665–3692. DOI: 10.1002/cssc.202101089

confirmed by XRD that a part component of chloride generated the $(\text{PEA})_2\text{MA}_{n-1}\text{Pb}_n\text{Cl}_{3n+1}$ (PbCl_6^{4-}) phase. Grazing-incidence wide-angle X-ray scattering (GIWAXS Fig. 5B) technique was used to understand the effect of Cl position on crystallinity of the film. Results proved that Cl on PEA prefers to form PbCl_6^{4-} compared to that on MAI. PVK prepared from mixed Cl and I precursor demonstrated a longer charge carrier lifetime (668.15 ns) and diffusion length. SEM results showed that the incorporation of chloride significantly improved the PVK morphology with increased grain size, enhanced crystallinity, and uniform and smooth surface. Finally, a best PCE of 12.78% was achieved for the I-I-Cl system in a ITO/PEDOT:PSS/PVK/PCBM/LiF/Al solar cell structure.

The role of Cl on the PVK synthesis mechanism can be explained by the formation of intermediate species that favor the growth and crystallization of the final compound. It results in improved carrier lifetime and diffusion length, defect passivation and a phase stabilization which are of great profit for the final performance.

2.4 Measurement of the residual chloride in the layers

We have seen that many studies have reported the application of chloride additives in PVK precursor solution to optimize the morphology and surface passivation but with little or no chloride incorporation into the bulk material. It is commonly known that Cl^- volatilizes (evaporates) during annealing of the PVK film but could also reside at the grain boundaries or on PVK film surface. Chloride compounds mainly act as film crystallization controllers or play a role in the passivation of the PVK-contact interface. The content of probably residual Cl in the bulk were investigated by EDS, XPS, XRD and so on. Cl^- content is always below the detection limit of these techniques. For instance, Pauporté et al.^[36, 67] could not detect a quantifiable amount of Cl by EDX in $\text{FA}_{1-x}\text{MA}_x\text{PbI}_3$ layers prepared with precursor solutions containing 48 mol% of MAI with respect to PbI_2 .

Moreover, the lattice parameters determined by XRD are easily influenced by other factors such as mechanical stress. Therefore, some researchers claimed that Cl^- is removed without incorporation into the crystal lattice. However, the content of Cl residual could be measured in some cases, depending on the doping level, source of Cl, halogen balance in the perovskite precursor solution/initial stoichiometry, and measurement technique.

Mosca et al.^[78] found in 2013 that low concentration of Cl incorporated in a iodide-based structure did not change the E_g , but improved the charge transport in the PVK layer. Devices with methyl ammonium lead iodide PVK (PS1) layer, methyl ammonium lead iodide chloride (PS2) layer (3:1 MAI:PbCl₂) and lead halide mixture

Cite this paper as: F. Cheng, J. Zhu, Th. Pauporté, Chlorides, other Halides and Pseudohalides as Additives for the Fabrication of Efficient and Stable Perovskite Solar Cells. ChemSusChem 14 (2021) 3665–3692. DOI: 10.1002/cssc.202101089

(PS3) layer (1:1MACl:PbI₂) were fabricated. Their bandgap was 1.60 ± 0.01 eV. PS1 was poorly crystal oriented, while PS2 had a high orientation. A 0.7% reduction of the unit cell volume with respect to PS1 proved Cl-doping in PS2. For PS3, a high orientation pointed out a further phase, cubic MAPbCl₃ ($a = 5.683(2)$ Å). The segregation of the cubic MAPbCl₃, besides the Cl-doped MAPbI₃ phase proved the low incorporation of Cl into I based PVK films. In 2015, Cojocaru et al.^[77] were the first to calculate the exact content of Cl⁻ in the final film by ion chromatography. CH₃NH₃PbI₃, CH₃NH₃PbCl₃, and CH₃NH₃PbI_{3-x}Cl_x layers were dissolved in 0.15 M sulfuric acid and injected into an ion analyzer equipped with an anion-exchange column and a conductivity detector. Standard solutions of known concentration were used for I⁻ and Cl⁻ calibration. As shown in Fig. 5C, for the film prepared with PbCl₂ and CH₃NH₃I in a 1:3 molar ratio, they found a 0.06:2.94 molar ratio of Cl to I which is equivalent to 2%.

In the work by Xu et al.^[49], MAPbCl₃ was employed into FA_{0.75}CS_{0.25}Pb(I_{0.8}Br_{0.2})₃ PVK. In contrast to prior reports that Cl additive increases the grain size by modifying the nucleation and crystal growth, enlargement of grain domains was not observed in this research (Fig. 5D). As shown by time-of-flight secondary ion mass spectrometry (TOF-SIMS) depth profiling (Fig. 5E), Cl was uniformly distributed throughout the film. Taken the EQE, XRD, SEM, XPS, and SIMS results together, it was concluded that Cl was incorporated into the PVK lattice and increased its E_g , rather than being eliminated in a volatile phase. In a further experiment, MACl was added alone into PVK, the band gap did not raise, in agreement with previous reports that MACl volatilize during the annealing process at the temperature from 100 °C to 140 °C.^[67,79-81] By replacing some of the iodine by bromine to shrink the lattice parameter, the solubility of Cl was improved, and it resulted in a factor of 2 increase in photocarrier lifetime and charge-carrier mobility.

2.5 Other applications of chloride additives

2.5.1 Fabricate lead-less PSC

Chloride additives have been employed with cations to partly replace Pb and thus fabricate more environmentally friendly PVK solar cells.^[23] Jin et al.^[82] replaced PbI₂ by 3% of ZnCl₂. The modified device showed a great improvement in PCE from 16.4% to 18.2%, and the corresponding J_{sc} , V_{oc} , FF under reverse scan were 22.04 mA.cm⁻², 1.09 V and 75.76 %. As illustrated in Fig. 6A, the grain size increased up to ~350 nm with 3% ZnCl₂ doping, without cracks nor pinholes. However, ZnI₂ doped film showed a similar increased

Cite this paper as: F. Cheng, J. Zhu, Th. Pauporté, Chlorides, other Halides and Pseudohalides as Additives for the Fabrication of Efficient and Stable Perovskite Solar Cells. ChemSusChem 14 (2021) 3665–3692. DOI: 10.1002/cssc.202101089

crystal in grain size, confirming the crucial impact of Zn on the nucleation and crystal growth process. The FWHM of the (110) peak in XRD measurements decreased with increasing ZnCl₂, indicating a better crystallinity, which is consistent with the SEM results. The film with 3% of ZnCl₂ showed the strongest intensity of PL and the maximum of 84.3 ns PL lifetime, which implies that ZnCl₂ doping reduces the traps and defects in the PVK layer. The MAI(PbI₂)_{0.97}(ZnCl₂)_{0.03}-based device had a 3% hysteresis index, much lower than the control device (10%). The recombination resistance (R_{rec}) of electrical impedance spectroscopy (EIS) increased from 202.4 Ω to 910.9 Ω, indicating a decrease in recombination. The modified device degraded 7% of its initial PCE value after aging for 30 days in an ambient environment at 25–28 °C with 30–55% humidity without encapsulation.

Tsai et al.^[83] replaced PbI₂ by 75% of SnCl₂. The device of FTO/TiO₂/Al₂O₃/MASn_yPb_{1-y}I₃(Cl)/NiO/C structure had a best 5.13% PCE with further addition of 30 mol % SnF₂. SnCl₂ modified the conduction band energy (E_{CB}), the valence band energy (E_{VB}) and lattice structure (0%, tetragonal structure; 25%, orthorhombic structure; 50% of which with a substantially smaller unit cell; 75%, pseudocubic structure.) of PVK (Fig. 6B and 6C). The device modified by SnCl₂ showed anomalous optical and optoelectronic properties compared to the SnI₂ control.

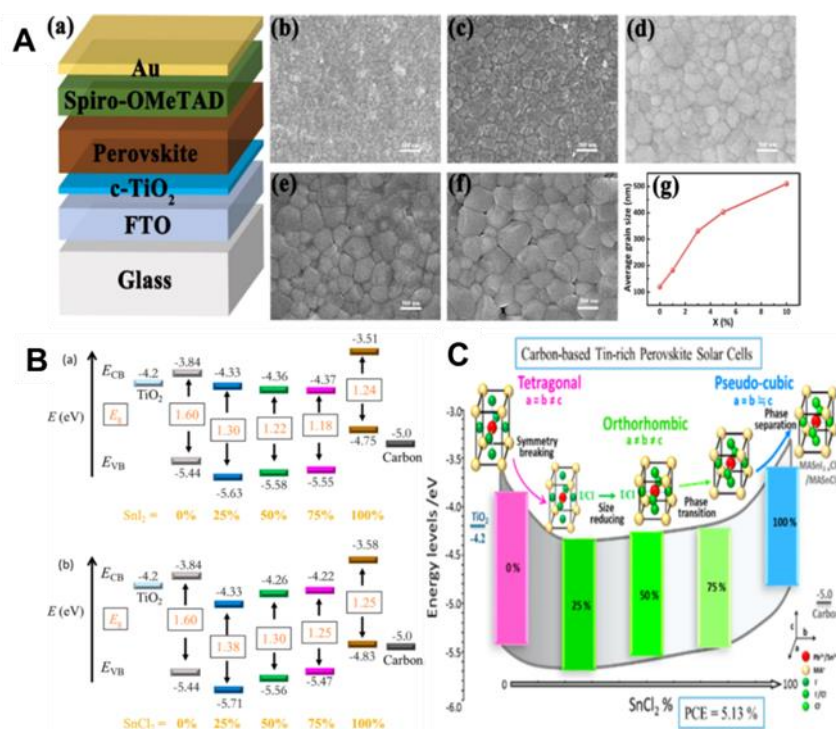


Fig. 6 (A) a) Schematic device architecture of MAI(PbI₂)_{1-x}(ZnCl₂)_x PVK solar cells. b–f) SEM surface images of the MAI(PbI₂)_{1-x}(ZnCl₂)_x PVK film with different ZnCl₂ (x = 0, 1, 3, 5, and 10%) content. g) Average grain size of MAI(PbI₂)_{1-x}(ZnCl₂)_x PVK film vs x.^[82] with permission from the American Chemical Society, copyright

Cite this paper as: F. Cheng, J. Zhu, Th. Pauporté, Chlorides, other Halides and Pseudohalides as Additives for the Fabrication of Efficient and Stable Perovskite Solar Cells.

ChemSusChem 14 (2021) 3665–3692. DOI: 10.1002/cssc.202101089

2017 (B) Potential energy diagrams (energies in eV with respect to vacuum) of a) $\text{CH}_3\text{NH}_3\text{Sn}_y\text{Pb}_{1-y}\text{I}_3$ and b) $\text{CH}_3\text{NH}_3\text{Sn}_y\text{Pb}_{1-y}\text{I}_3(\text{Cl})$ films with Sn/Pb ratios controlled with $\text{SnI}_2/\text{PbI}_2$ and $\text{SnCl}_2/\text{PbI}_2$ precursors, respectively, at varied concentrations as indicated. (C) The lattice structure of PVK modified by SnCl_2 concentration.^[83] with permission from the American Chemical Society, copyright 2016

2.5.2 Fabrication of 2D/3D dimensional PVKs.

Hybrid 2D/3D PVKs are gaining an increasing interest in the field of halide PSC, the 3D component acts as an active material, while its 2D part provides protection against environmental degrading agents.

Wu et al.^[84] added dodecylammonium-chloride (DACl) into the precursor solution of $\text{FA}_{1-x}\text{MA}_x\text{PbI}_3$. On the XRD pattern, the 3D-PVK peaks shifted towards higher angles and three peaks below 10° were present, indicating the formation of 2D-PVK. SEM images of PVKs films with increasing concentration of DACl showed denser and larger jigsaw-like crystals oriented perpendicular to the substrates. The PL-lifetime was improved from 3.15 ns to 26 ns by lowering the dimensionality. Incorporation of 8% DACl into the film reduced the defect levels by 2D-PVK formation. The moisture stability test showed that PVK retained the absorption structural characteristics even after being exposed to a humid environment ($\text{RH} > 50\%$) for more than 50 days. The best performance device exhibited a PCE of 5%, 82% of which was maintained after 6 days and 64% after 9 days in RH 50% and at a temperature of 85 °C.

Cl additive is also used in LED. It enables PVK blue-LEDs with narrowband and spectrally stable, without wavelength shift^[85, 86] and it enhances the photoluminescence quantum efficiency.^[86]

The list of the main chloride additives employed in PSC, cell structure, PCEs and $J-V$ curve parameters are summarized in the Table 3.

In summary, the role of chloride on the PVK synthesis mechanism has been explained by the formation of intermediate species. They favor the growth and crystallization of the final compound. They endow PVKs with high crystallinity as well as enhanced the grain orientation and increased charge carrier lifetime, increased diffusion length and electron-hole collection efficiency. Chloride additives have been employed to passivate the charged defects of the surface and grain boundaries as well as to control of crystallization and formation of PVK films for attaining efficient and stable photovoltaics. K^+ counter cation passivates trap states due to defects and blocks the iodide mobility. Many groups have investigated the possible mechanism of chloride additives engineered PVK crystallization process. Cl^- additives slows down the PVK formation rate to give uniform PVK film *via* forming the intermediate phase with PbI_2 and reducing the reaction rate between PbI_2 and MAI.

Cite this paper as: F. Cheng, J. Zhu, Th. Pauporté, Chlorides, other Halides and Pseudohalides as Additives for the Fabrication of Efficient and Stable Perovskite Solar Cells. ChemSusChem 14 (2021) 3665–3692. DOI: 10.1002/cssc.202101089

However, just little or no chloride is incorporated into the bulk PVK: most Cl⁻ evaporates during PVK annealing. Interestingly, Cl⁻ additives can be used to stabilize the black α -phase FAPbI₃, because Cl⁻ additive can enhance the intensity of the p orbital of I at the HOMO state and the interaction of FA and I. Finally, with synergy effect of other passivator, efficiency of 24.02% for (MA)FAPbI₃ PVK has been achieved.

Cite this paper as: F. Cheng, J. Zhu, Th. Pauporté, Chlorides, other Halides and Pseudohalides as Additives for the Fabrication of Efficient and Stable Perovskite Solar Cells.

ChemSusChem 14 (2021) 3665–3692. DOI: 10.1002/cssc.202101089

Table 3. Main chloride additives used in PVK, concentration, cell structure, PCE and J-V curve parameters.

Chloride additives in the precursor	Concentration/ PbI ₂ ^a	Device structure	PCE (%)	J _{sc} (mA.cm ⁻²)	V _{oc} (V)	FF (%)	Year ^{Ref.}
KCl	9 mol%	FTO/c-TiO ₂ /mp-TiO ₂ /Cs _{0.1} FA _{0.9} PbI ₃ /PEAI/spiro-OMeTAD/Au	19.16	25.24	0.992	76.54	2021 ^[50]
KCl	0.75 mol%/ DMSO	ITO/PEDOT:PSS/MAPbI ₃ /PC61BM/C60/BCP/Al	15.08	18.33	1.04	74.67	2016 ^[54]
KCl + NH ₄ Cl	5 mol%, 30 mol%	FTO/c-TiO ₂ /mp-TiO ₂ /Cs _{0.1} FA _{0.9} PbI ₃ /PEAI/spiro-OMeTAD/Au	20.05	25.21	1.012	78.61	2021 ^[50]
FACl	10 mol%	FTO/TiO ₂ /MAPbI _{3-x} Cl _x /spiro-OMeTAD/Au	13.75	22.5	0.888	69.00	2019 ^[70]
FACl, ADAHCl	10 mg.mL ⁻¹ ; 3 mg.mL ⁻¹ (CB)	FTO/SnO ₂ /(FAPbI ₃) _{0.87} (MAPbBr ₃) _{0.13} /spiro-OMeTAD/Au	21.20	23.4	1.152	78.30	2019 ^[71]
Cl-FACl	5 mol%	ITO/P ₃ CT-N/MAPbI _{3-x} Cl _x /PC ₆₁ BM/BCP/Ag	20.36	22.1	1.12	81.97	2019 ^[87]
PbCl ₂	2.50 mol%	FTO/TiO ₂ /MAPbI ₃ /spiro-OMeTAD/Au	18.10	23.5	1.04	75.00	2013 ^[52]
PbCl ₂	5 mol%	FTO/TiO ₂ /MAPbI ₃ /spiro-OMeTAD/Au	17.05	21.53	1.04	75.90	2019 ^[53]
DACl	8 vo%/PPS ^b	ITO/PEDOT:PSS/FAMAPbI ₃ /PCBM/BCP/Ag	5	13.57	0.845	44.00	2019 ^[84]
NH ₄ Cl	0.8 mol%	FTO/BL-TiO ₂ /ML-TiO ₂ /SL-ZrO ₂ /MAPbI ₃ /C	9.89	22.38	0.878	50.30	2019 ^[56]
NH ₄ Cl	0.2 M	ITO/PEDOT:PSS/MAPbI ₃ /PCBM/Ag	12.50	20.6	0.83	73.00	2020 ^[55]
NH ₄ Cl	0.3 M	MgF ₂ /Willow Glass/ITO/PTAA/MAPbI ₃ /C60/BCP/Cu	19.72	22.83	1.092	79.10	2020 ^[88]
NH ₄ Cl	30 mol%	FTO/c-TiO ₂ /mp-TiO ₂ /Cs _{0.1} FA _{0.9} PbI ₃ /PEAI/spiro-OMeTAD/Au	19.34	25.32	1.004	76.08	2021 ^[50]
MACl	48 mol%	FTO/c-TiO ₂ /mp-TiO ₂ /FA _{0.94} MA _{0.06} PbI ₃ /PEAI/spiro-OMeTAD/Au	22.18	25.94	1.06	80.62	2020 ^[67]
MACl	20 mol%	FTO/c-TiO ₂ /MAPbI ₃ /spiro-OMeTAD/Au	17.70	21.3	1.02	81.00	2019 ^[89]
MACl	15 mg.mL ⁻¹	FTO/TiO ₂ /SnO ₂ /(FAPbI ₃) _{0.87} (MAPbBr ₃) _{0.13} /spiro-OMeTAD/Au	21.65	23.2	1.193	78.20	2019 ^[66]
MACl	40 mol%	FTO/c-TiO ₂ /mp-TiO ₂ /FAPbI ₃ /PEAI/spiro-OMeTAD/Au	24.02	25.92	1.13	82.00	2019 ^[38]
MACl	20 mg.mL ⁻¹	FTO/SnO ₂ /FA _x MA _{1-x} PbI ₃ /spiro-OMeTAD/Au	20.40	23.88	1.08	78.38	2020 ^[75]
MACl, CNT-NH ₂	0.21 M; 0.05 mg.mL ⁻¹	FTO/c-TiO ₂ /SnO ₂ /MA _{0.85} FA _{0.15} PbI ₃ /Spiro-OMeTAD/Ag	21.05	23.52	1.091	82.00	2019 ^[65]
MACl	10 mg.mL ⁻¹	FTO/c-TiO ₂ /(GA)(MA) _n Pb _n I _{3n+1} (n = 3)/spiro-OMeTAD/Au	18.48	22.26	1.14	72.67	2019 ^[64]
MACl	0.5 M	FTO/TiO ₂ /SnO ₂ /FA _{0.87} MA _{0.13} (Ge _{0.03} Pb _{0.97})(I _{0.9} Br _{0.1}) ₃ /spiro-OMeTAD/Au	22.70	24.67	1.18	78.00	2020 ^[68]
ZnCl ₂	3 mol%/ MAI	FTO/c-TiO ₂ /MAI(PbI ₂) _{1-x} (ZnCl ₂) _x /spiro-OMeTAD/Au	18.20	22.04	1.09	75.76	2017 ^[82]

Cite this paper as: F. Cheng, J. Zhu, Th. Pauporté, Chlorides, other Halides and Pseudohalides as Additives for the Fabrication of Efficient and Stable Perovskite Solar Cells.

ChemSusChem 14 (2021) 3665–3692. DOI: 10.1002/cssc.202101089

SnCl ₂	75 mol% / MAI	FTO/TiO ₂ /Al ₂ O ₃ /MASn _y Pb _{1-y} I _{3-x} Cl _x /NiO/C	5.13	19.63	0.457	57.20	2016 ^[83]
-------------------	---------------	---	------	-------	-------	-------	----------------------

^a Compared to PbI₂ precursor if not otherwise precised. ^b PPS : perovskite precursor solution.

3. Other halides and pseudo-halides additives for PVK films

3.1 Halogen acids additives for PVK films

The PVK precursor solution is made of colloids of a lead polyhalide framework between organic and inorganic components.^[17, 90] These colloids act as a nucleation center and determine the coverage and morphology of deposited thin films, especially large colloids induce a poor film morphology. Hydrohalic acids can dissolve large colloid particles and manipulate the colloidal concentration in the precursor solution, resulting in the modulation of the PVK morphology during the deposition process. Compared to neutral additives, the addition of acids can disrupt the interaction between solvent molecules and lower the solution viscosity, which, in turn, affects the solvent evaporation rate and determine the PVK crystallization rate.

Acids can improve the solubility of PVK precursors and help to obtain uniform and well-covering PVK films. In 2014, Eperon et al.^[91] reported that the addition of HI helps to form uniform and continuous thin film. McMeekin et al.^[92] investigated the nucleation and growth stages of PVK films by adding HI and HBr acids into $\text{FA}_{0.83}\text{Cs}_{0.17}\text{Pb}(\text{Br}_{0.2}\text{I}_{0.8})_3$ precursor solution. As shown in Fig. 7A, the colloids in suspension gradually dissolved, and the content of small colloidal particles increased with longer aging time after addition of acid. It critically impacted the crystallization kinetics and morphology of the thin films since colloids act as nucleation center (Fig. 7B, C). Finally, large grains and well-covering films were obtained by reducing the density of nucleation sites. However, a distinct trade-off between the grain sizes and pinhole density was observed. Since crystal growth also occurred in the vertical direction, the large crystal grains tended to be accompanied with undesirable pinholes. Heo et al.^[93] deposited dense MAPbBr_3 PVK films with well-surface coverage by adding HBr into MAPbBr_3 precursor solution. The nucleation time of MAPbBr_3 was retarded during spin-coating process due to the improved solubility of MAPbBr_3 in DMF+HBr solution. A more-concentrated MAPbBr_3 in DMF + HBr solution helped to yield thinner and better-covering PVK layers. It was noticed that the addition of the same amount of H_2O also enabled the formation of fully-covering MAPbBr_3 layers, but the H_2O produced the decomposition of MAPbBr_3 into MABr and PbBr_2 .

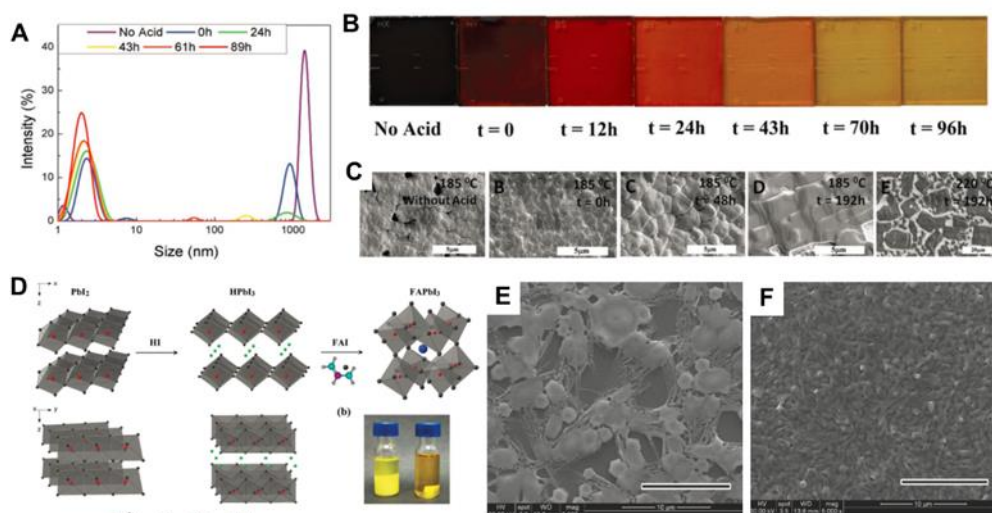


Fig. 7 Effect of acid additive on the colloid in the precursor solution. (A) Colloidal hydrodynamic size distribution of various PVK solutions. (B, C) Photographs and SEM views of thin films prepared with aged solution after the addition of Halogen acid.^[92] with permission from Wiley-VCH, copyright 2017. (D) Schematic illustration of FAPbI₃ formation from PbI₂ with HI additive. (E, F) SEM images fabricated from FAI/PbI₂ and FAI/HPbI₃, respectively.^[94] with permission from Wiley-VCH, copyright 2015.

HI can react with PbI₂ to form HPbI₃ or HPbI_x, which show better solubility than PbI₂ in DMF solution. Wang et al.^[94] developed HPbI₃ to replace lead iodide and obtained highly uniform FAPbI₃ films (Fig. 7D). They proposed that the best performances of the HPbI₃ based PVK films may benefit from the slow crystallization process with exchange of H⁺ and FA⁺ ions in the PbI₆ framework (Fig. 7E and 7F). Pang et al.^[95] demonstrated that the HPbI₃ can serve as precursor compounds to deposit uniform MAPbI₃ PVK film upon CH₃NH₂ gas treatment. Upon exposed HPbI₃ into CH₃NH₂ atmosphere, the CH₃NH₂ molecules can react with H⁺ to form CH₃NH₃⁺. After annealing, 1D HPbI₃ structure transformed into 3D MAPbI₃ PVK structure. H⁺ plays a critical role in the formation of a stoichiometric, ultrasmooth and fully covering MAPbI₃ PVK thin films. Eperon et al.^[96] first introduced HI additive into CsPbI₃ precursor solution, which made the conversion temperature from yellow to the black phase decreased to 100°C. It resulted in the formation of smooth and uniform black CsPbI₃ films. HPbI₃ was also employed to fabricate CsPbI₃ PSCs with improved stability and performance.^[97]

In summary, halogen acid additives can modulate the morphology of PVK film via affecting the colloid particles and concentration in the precursor solution and reducing the crystallization rate. It results in better PVK morphology and trap states reduction.

3.2 Fluoride additives for PVK films

Due to the small size and large electronegativity of fluorine, fluoride species can form strong ionic and intermolecular bonding with PVK. Such strong chemical reactivity between fluoride and PVK is beneficial for passivating surface and crystal boundaries defects. Generally, when fluoride is incorporated into PVK film, it is typically present on the surface of PVK, exhibiting surface hydrophobicity and therefore protect the PVK from moisture erosion. Metal fluoride, such as SnF₂ and alkali fluoride, have been used in PSCs, especially, SnF₂ is employed in the tin halide PVK for suppressing the oxidation from Sn²⁺ to Sn⁴⁺. Due to the toxicity of Pb which may limit the diffusion of the PSC technology, lead-free PVKs ASnX₃ have been intensively investigated. It is reported that MASnI₃ has a bandgap around 1.2 to 1.3 eV and an expected large short-circuit photocurrent. However, the PCEs of Sn-doped or entirely Sn-based PSCs are well-below that of Pb-based PSCs, and a large fraction of them is short-circuited. This mainly results from the oxidation of Sn²⁺ to Sn⁴⁺ in air and the intrinsic Sn-cation vacancies, as well as the poor morphology.

SnF₂ additive can suppress the oxidation of Sn²⁺ to Sn⁴⁺. The tin-based PVK ASnX₃ are unintentionally hole-doped to a high degree, due to the Sn vacancies and the oxidation of Sn²⁺. Recently, SnF₂ additive in the lead-free PVK was shown to increase the Sn chemical potential and the formation energy of Sn vacancies, and then reduce the background carrier density and Sn defects.^[98, 99] Handa et al.^[100] reported a blue-shifted absorption edge for pure MASnI₃ thin film compared to the MASnI₃ with SnF₂ additive (Fig. 8A). It was assigned to the unintentional hole doping which induces a Burstein-Moss shift in the SnF₂-free MASnI₃ samples. They demonstrated that SnF₂ additive reduces the hole density by about 1–2 orders of magnitude and suppresses the Sn⁴⁺ formation. The PL lifetime of MASnI₃ with SnF₂ additive increased by one order of magnitude, resulting in improved performance of devices. For the effect of SnF₂ additive, Ma et al. proposed that SnF₂ just act as an inhibitor of Sn²⁺ oxidation in the CH₃NH₃SnI₃ precursor solution for preparing undoped (Sn⁴⁺-free) film with lower defect concentration. Based on SEM images, XRD and UV-Vis spectra of CH₃NH₃SnI₃ film with 20 mol% SnF₂, no SnF₂ or SnI₂ was found in the CH₃NH₃SnI₃ film.^[101]

SnF₂ additive was used to modulate the crystallization process and improve the morphology of PVK films. F has a much smaller ionic radius (1.33 Å) than I (2.20 Å), therefore F doping of iodide PVK would not induce a significant variation in the lattice parameter and unwanted phases of film. Liao et al.^[102] investigated the effect of SnF₂ additive on the morphology of FASnI₃ thin films. As shown in Fig. 8B, a flower-like structure with

Cite this paper as: F. Cheng, J. Zhu, Th. Pauporté, Chlorides, other Halides and Pseudohalides as Additives for the Fabrication of Efficient and Stable Perovskite Solar Cells. ChemSusChem 14 (2021) 3665–3692. DOI: 10.1002/cssc.202101089

many pinholes was observed for the pure FASnI₃ thin film. With increasing SnF₂ concentration, the flower-like structures disappeared and the FASnI₃ films became more uniform. It was noticed that a higher amount of SnF₂ (>10%) induced severe phase segregation, resulting in obvious aggregates formation in the PVK film. As a result, the PCEs of Sn-based PSCs with optimized 10 mol% SnF₂ additives increased to 6.22% in 2016. Lee et al.^[103] selected SnF₂-pyrazine complex as additive in FASnI₃ precursor solution to restrict the phase separation and reduce Sn vacancies formation. They also demonstrated the role of DMSO in forming a uniform PVK layer. During the spin-coating process, the crystallization of FAI and SnI₂ was retarded by using DMSO as solvent, thereby producing a film with much better quality. Finally, FASnI₃ PSCs with addition of SnF₂-pyrazine complex achieved a high PCE of 4.8%, and showed high reproducibility and stability for the encapsulated devices.

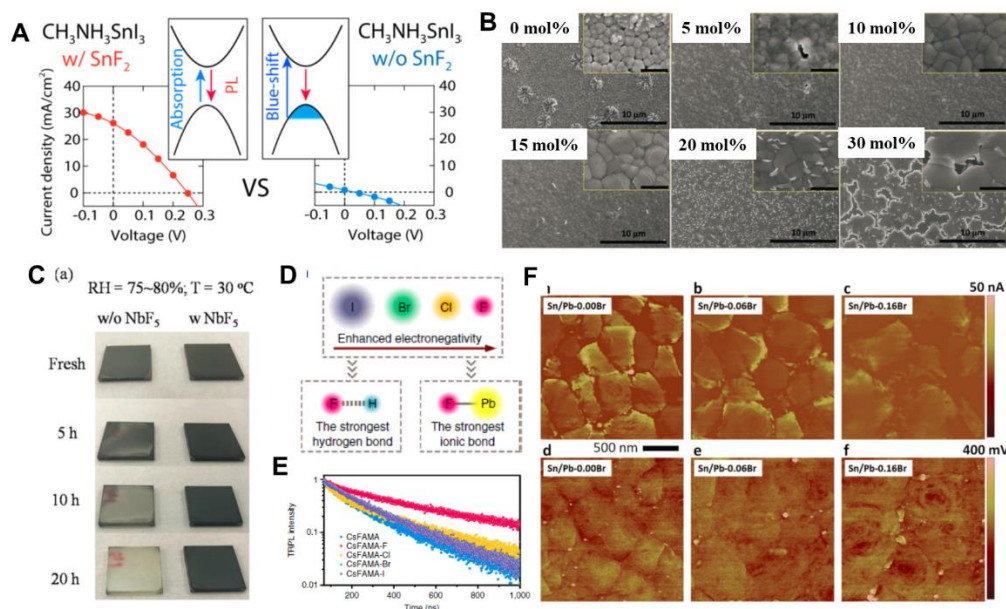


Fig. 8 (A) Current–voltage curves of a MASnI₃ solar cells (prepared with and without SnF₂) recorded under AM 1.5G 1-sun irradiation.^[100] with permission from the American Chemical Society, copyright 2020. (B) SEM images of FASnI₃ PVK films with varying concentration of SnF₂, scale bar in all images are 10 μm and 1 μm (inset images).^[102] with permission from Wiley-VCH, copyright 2017. (C) Humidity stability of FA_{0.85}MA_{0.15}PbI₃ PVK films without and with NbF₅.^[104] with permission from Wiley-VCH, copyright 2019. (D) Schematic illustration of hydrogen bond between halogen and MA/FA ions. (E) TRPL spectra for the (Cs_{0.05}FA_{0.54}MA_{0.41})Pb(I_{0.98}Br_{0.02})₃ PVK film with different sodium halide additives.^[105] with permission from Springer Nature, copyright 2019. (F) AFM and (d) KPFM images of (FASnI₃)_{0.6}(MAPbI₃)_{0.4-x}(MAPbBr₃)_x (x = 0, 0.06, 0.16) PVK films.^[106] with permission from Wiley-VCH, copyright 2018.

SnF₂ additive was used to improve the phase stability. The use of Sn²⁺ cation results in a lower bandgap of

Cite this paper as: F. Cheng, J. Zhu, Th. Pauporté, Chlorides, other Halides and Pseudohalides as Additives for the Fabrication of Efficient and Stable Perovskite Solar Cells. ChemSusChem 14 (2021) 3665–3692. DOI: 10.1002/cssc.202101089

PVK compared to Pb^{2+} ,^[107] while the phase transformation and facile oxidation of Sn^{2+} to Sn^{4+} lead to the instability and poor performance for the PSCs. It is known that the tolerance factors of the stable PVK materials ABX_3 should lie between 0.78–1.05, where the tolerance factor is defined as: $t = (R_A + R_X)/2(R_B + R_X)$ with R_A , R_B and R_X the ionic radii of A, B and X ions, respectively. When F ion (as SnF_2) is introduced stoichiometrically, into the ASnI_3 PVK, forming a $\text{ASnI}_{3-x}\text{F}_x$ PVK layer, the tolerance factor t becomes larger as x increases due to the smaller F ionic radius, and enhances the phase stability of Sn-based PVK. Therefore, fluoride complex was introduced as additive to improve the stability of Sn-based PVK. Wu et al.^[108] demonstrated that F ion dopant inhibits the oxidation process, and slows down the phase transformation of CsSnI_3 into Cs_2SnI_6 .

Alkali fluoride is beneficial for reducing the positive and negative charged defects by forming chemical bonds with lead-based PVK. Yuan et al.^[104] presented an efficient method to prevent the phase transformation from black α -phase to yellow non-PVK δ -phase by adding NbF_5 material (Fig. 8C). The $\text{FA}_{0.85}\text{MA}_{0.15}\text{PbI}_3$ PVK film with NbF_5 could maintain the black color without bleaching to transparent after 20 h, and the stability of PSC was much improved. The fluorine and niobium elements were distributed over the PVK surface, the strong Pb-F and Nb-I interactions between NbF_5 and $\text{FA}_{0.85}\text{MA}_{0.15}\text{PbI}_3$ were probably the main reasons for the improved phase stability after NbF_5 addition. Li et al.^[105] explored an effective passivation of cation and anion vacancy defects via adding NaF into the triple-cation PVK ($\text{Cs}_{0.05}\text{FA}_{0.54}\text{MA}_{0.41}$) $\text{Pb}(\text{I}_{0.98}\text{Br}_{0.02})_3$ layer. They compared the passivation effect of NaX ($X=\text{Cl}, \text{Br}, \text{F}$) with tunable bond strength of halide with PVK layer (Fig. 8D). Although all sodium halides could improve the PVK quality, the fluoride-containing material gave the best results (Fig. 8E). Since the F ions can form hydrogen bonds ($\text{N-H}\dots\text{F}$) with organic cations and ionic bonds with Pb at the PVKs surface, F ions are effective in passivating both the organic cations and halide vacancies. Meanwhile, the increased ionic bonding of PVK with fluoride ions also immobilized both organic cations and halide anions. Finally, the addition of NaF resulted in a best PCE of 21.46% in planar PSCs, and superb thermal and environmental stability for the PVK layer and devices.

3.3 Bromide additives for PVK films

The bandgap of organic halide PVK can be tuned by the p -orbital of halide, since the electronic structure of PVK is related to both halide and metal p -orbitals. Substitute iodide by bromide anion to create mixed-halide PVK can broaden the band gap of PVK film, generate longer lifetimes and improve stability.^[109] The mixed-halide PVK films also exhibit enhanced stability toward ambient conditions.^[110] Noh et al.^[111] first tuned the

Cite this paper as: F. Cheng, J. Zhu, Th. Pauporté, Chlorides, other Halides and Pseudohalides as Additives for the Fabrication of Efficient and Stable Perovskite Solar Cells. *ChemSusChem* 14 (2021) 3665–3692. DOI: 10.1002/cssc.202101089

bandgap of MAPbX₃ from 1.6 eV to 2.2 eV covering almost the entire visible spectrum via adjusting the Br/I ratios. With this approach, Huang et al.^[112] designed a novel prismatic PSC by connecting four MAPbI_xBr_{3-x} (x=3, 2, 1, 0) subcells with different bandgaps in the same horizontal plane. Thermodynamic losses are mitigated by this approach and the incident high-to-low energy photons are harvested by horizontally aligned MAPbI_xBr_{3-x} subcells. As a result, the corresponding newly designed PSC generated a record V_{oc} of 5.3 V and PCE of 21.3%. The PVK with bandgap of 1.3-1.4 eV is pivotal for single junction PSCs because of the balance between absorption loss of sub-bandgap photons and thermalization loss of above-bandgap photons. Yang et al.^[113] incorporated 20% Br into MASn_{0.5}Pb_{0.5}I₃ to obtain an ideal bandgap (1.35 eV) absorber layer for single junction PSCs. This mixed-halide MAPb_{0.5}Sn_{0.5}(I_{0.8}Br_{0.2})₃ PVK reduced the V_{oc} loss at 0.45 V and improved PCE to 17.63%.

Bromine incorporation can passivate grain boundaries. It is known that low-E_g mixed Pb-Sn PSCs exhibits large V_{oc} deficits and low FF, because of the high dark saturation current density caused by high leakage current from grain boundaries.^[114, 115] Li et al.^[106] demonstrated that Br incorporation can passivate defects at grain boundaries and lower the dark saturation current density of low E_g mixed Sn-Pb PSCs. PVK films were prepared by spin-coating (FASnI₃)_{0.6}(MAPbI₃)_{0.4-x}(MAPbBr₃)_x (x = 0, 0.04, 0.06, 0.08, and 0.16) precursor solutions. In the fabrication process of annealing at 100 °C, the high temperature would drive Br out of PVK crystal lattice, resulting in higher Br concentration at grain boundaries than in grain bulk. Consequently, the grain boundaries contain a higher density of negatively charged defects than grain interiors confirmed by KPFM map (Fig. 8F). With Br additive, the mixed low-E_g (1.272 eV) Sn-Pb PSCs have achieved low V_{oc} deficits of 0.384 V, high FF of 75% and a PCE of >19%. Although mixed Sn-Pb PVK layer possesses ideal-bandgap for photovoltaic application, the best PCEs of Sn-Pb binary PSCs with <18% are lower than 1.5-1.6 eV bandgap pure-Pb-based PSCs with PCE of 24%.^[116] The poor efficiency of Sn-Pb binary PSCs is attributed to the high defect density associated with Sn²⁺ oxidation, which leads to lower open circuit voltage (<0.9 V).^[117] Therefore, some organic substances, such as SnF₂-Prazine,^[103] guanidinium thiocyanate,^[118] have been used as additive to reduce the high defect density caused by Sn²⁺ oxidation. Zhou et al.^[119] discovered that guanidinium bromide (GABr) in the PVK film can passivate the defect related with Sn²⁺ oxidation, which improved the structural and photoelectric characteristics of Sn-Pb binary PVK (FA_{0.7}MA_{0.3}Pb_{0.7}Sn_{0.3}I₃) thin films. With optimized GABr concentration of 12%, Sn-Pb binary PVK films display increased grain size, decreased charge-carrier recombination, and reduced trap state densities, resulting in best PCE of 20.63% with a small V_{oc} deficit of 0.33 V.

Cite this paper as: F. Cheng, J. Zhu, Th. Pauporté, Chlorides, other Halides and Pseudohalides as Additives for the Fabrication of Efficient and Stable Perovskite Solar Cells. ChemSusChem 14 (2021) 3665–3692. DOI: 10.1002/cssc.202101089

Lewis base usually act as electron donor, which can interact with positively charged under-coordinated Pb^{2+} ions. Organic Lewis base, such as thiophene, pyridine, thiourea etc, could efficiently passivate the under-coordinated Pb^{2+} and thus enhance the PCE and stability of PSCs. Zhang et al.^[120] applied N-(4-bromophenyl)-thiourea (BrPh-ThR) as the Lewis base in the PVK solution precursor to investigate the cooperation passivation effect of organic cation and bromide. BrPh-ThR as an S-donor has a strong ability to coordinate with PbI_2 , which is beneficial for the large grain PVK formation and defect passivation of the Pb^{2+} defects at crystal grain boundaries and surface. As a result, they obtained a 20.4% device efficiency with BrPh-ThR additive in precursor solution, compared with 19.3% for the control PSCs.

3.4 Iodide additives for PVK films

Recent studies show that the performance of PVK film could be improved through addition of solid iodine (I_2), organic iodide, PbI_2 and alkali metal iodides, LiI, NaI, KI, RbI and CsI. A complete understanding of these issues is important for obtaining high efficiency PSCs.

3.4.1 Iodide ions additive

A large number of iodide additives have been employed in the literature to prepare 2D/3D PVK layers. The complete reporting of this research field is out of the scope of the present review and one can report on the recent review by Zhang et al.^[121] to have an overview on the topic. The most successful approach developed up to now for getting highly stable PSCs has been to adopt a triple mesoscopic architecture where the HTL/metal back contact is replaced by a mesoporous carbon counter-electrode.^[58, 122, 123] Such cells have recently successfully passed items of the IEC61215:2016 PV qualification test.^[124] The employment of 5-Ammonium valeric acid iodide (5-AVAI) additive was shown important to facilitate the porous scaffold filling, to improve the contact with the oxide scaffold and to strengthen the MAPbI_3 grain boundaries due to bifunctionality.^[124] 4-(aminomethyl) benzoic acid hydroiodide additive has also been employed efficiently for the same purpose.^[125] Yang et al.^[126] reported a defect-engineering strategy with iodide management for fabricating formamidinium-lead-halide-based PVK. Solid iodine (I_2) was dissolved in isopropanol (IPA) and formed to I_3^- ions, which was added into the dripping solution of FAI (+ MABr) for increasing the proportion of the crystalline α -FAPbI₃ phase and reducing the concentration of defects in the entire PVK layer. The fabricated PSCs exhibited a

certified power conversion efficiency of 22.1% in small cells and 19.7% in 1-square-centimeter cells.

3.4.2 Excess amount of PbI_2 and other inorganic iodide additives

Although the precise stoichiometry of halide PVK precursor solution is important for making PVK film, a slight excess of PbI_2 on the PVK grains is beneficial for the performances of PSCs.^[127] The mechanism for the effect of PbI_2 on the PSCs performances have been investigated. Lead iodide, a p-type semiconductor with a large bandgap of 2.3 eV,^[128] could passivate and eliminate defect states due to a band edge matching between PVK, PbI_2 , and the HTL.^[129, 130] Zhang et al.^[13] investigated the MAPbI_3 could decomposed into PbI_2 and organic species with annealing time excess. By releasing the organic species, PbI_2 formed in PVK films could passivate and eliminate defect states and enhance the device performance. Chen et al.^[130] demonstrated a self-induced passivation strategy of PbI_2 for the MAPbI_3 PVK to control the carrier injection and transfer behavior across the corresponding heterojunction. They discovered that the MAPbI_3 would slightly decompose to PbI_2 upon heating at 150 °C for more than 30 min. As shown in Fig. 9A, PbI_2 excess can fill PVK grain boundaries, thereby reducing the number of trapping sites and form a favorable type I band alignment. This PbI_2 passivator can reduce the carrier recombination at the interface of TiO_2/PVK and alleviate the barrier of charge extraction from PVK to HTL. The excess of PbI_2 formed a passivating layer at the PVK gain boundaries and surface which induced to a longer recombination time, but too much PbI_2 could act as an insulating layer and impair the device performance.^[131] However, it is difficult to control the amount of PbI_2 by such self-induced approach with annealing technique. Kim et al.^[127] incorporated different amount of PbI_2 into the PVK layers. They demonstrated that PbI_2 excess in the PVK phases is highly beneficial for reducing the hysteresis of J - V characteristics and ion migration. Finally, the best PSC fabricated using $(\text{FAPbI}_3)_{0.85}(\text{MAPbBr}_3)_{0.15}$ achieved a PCE of 20.1% with 5.7 mol% PbI_2 excess incorporated. Zhang et al.^[132] developed a novel approach to fabricate PVK passivated by a controllable PbI_2 amount by using hydrohalide deficient $\text{PbI}_2 \cdot x\text{HI}/\text{Br}$ ($x < 1$) precursors reacted with CH_3NH_2 . Both MAPbI_3 and MAPbI_2Br PVK solar cells prepared via $\text{MA}+(\text{PbI}_2+0.95\text{HI}/\text{Br})$ exhibited improved PV performance with a V_{oc} enhancement due to less charge recombination by PbI_2 passivation. Moreover, authors have hypothesized that a small excess of PbI_2 is beneficial for preparing larger PVK grains or improving their crystallinity, resulting in enhanced devices' performances.^[131, 133, 134] Jiang et al.^[134] investigated the synergistic effect of PbI_2 passivation and Cl inclusion for improving the $\text{CH}_3\text{NH}_3\text{PbI}_3(\text{Cl})$ PVK film growth and suppressing nonradiative recombination. It resulted in a record-high V_{oc} over 1.15V for

the $\text{CH}_3\text{NH}_3\text{PbI}_3(\text{Cl})$ PSCs.

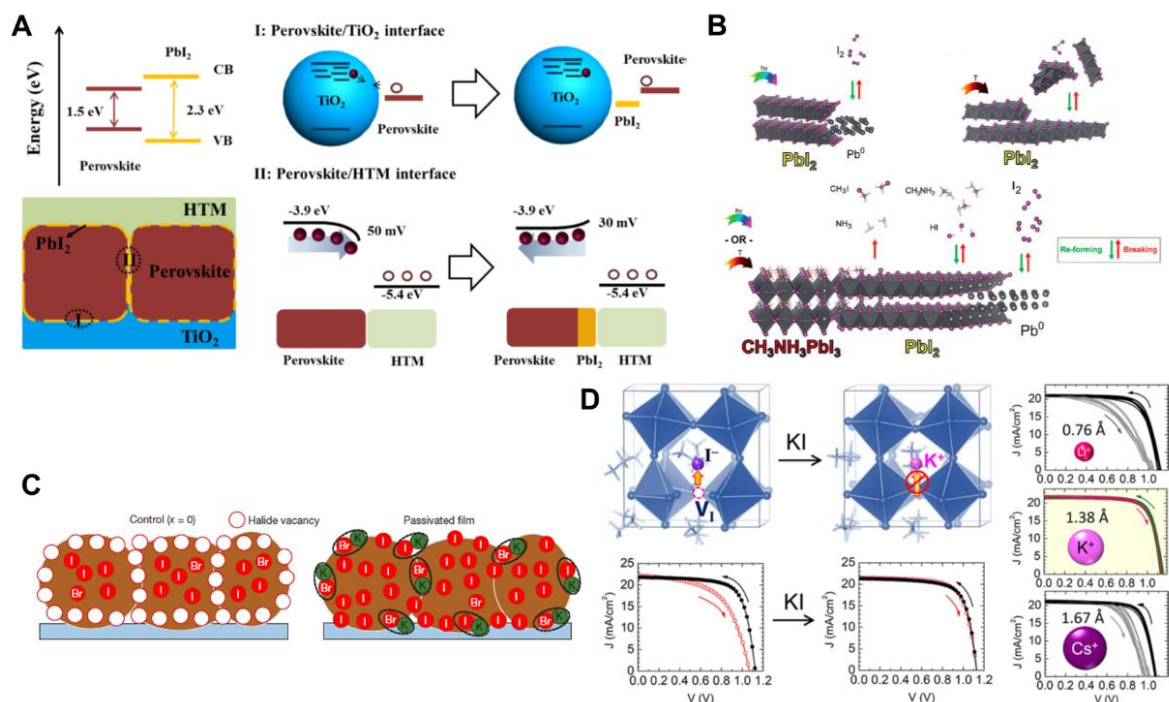


Fig. 9 (A) Proposed mechanism for PbI_2 passivation in $\text{CH}_3\text{NH}_3\text{PbI}_3$ Film.^[130] with permission from the American Chemical Society, copyright 2014. (B) The photodecomposition and thermal degradation processes of PbI_2 and MAPbI_3 .^[135] with permission from The Royal Society of Chemistry, copyright 2018. (C) Schematic illustration of PVK film showing halide-vacancy management and the potassium passivation effect.^[136] with permission from Springer Nature, copyright 2018. (D) Schematic view of MAPbI_3 hybrid PVK structure with I_Frenkel defect, and the passivation effect of KI on the device performance.^[137] with permission from the American Chemical Society, copyright 2018.

PbI_2 excess at the surfaces and grain boundaries of PVK films, due to a larger bandgap than PVK, results in electronic insulation and negative effect for the cell performance.^[138, 139] Especially, a small excess amount of PbI_2 has a detrimental effect on the stability of PVK.^[140] As shown in Fig. 9B, PbI_2 suffers photodecomposition to iodine gas (I_2) and lead (Pb^0) upon interaction with visible light.^[135] I_2 gas is released from MAPbI_3 even in dark conditions during heating at temperatures as low as 40 °C to 80 °C, which correspond to solar cell working temperatures. Such intrinsic photolysis of PbI_2 is related to the devices' instability under continuous light illumination.^[135] Tumen-Ulzii et al.^[141] further confirmed the detrimental effect of unreacted PbI_2 on the long-term stability of PSCs. The PVK films were deposited from 1.12 M $\text{Cs}_{0.05}(\text{FA}_{1-x}\text{MA}_x)_{0.95}\text{Pb}(\text{I}_{1-y}\text{Br}_y)_3$ precursor solution. Unreacted PbI_2 were deposited at the surfaces and grain boundaries of PVK when the PbI_2 concentrations in precursor solutions increased. The PCE of PSCs prepared with unreacted PbI_2 reduced to 47%

Cite this paper as: F. Cheng, J. Zhu, Th. Pauporté, Chlorides, other Halides and Pseudohalides as Additives for the Fabrication of Efficient and Stable Perovskite Solar Cells. ChemSusChem 14 (2021) 3665–3692. DOI: 10.1002/cssc.202101089

of its initial value after 520 h of continuous illumination. However, the PCEs of PSCs without unreacted PbI_2 retained 99% of their initial values. SEM images revealed that unreacted PbI_2 in the original PVK film almost disappeared, but defects and pinholes increased after 520 h of continuous illumination. They proposed that the degradation of $\text{Cs}_{0.05}(\text{FA}_{1-x}\text{MA}_x)_{0.95}\text{Pb}(\text{I}_{1-y}\text{Br}_y)_3$ PSCs was due to the photolysis of unreacted PbI_2 into Pb^0 and I_2 gas under light illumination.

In addition to PbI_2 , alkali metal iodides are considered as important additives to enhance the performance of PVK, especially for eliminating hysteresis in PSCs. In 2017, Tang et al.^[142] were the first to report hysteresis-free PVK solar cells after adding a small amount of KI (5%) into the $(\text{FA}_{0.85}\text{MA}_{0.15}\text{Pb}(\text{I}_{0.85}\text{Br}_{0.15})_3)$ PVK. With incorporation of KI, the electron transfer barrier between TiO_2/PVK is minimized, resulting in the elimination of J - V hysteresis and a PCE of more than 20%. Then after, Abdi-Jalebi et al.^[136] demonstrated that the KI fills the halide vacancies and acts as a passivation layer decorating the PVK surface and grain boundaries. As shown in Fig. 9C, the potassium-rich, halide-sequestering species at the grain boundaries and surfaces would inhibit halide migration and suppress any additional non-radiative decay arising from interstitial halides. They obtained a champion PCE of 21.5% with KI at ~9.09%, based on the $(\text{Cs,FA,MA})\text{Pb}(\text{I}_{0.85}\text{Br}_{0.15})_3$ PVK, with the elimination of PSC hysteresis. A series of alkali metal iodides of LiI, NaI, KI, RbI and CsI were introduced into PVK films by Cao et al.^[143]. They demonstrated that alkali cations can occupy the interstitial sites of the PVK lattice and suppress ion migration, which results in elimination of J - V hysteresis and enhancement of photostability of PSCs. On the other hand, Son et al.^[137] found from DFT calculation that the hysteresis of PVK solar cells arises from the formation of iodide Frenkel defect not the migration of iodide vacancy. They compared the effect of adding alkali metal iodides (LiI, NaI, KI, RbI and CsI) in PVK material on reducing current–voltage hysteresis. KI was found the best candidate for preventing the formation of iodide Frenkel defect, because K interstitials are energetically the most stables. As a result, they prepared mixed PVK $(\text{FA}_{0.875}\text{MA}_{0.125}\text{PbI}_{2.55}\text{Br}_{0.45})$ based PSCs with complete removal of hysteresis (Fig. 9D). Meanwhile, the alkali halide additive is able to homogenize the halide distribution, which help for the formation of uniform and continuous PVK film, leading to hysteresis-free PSCs with improved performance.^[144, 145]

3.5 Pseudo-halides additives for PVK films

Pseudo-halides, such as thiocyanate (SCN^-) or cyanide (CN^-) have similar chemical behaviors and properties to halogen. The ionic radii of thiocyanate (SCN^-) is ~217 pm, which is close to the iodine ionic radius of 220

Cite this paper as: F. Cheng, J. Zhu, Th. Pauporté, Chlorides, other Halides and Pseudohalides as Additives for the Fabrication of Efficient and Stable Perovskite Solar Cells. ChemSusChem 14 (2021) 3665–3692. DOI: 10.1002/cssc.202101089

pm and is expected to act as a substitute of halogen atoms in halide PVK.^[146-148] To date, various pseudo-halide, such as Pb(SCN)₂, NH₄SCN and MASCN, have been incorporated into PVK film to adjust the PVK crystal nucleation and growth process and passivate the crystal defects, effectively enhancing the performance of PSCs.

The incorporation of pseudo-halide in the PVK layer can improve the grain size, material crystallinity and optical properties of PVK layers.^[149] In 2015, Halder et al.^[146] reported that the incorporation of pseudo-halide in MAPbI₃ can increase the optical bandgap up to ~80 meV, and gives rise to a remarkable improvement in the photoluminescence (PL) emission quantum yield. Chen et al.^[150] reported the two-step preparation of CH₃NH₃PbI_{3-x}(SCN)_x PVK via adding a small amount of Pb(SCN)₂ into PbI₂ solution. They revealed that the CH₃NH₃PbI_{3-x}(SCN)_x with optimized 5 wt% Pb(SCN)₂ leads notably to stronger absorption at 400-625 nm. In addition, Zhou et al.^[151] compared several preparation routes for investigating the effect of Pb(SCN)₂ on the performance of PVK film (Fig. 10A). The Cs_{0.17}FA_{0.83}PbI_{3-x}Br_x (x=0.8) films deposited by the direct spin-coating of Cs_{0.17}FA_{0.83}PbI_{3-x}Br_x from (CsI)_{0.17}(FAI)_{0.83}(PbI₂)_{1-0.5x}(PbBr₂)_{0.5x} (precursor solution A) exhibited small grains and low crystallinity (Route 1). Then, they added 5 vol.% of Pb(SCN)₂ solution into solution A (Route 2). It led to increased grain size and crystallinity but PbX₂ (X = I and Br) impurity byproduct segregated randomly at the grain boundaries. Accordingly, they deposited PVK from (CsI)_{0.17}(FAI)_{0.83}(Pb(SCN)₂ + 2FAI)_{0.6}(Pb(SCN)₂ + 2FABr)_{0.4} (precursor solution C), in which the molar ratio FAX: Pb(SCN)₂ = 2:1. It resulted in a film with large grain size and high crystallinity without PbX₂. Since the excess of MAX can passivate the defects, solution B but with higher FAX: Pb(SCN)₂ ratio to 3:1 (route 4) was used to deposit PVK film. Highly crystallized and large grain ~1300 nm PVK (Fig. 10A) was obtained by this Route 4. With the synergistic effects of Pb(SCN)₂ assisted crystallization and FAX grain boundary healing, the well-passivated PSC showed greatly reduced hysteresis and excellent photovoltaic performance.

Pb(SCN)₂ affects the reaction between PbI₂ and MAI, leading to the PbI₂ residual in the PVK films. PbI₂ is an undesirable byproduct that can be detected in the PVK film and which is detrimental for the stability of PSC. Yu et al.^[152] developed an efficient strategy combining Pb(SCN)₂ additive (1.0 mol % Pb(SCN)₂) and a solvent annealing process to get large PVK grain size and avoiding PbI₂ excess formation (Fig. 10B). As a result, the average grain size of wide-bandgap FA_{0.8}Cs_{0.2}Pb(I_{0.7}Br_{0.3})₃ PVK thin films ($E_g = 1.75$ eV) increased from 66 ± 24 to 1036 ± 317 nm, and the mean carrier lifetime increased by more than 3-fold, from 330 to over 1000 ns. Kim et al.^[153] developed (FA_{0.65}MA_{0.20}Cs_{0.15})Pb(I_{0.8}Br_{0.2})₃ PSCs with an PCE of ~20% by using PEAI and Pb(SCN)₂ as additives. The cooperation of PEA⁺ and SCN⁻ provided a synergistic effect that enhanced

Cite this paper as: F. Cheng, J. Zhu, Th. Pauporté, Chlorides, other Halides and Pseudohalides as Additives for the Fabrication of Efficient and Stable Perovskite Solar Cells. ChemSusChem 14 (2021) 3665–3692. DOI: 10.1002/cssc.202101089

PVK morphology and reduced PbI_2 formation. As a result, using both additives increased the charge-carrier mobility and lifetime of PVK to near $50 \text{ cm}^2 \text{ V}^{-1} \text{ s}^{-1}$ and $3 \mu\text{s}$, higher values than that of control samples. The average PCE of PSCs increased from 16.3% to 18.7%.

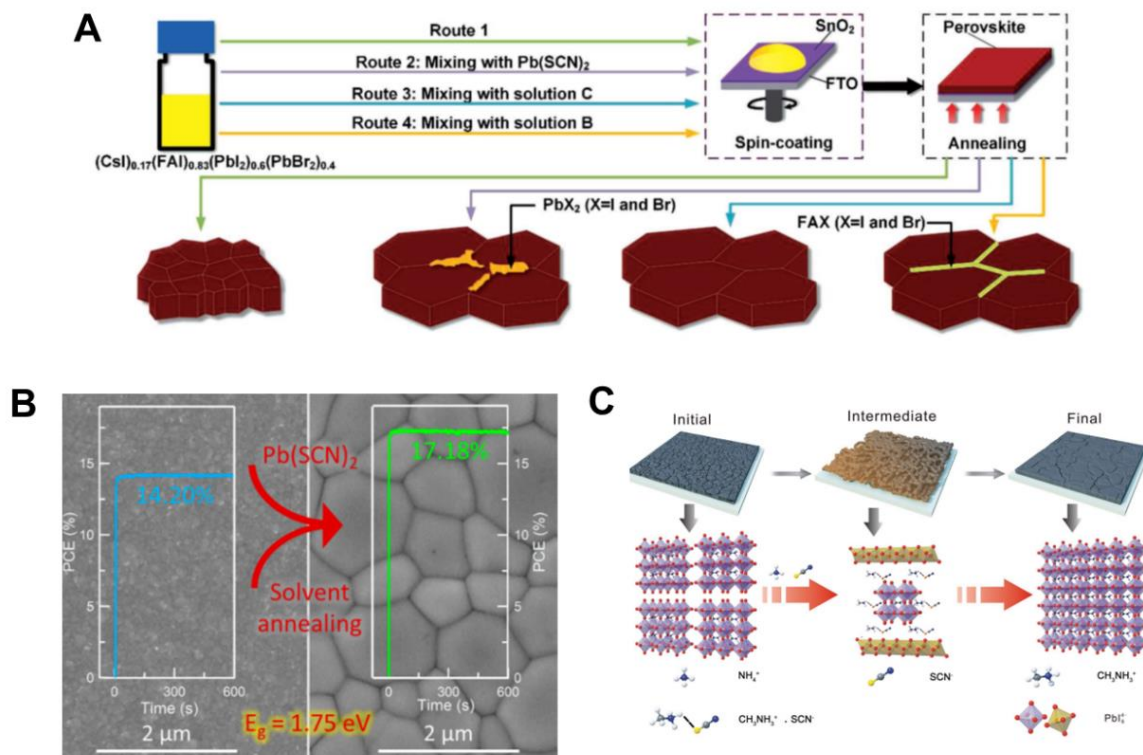


Fig. 10 (A) Schematics of different routes to prepare the $\text{FA}_{0.17}\text{Cs}_{0.83}\text{PbI}_{3-x}\text{Br}_x$ ($x = 0.8$) PVK thin films.^[151] with permission from Wiley-VCH, copyright 2018. (B) SEM images of $\text{FA}_{0.8}\text{Cs}_{0.2}\text{Pb}(\text{I}_{0.7}\text{Br}_{0.3})_3$ PVK thin films before and after the synergistic effects of $\text{Pb}(\text{SCN})_2$ and solvent annealing process.^[152] with permission from the American Chemical Society, copyright 2017. (C) Schematic diagram of the recrystallization process: morphological evaluation and structure dynamic process of the $\text{CH}_3\text{NH}_3\text{PbI}_3$ film with NH_4SCN treatment.^[154] with permission from Wiley-VCH, copyright 2017.

In addition to $\text{Pb}(\text{SCN})_2$, volatile additives such as NH_4SCN and MASCN have also been adopted to improve the crystallinity of PVK films and enhance cells performance.^[154, 155] Dong et al.^[154] demonstrated a NH_4SCN -induced recrystallization process (Fig. 10C) through an antisolvent method for improving the morphology and crystalline quality of the PVK film. First, when the prepared MAPbI_3 (Initial film) was dipped into NH_4SCN in IPA solution, it was partially dissolved and formed the mesoporous framework (Intermediate film) with PbI_2 compound. Since SCN^- has a stronger ionic bonding with CH_3NH_3^+ than I^- , CH_3NH_3^+ is preferred to form ionic bonding with SCN^- than I^- in this intermediate state (Equation 2). Upon the annealing process, the formed NH_3 and HSCN volatilized quickly (Equation 3). Subsequently, the undissolved polycrystal could play the role of

Cite this paper as: F. Cheng, J. Zhu, Th. Pauporté, Chlorides, other Halides and Pseudohalides as Additives for the Fabrication of Efficient and Stable Perovskite Solar Cells. ChemSusChem 14 (2021) 3665–3692. DOI: 10.1002/cssc.202101089

nucleus for the recrystallization process, new well-crystallized MAPbI₃ (Final film) was formed and PbI₂ impurity disappeared (Equation 4).



As a result, MAPbI₃ prepared through such intermediate catalytic effect of NH₄SCN exhibited large crystal grain sizes, as well as lower trap density, leading to a higher PCE of 19.44%. NH₄SCN additive strategy was also used in Cs-based and Sn-based PVK films for improving the crystallinity, stability and oxidation resistance in air atmosphere, promoting charge transfer and performances of devices.^[156, 157]

Zhang et al.^[158] employed ammonium thiocyanate (NH₄SCN) as additive for the preparation of MAPbX₃ layers. This compound was the most efficient at 15 mol% in the PPS and provided better benefits compared to NH₄I or Pb(SCN)₂ additives. They showed a synergistic effect of both cation and anion for the control of the nucleation and growth of the perovskite layer which gave rise to bigger grains and more stable layers. The final composition of the layer was MAPbI_{3-x}SCN_x and these authors showed the formation of the NH₄PbI_{3-x}SCN_x intermediate, more stable than the MAPbI₃ one. It induces less defects and slow down the rate of crystallization. They have also linked the good stability of MAPbI_{3-x}SCN_x with the linear shape of SCN⁻ ions, strongly coordinated with Pb²⁺ ions.

The list of the main other halides and pseudo-halides employed as additives for PSC, the cell structure, PCEs and *J-V* curve parameters are gathered in the Table 4.

We have reported that fluoride species can form strong ionic and intermolecular bonding with PVK, which is beneficial for passivating surface and crystal boundaries defects. They can endow the surfaces with hydrophobic properties and then protect the PVK from moisture erosion. In lead-free PVK, SnF₂ can suppress the oxidation from Sn²⁺ to Sn⁴⁺, reducing the background carrier density and Sn defects for improving the performance of Sn-based PSCs. Bromide additives can broaden the band gap of PVK, control the PVK growth to get large grains. They passivate grain boundaries, passivate defects related to Sn²⁺ oxidation. It results in longer lifetimes, improve stability. Iodide additives act as candidates for preventing the formation of iodide Frenkel defect, forming uniform and continuous PVK film and leading to hysteresis-free PSCs with improved performances. Regarding pseudo-halides, they can act as a substitute of halogen atoms in the halide PVK, and the incorporation of pseudo-halide can improve the grain size, material crystallinity and optical properties of PVK layers.

Cite this paper as: F. Cheng, J. Zhu, Th. Pauporté, Chlorides, other Halides and Pseudohalides as Additives for the Fabrication of Efficient and Stable Perovskite Solar Cells. ChemSusChem 14 (2021) 3665–3692. DOI: 10.1002/cssc.202101089

Cite this paper as: F. Cheng, J. Zhu, Th. Pauporté, Chlorides, other Halides and Pseudohalides as Additives for the Fabrication of Efficient and Stable Perovskite Solar Cells.

ChemSusChem 14 (2021) 3665–3692. DOI: 10.1002/cssc.202101089

Table 4. Other halides and pseudo-halides additives used in PVK, concentration, cell structure, PCE and J-V curve parameters.

Other halides and pseudo-halides additives in the bulk	Concentration	Device structure	PCE (%)	J _{sc} (mA.cm ⁻²)	V _{oc} (V)	FF (%)	Year ^{Ref.}
SnF ₂	20 mol%	FTO/TiO ₂ /MASnI ₃ /PTAA/Au	1.94	26.1	0.25	30.00	2017 ^[100]
SnF ₂ -Pyrazine	20 mol%	FTO/TiO ₂ /FASnI ₃ /Spiro-OMeTAD/Au	4.00	24.5	0.29	55.00	2016 ^[103]
NaF	0.1 mol%	ITO/SnO ₂ /(Cs _{0.05} FA _{0.54} MA _{0.41})Pb(I _{0.98} Br _{0.02}) ₃ /spiro-OMeTAD/	21.92	24.23	1.126	80.35	2019 ^[105]
NbF ₅	3 mg.mL ⁻¹	FTO/TiO ₂ /PVK(NbF ₅)/PCBM/Ag	20.56	25.4	1.05	77.08	2019 ^[106]
guanidinium bromide (GABr)	12 mol%	ITO/EMIC-PEDOT:PSS/FA _{0.7} MA _{0.3} Pb _{0.7} Sn _{0.3} I ₃ /S-acetylthiocholine chloride passivation layer /C60/BCP/Ag	20.63	26.61	1.02	76.00	2020 ^[119]
N-(4-bromophenyl)-thiourea (BrPh-ThR)	0.6 mg.mL ⁻¹	FTO/TiO ₂ /(FAI) _{0.81} (PbI ₂) _{0.85} (MABr) _{0.15} (PbBr ₂) _{0.15} /Spiro-OMeTAD/Au	21.7	23.93	1.12	78.00	2018 ^[120]
RbI; CsI	5 mol%; 5 mol%	FTO/TiO ₂ /(MAPbBr ₃) _{0.17} (FAPbI ₃) _{0.83} /Spiro-OMeTAD/Au	19	22.7	1.1	76.00	2019 ^[145]
ethylenediammonium diiodide	1 mol%	ITO/PEDOT:PSS/FASnI ₃ /C60 /BCP/Ag	8.9	21.3	0.583	71.80	2018 ^[159]
MASCN	40 mol%	FTO/TiO ₂ /MAPbI ₃ /Spiro-OMeTAD/Au	18.22	23.2	1.064	76.94	2017 ^[155]
PEAI; Pb(SCN) ₂	1 mol%; 2 mol%	ITO/PTAA/(FA _{0.65} MA _{0.20} Cs _{0.15})Pb(I _{0.8} Br _{0.2}) ₃ /C60/BCP/Ag	19.8	21.2	1.17	79.80	2019 ^[153]
FASCN; PEA	5 mol%; 10 mol%	ITO/PEDOT:PSS/FASnI ₃ /PCBM/Al	8.17	22.5	0.53	68.30	2018 ^[160]
Pb(SCN) ₂	2 mol%	FTO/PEALD SnO ₂ /C60-SAM/(MA _{0.7} FA _{0.3} PbI ₃) _{1-x} (CsPbI ₃) _x /spiro-OMeTAD/Au	20.49	23.05	1.11	80.09	2018 ^[161]
GuaSCN	7 mol%	ITO/PEDOT:PSS/(FASnI ₃) _{0.6} (MAPbI ₃) _{0.4} /C60/bathocuproine/Ag	18.7	28.7	0.82	79.00	2019 ^[118]
NH ₄ SCN	1.5 mol%	ITO/TiO ₂ /CsPbBr ₃ /Spiro-OMeTAD/Au	8.47	7.76	1.375	79.31	2020 ^[156]
NH ₄ SCN	0.03 M.mL ⁻¹	ITO/PTAA/CH ₃ NH ₃ PbI ₃ /PCBM/BCP/Ag	19.44	22.55	1.103	78.20	2017 ^[154]
NH ₄ SCN	15 mol%	ITO/PEDOT:PSS/ MAPbI _{3-x} SCN _x /PC61BM/LiF/Al	16.47	23.31	0.96	73.84	2018 ^[158]
Pb(SCN) ₂	2 mol%	FTO/TiO ₂ /CsPbI ₃ /PTAA/Au	17.03	20.34	1.09	77.00	2019 ^[162]

4. Halides at the interfaces of PSCs

The ETL/PVK and HTL/PVK interfaces play a critical role on the performances of PSCs. They must be engineered to improve the PSC characteristics. Especially, interfacial modification is key to passivate the defects of metallic oxide ETL and PVK, improving the charge transfer and reducing the charge recombination. Moreover, they can induce PVK crystal modification, adjustment of the energy-level alignment and the stabilization of the PVK towards UV-light, humidity and oxygen degrading agents. Normally, the modification is obtained by adding the halide additive into the charge carrier precursor solution, spin-coating halide additive solution onto the charge carrier layers or by soaking the well-formed layer in an additive solution.

4.1 Introduction of halogen atoms at the ETL/PVK interface

Chlorine serves as contact passivator to mitigate the interfacial recombination. Defects at the ETL/PVK interface and induces charge recombination which has a negative effect on the performance and stability of PSCs and that must be addressed by passivating the surface of active layers. Tan et al.^[163] employed chlorine-capped TiO₂ colloidal nanocrystal to suppress TiO₂ deep trap states and reduce the interface recombination at the TiO₂/PVK contact. DFT calculation showed that Cl at the interface results in a lower density of interfacial trap states, as well as in a stronger binding of PVK to TiO₂ interface. As a result, the hysteresis-free planar PSCs with champion PCE of 20.1% for small-area devices (0.049 cm²) was obtained. F doping of SnO₂ was used to adjust the Fermi level of ETL.^[164] The device V_{oc} could be tailored by modulating the band offset at the interface of ETL and PVK. The grain boundary barriers and defects within the bilayer ETL could be largely restrained due to a matched lattice constant.

4.2 Halides at the ETL/PVK interface

Organic monolayer on ETL surface have been introduced to enhance the interfacial optoelectronic properties of PSCs. The metallic oxide and PVK can undergo chemical interaction with organic molecules, which can improve the PVK film quality and promote the electron extraction while

Cite this paper as: F. Cheng, J. Zhu, Th. Pauporté, Chlorides, other Halides and Pseudohalides as Additives for the Fabrication of Efficient and Stable Perovskite Solar Cells. ChemSusChem 14 (2021) 3665–3692. DOI: 10.1002/cssc.202101089

restricting the charge recombination between ETL and PVK. With this motivation, organic small molecular materials have been used for interfacial modification such as benzoic acid derivatives onto the TiO₂ in PSCs.^[165] Pauporté et al.^[166] investigated the effect of self-assembled monolayers (SAMs) prepared by spin-coating benzoic acid derivatives onto the TiO₂ of PSCs. As shown in Fig. 11A, a series of organic compounds with benzene and various terminal groups were tested (Cl, NO, Br, O-CH₃, NH₂) and compared to β-alanine, an amino acid. The –COO anchoring group passivates the ETL surface via chemical bonding. The best functional group was found to be Cl (CBA) with a stabilized PCE reaching 20.9% (20.0% for the pristine cell). The para-Cl group can establish a stable bonding with the PVK. The presence of this monolayer decreased interfacial trap states, improved the global PVK quality and created a structural continuity between TiO₂ and PVK. This system was further studied by DFT^[167] that showed the bonding between Cl and Pb of the PVK (Fig. 11B). The computed density of states revealed that the PVK (MAPbI₃ employed as a model PVK) contributes to the top of the valence band while TiO₂ ETM contributes to the bottom of the conduction band. It indicated that an electron transfer from MAPbI₃ to TiO₂ is possible. Furthermore, these authors quantified the spin density of the reduced MAPbI₃/CBA/TiO₂ system and calculated a quantitative (99.94%) electron transfer from MAPbI₃ to TiO₂ to the interfacial engineering. They have also calculated an ultrafast electron injection time at 24 fs, and the dipole moment of 0.61 D induced by CBA at the interface which is favorable for the charge transfer from MAPbI₃ to TiO₂.

Introducing inorganic metal halide materials at the ETL/PVK interface can adjust the band alignment, passivate the surface trap states and suppress the recombination process. As shown in Fig. 11C, p-type CuI on TiO₂ surface was used to modify the TiO₂ band alignment by shifting the conduction band bottom from -4.13eV to -3.93eV. It resulted in a barrier-free contact and an increased open-circuit voltage. Meanwhile, the polarity of the CuI-modified TiO₂ surface was favorable to pull electrons from PVK to the interface of ETL/PVK, improving electron extraction and reducing nonradiative recombination.^[168] In a similar manner, inorganic alkaline halide was used to passivate ionic defects with their cations and anions. Li et al.^[169] introduced CsBr onto the compact c-TiO₂ surface in planar heterojunction solar cells, which reduced the pinholes density and resulted in the shifts of work function of TiO₂ from 4.07 to 3.09 eV. Such CsBr surface modification enhanced the electron transfer and the stability of planar heterojunction devices under ultraviolet (UV) light soaking. It is reported that alkaline halides can

Cite this paper as: F. Cheng, J. Zhu, Th. Pauporté, Chlorides, other Halides and Pseudohalides as Additives for the Fabrication of Efficient and Stable Perovskite Solar Cells. ChemSusChem 14 (2021) 3665–3692. DOI: 10.1002/cssc.202101089

passivate both types of charged defects (positive and negative) with alkaline cation and halide anion. Yuan et al.^[170] demonstrated the interfacial passivation effect of LiF at the SnO₂/PVK interface (Fig. 11D). The intermediate layer of LiF effectively blocks holes and promotes the electron transport. In order to identify the interfacial passivation by Li⁺ and F⁻, devices with PbF₂ (F⁻ only) or LiTFSI (Li⁺ only) modified layer were fabricated. It was found that F⁻ ion play a main role in the device performance improvement. Hysteresis-less planar PSCs with a PCE of 18.3% were fabricated by Ma et al.^[171] via passivating the compact TiO₂/PVK interface with NaCl. They immersed the TiO₂ substrate in 0.5 mg.mL⁻¹ NaCl solution and then heated at 500 °C for 15 min. By varying light intensities from 0.1 to 100 mW cm⁻², the V_{oc} versus light intensity slope of the devices based on pristine TiO₂ and NaCl modified TiO₂ were 1.23 kT/q and 1.14 kT/q, respectively (where k is the Boltzmann constant, T is absolute temperature, and q is the elementary charge). It indicated that the doping treatment reduced the trap density at the TiO₂/PVK interface and improved the electrical property of TiO₂. To further understand the mechanism of charge transfer and recombination, transient photocurrent (TPC) under short-circuit condition and transient photovoltage (TPV) under open-circuit conditions measurements were performed. TPC decay lifetime was faster at 0.51 μs for TiO₂-NaCl while TPV exhibited a longer decay lifetime of 24.67 μs for TiO₂-NaCl. It indicated more efficient charge transfer, extraction process and efficient suppression of charge recombination, respectively. The hysteresis index was reduced from 12.6% to 2.7% after the doping treatment. The trap density of TiO₂ and TiO₂-NaCl measured by space charge limited current (SCLC) were 7.08×10¹⁶ cm⁻³ and 5.19×10¹⁶ cm⁻³, respectively. The electron mobility of TiO₂-NaCl increased to 7.20×10⁻⁴ cm²V⁻¹s⁻¹ compared to that of pristine TiO₂ (3.48×10⁻⁴ cm²V⁻¹s⁻¹). Finally, the film was more homogeneous after NaCl doping.

Jang et al.^[172] developed a deposition and diffusion method of alkaline chlorides onto ZnO ETL to effectively passivate both shallow and deep trap states, which were present in PVK crystallized layer and at the PVK/ETL interface. Dual trap passivation dramatically improved the PCE, reduced the photocurrent hysteresis, and enhanced the long-term stability of PSCs. The ZnO layers were modified by immersing them in aqueous alkaline chloride (LiCl, NaCl, KCl, CsCl), the reduction in defect-related PL emissions was the most prominent in the 10 mM KCl modified ZnO sample. Interfacial defect passivation was due to both K and Cl. As a result of time-correlated single-photon counting (TCSPC) analysis, the ZnO-KCl sample exhibited a substantially shorter decay time (2.73 ns). The charge

Cite this paper as: F. Cheng, J. Zhu, Th. Pauporté, Chlorides, other Halides and Pseudohalides as Additives for the Fabrication of Efficient and Stable Perovskite Solar Cells. ChemSusChem 14 (2021) 3665–3692. DOI: 10.1002/cssc.202101089

recombination lifetime and charge transport time of the modified PSCs were 204 μ s and 1.7 μ s, respectively. The average grain size of the KCl modified PVK sample was about 450 nm, whereas that of the unmodified sample was about 300 nm. TEM coupled with EDS mapping showed the penetration of K and Cl atoms throughout the PVK layers. The KCl modified low-temperature processed PSCs (L-PSC) achieved the highest PCE of 22.6%. With an active area of 1.12 cm², L-PSC-KCl reached 21.3%, which was one of the highest values among the reported L-PSCs with an active area of >1 cm² thus far. The long-term shelf-life of unencapsulated L-PSCs was tested following the ISOSD-1 protocol (in the dark, 25 °C, 40% humidity, in air).^[173] The L-PSC-KCl maintained 90% of its initial PCE after 1400 h. Moreover, Liu et al.^[174] also observed that the inorganic binary alkaline halide salts treatment of the SnO₂/PVK interface can significantly increase the open-circuit voltage and eliminate hysteresis.

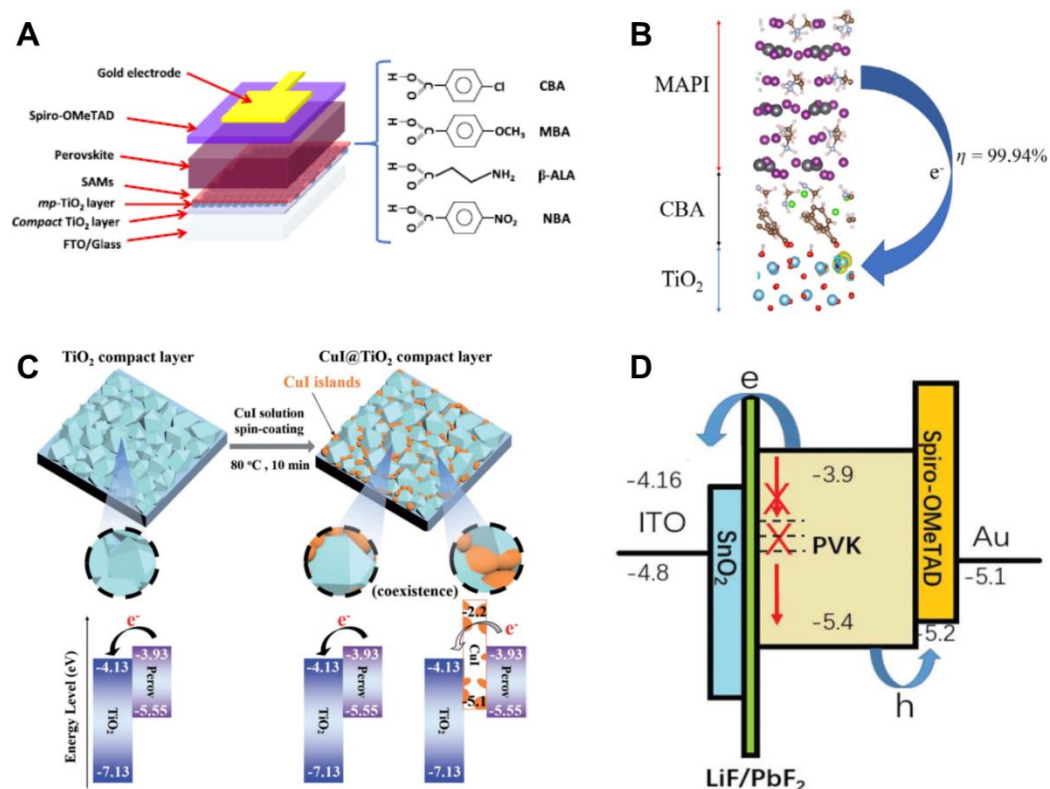


Fig. 11 (A) PSC cell structure and mesoporous *mp*-TiO₂ layer covered by SAMs (in red) of *para*-substituted benzoic acid derivatives and β -alanine.^[166] with permission from The American Chemical Society, copyright 2020. Spin density of the reduced MAPI-CBA-TiO₂ interface system and calculated charge injection efficiency.^[167] with permission from Wiley-VCH, copyright 2020. (C) Schematic illustration of the deposition of CuI on TiO₂ compact layer. In CuI@TiO₂-based devices, electrons transfer from PVK to exposed TiO₂ not CuI due to the high conduction band energy level of CuI.^[168] with permission from Wiley-VCH, copyright 2018 (D) Structure of the PSC with a thin layer of LiF or PbF₂ on SnO₂ layer.^[170] with permission from The Royal Society of Chemistry, copyright 2018.

4.3 PVK layer surface engineering

Due to the ionic nature of PVK materials, undesirable electronic defects and pinholes can be observed at the surface and grain boundaries of PVK layers. Such defects decrease the charge collection efficiency and increase the charge recombination during the photoelectric conversion process, the best performance of PSCs still lags behind the theoretical limit of Shockley–Queisser efficiency. Moreover, the crystal defects and uncoordinated ions at the surface and grain boundaries are supposed to affect the stability of PSCs. Thus, in order to develop the high-efficiency and stable PSCs, it is essential to passivate the crystal defects at the crystal surface and grain boundaries.

4.3.1 Hydrophobic organo-halogen at the surface of PVK

Some organic insulating tunneling layers consisting of hydrophobic groups can cover the surface of PVK film, suppressing carrier recombination and protecting the PVK from decomposition caused by moisture. The fluorinated organic compounds are known to be hydrophobic, and have been used to improve the stability of PVK by grafting on the surface of PVK crystals. Wang et al.^[175] chose a hydrophobic insulating fluoro-silane, trichloro(3,3,3-trifluoropropyl)silane, as a tunneling layer deposited on the top of MAPbI₃ PVK film to fabricate water-resistant devices (Fig. 12A). As shown in Fig. 12B, the silanes were hydroxylated to the silanols with tiny amount of H₂O. Then, they underwent a cross-linking by forming Si-O-Si bonds, this fluoro-silane insulating organic layer protected the underneath PVK films from water attack. Meanwhile, this tunneling layer spatially separated photogenerated electrons and holes at the PVK/polymer HTM interface. It reduced the carrier surface recombination and significantly increased the device performance. Considering the conductivity of fluorinated compounds, the conductive fluorinated perylenediimide (F-PDI) was introduced to fill in at grain boundaries and surface of the PVK film (Fig. 12C).^[176] The conductive F-PDI chemical bonding to PVK film effectively passivated defects and promoted the charge transport. Meanwhile, hydrogen bond formed between F-PDI and MA⁺ reduced the mobility of MA⁺ in the MAPbI₃ PVK and therefore improved the thermal and moisture stability. F-PDI-incorporated device based on the

Cite this paper as: F. Cheng, J. Zhu, Th. Pauporté, Chlorides, other Halides and Pseudohalides as Additives for the Fabrication of Efficient and Stable Perovskite Solar Cells. ChemSusChem 14 (2021) 3665–3692. DOI: 10.1002/cssc.202101089

(FA_{0.83}MA_{0.17})_{0.95}Pb(Br_{0.17}I_{0.83})₃ absorber showed champion efficiencies of 19.26%, and maintains 80% of its initial efficiency even after exposure to RH of 50% for 30 days. In another work, Wu et al.^[177] developed a CF₄ plasma treatment for fluorinating the whole PSC device. A strongly bonded C-F_x layer covered the top and lateral surface of PSCs, which exhibited an excellent water-repellent property, without any change after immersion into water for 5 min. Liu et al.^[178] introduced a two-dimensional (2D) A₂PbI₄ PVK layer using pentafluorophenylethylammonium (FEA) as a fluoroarene cation inserted between the 3D light-harvesting PVK film and the hole-transporting material (HTM). The perfluorinated benzene moiety conferred an ultra-hydrophobic character to the spacer layer, protecting the PVK material from ambient moisture while mitigating ionic diffusion in the device.

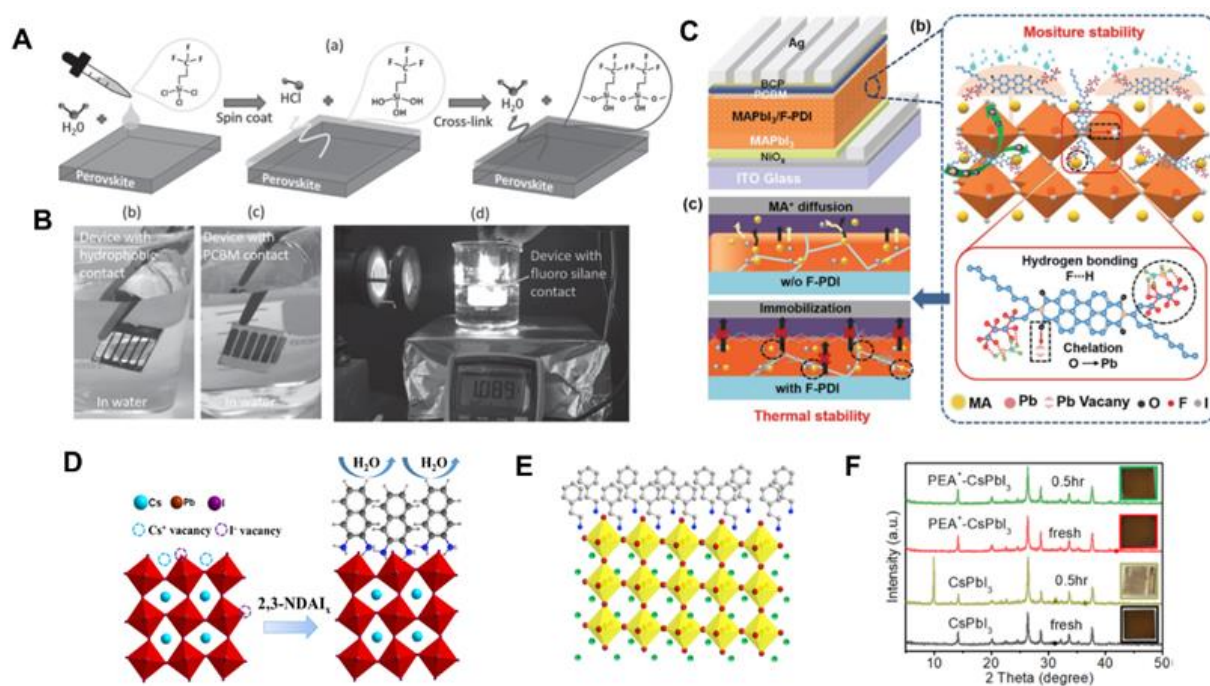


Fig. 12 (A) Schematic illustration for the cross-link process of fluoro-silane layer on the PVK film. (B) The humidity stability test for the PVK layers with and without fluoro-silane contact.^[175] with permission from Wiley-VCH, copyright 2016. (C) Schematic illustration of PSCs structure, the interactions between F-PDI and MAPbI₃ PVK.^[176] with permission from Wiley-VCH, copyright 2019. (D) Schematic illustration of defect passivation and water resistance effect with naphthalenediammonium iodide.^[191] with permission from The Royal Society of Chemistry, copyright 1996. (E) Schematic illustration of PEA⁺ cations at CsPbI₃ surface termination (F) XRD patterns and photographs of the CsPbI₃ and PEA⁺-CsPbI₃ thin films after exposed to ambient environment with 85%–90% RH at RT for 0.5 hr.^[179] with permission from Elsevier, copyright 2018.

4.3.2 Passivation of PVK defects and near surface film modification

It is known that the imperfections in hybrid perovskite could induce a large density of traps. There are three types of defects in the MAPbI₃: vacancies (V_{MA} , V_{Pb} , V_I), interstitials (MA_i , Pb_i , I_i) and antisite substitutions (MA_{Pb} , Pb_{MA} , MA_I , Pb_I , I_{MA} , I_{Pb}), where in the latter A_B indicates that A is substituted by B. The first-principles calculations are performed to investigate the electronic structure, dielectric properties and defect properties of perovskite. Buin et al.^[180] showed the origin of major sources of deep traps for the perovskite materials *via* analysis of defect aggregation in terms of defect binding energies with DFT calculations. They concluded that the halide vacancies are the major source of deep traps in Cl-based perovskite, while lead interstitials are the dominant source of defects in Br-based perovskites. M. H. Du^[181] calculated defects in MAPbI₃ and showed that iodine vacancy is a low energy deep trap and non-radiative recombination centre. Thus, alloying iodide with chloride can reduce the lattice constant of the iodide and increases the formation energy of interstitial defects. As mentioned above, excess of halide or using mixed halides approach can prevent the formation of deep energy level.

Contrary to organo-halogen molecules, halide compounds are often used to passivate Pb interstitial and halide vacancies. Ammonium derivative halide salts are popular passivators that can reduce the cation and anion defects at PVK/HTL interface through hydrogen bonding or ionic bonding with PVK bulk. Until now, PTN-Br,^[182] MAI,^[183] FABr,^[184] phenyltrimethylammonium bromide (PTABr),^[185] imidazolium iodide (IAI),^[186] ethylammonium iodide (EAI),^[187] guanidinium hydroiodide (GAI),^[188] NH₄F,^[189] Phenylhydrazinium iodide (PHAI),^[190] Phenylethylammonium iodide (PEAI),^[67] Naphthalenediammonium (2,3-NDA^{x+}),^[191] 5-Ammonium valeric acid iodide (5-AVAI),^[192] n-propylammonium iodide (PAI) and propane-1,3-diammonium iodide (PDAI₂)^[67] have been notably inserted between PVK/HTL interface to passivate defects and to accelerate the carrier transfer to the contact and to reduce the recombination in devices. Among those, PTABr on CsPbI₃ only induces a less than 5 nm blue shift in UV–vis absorbance, while the gradient of Br doping on the surface enhances the phase stability and significantly improves the stability of PSCs.^[185] Wang et al.^[193] reported that choline iodide (CHI) treatment of CsPbI₃ increases the charge carrier and improves the energy-level alignment of PVK/ETL interface by 120 mV. PCE of CHI-modified PSCs reached 18.4%. Zhang et al.^[191] introduced the π -conjugated naphthalenediammonium onto the surface of CsPbI₃ PVK film *via*

Cite this paper as: F. Cheng, J. Zhu, Th. Pauporté, Chlorides, other Halides and Pseudohalides as Additives for the Fabrication of Efficient and Stable Perovskite Solar Cells. ChemSusChem 14 (2021) 3665–3692. DOI: 10.1002/cssc.202101089

anchoring ammonium groups occupying A-site vacancies (**Fig. 12D**). This strategy largely improved humidity stability of CsPbI₃ PVK film and gave highly reproducible inorganic PSCs with a champion stabilized efficiency of 16.69% and a V_{oc} of 1.08V. Zheng et al.^[194] reported that choline zwitterions, such as L-a-phosphatidylcholine, choline chloride and choline iodide, can effectively passivate ionic defects in hybrid PVK with their negative- and positive-charged components. This defect passivation reduced the open-circuit-voltage deficit of PSCs to 0.39V, boosted the PCE up to 20.66 % and enhanced the stability of films in ambient conditions. However, the mechanism of passivation effect with organic halide salts is not clear.

For the organic-inorganic hybrid PVK, a thin layer of 2D PVK can be formed on top of 3D PVK after post-treatment with an isopropyl alcohol (IPA) solution containing bulky organic cations ammonium. In this case, IPA partly dissolves the organic cation and favors the generation of a surface layer.^[67] This layer improves the interface between the PVK and the HTL. PEAI has attracted much attention for the passivation of the PVK grain boundaries and surfaces in several studies.^[67, 195] You et al.^[37] found that PEAI itself can effectively passivate the PVK defects and therefore improves the efficiency of the devices. PEAI can also form a (PEA)₂PbI₄ 2D PVK layer after reaction with I and Pb sources.^[156] Pauporté et al.^[67] employed PEAI to treat FA_{0.94}MA_{0.06}PbI₃ PVK layers. They showed that this treatment, without any thermal annealing, leads to the spontaneous formation of a crystallized (PEA)₂PbI₄ 2D PVK nanolayer at the PVK film surface due to partial organic cation dissolution. It favored a fast transfer of photogenerated holes toward the HTL and reduced the recombination at and near the PVK/HTL interface in PSCs. The solar cell PCE was improved from 20.4% to 22.2% and the hysteresis became negligible. However, the reaction of PEAI seems to depend on the type of PVK. Actually, Wang et al.^[179] demonstrated that CsPbI₃ could not cation exchange with PEAI to form 2D PVK layer, the PEAI on the CsPbI₃ layer just formed a surface termination layer (**Fig. 12E**), which enhanced phase stability and moisture resistance (**Fig. 12F**). Li et al.^[197] investigated the surface treatment of methylammonium-free PVK layers by PAI and propane-1,3-diammonium (PDA) iodide. They observed a boosting of the PCE and an improvement of the solar cell stability for both treatments compared to the untreated PVK layer. Exceptional thermal and humidity stabilities were attained with PDA.

Hybrid 3D/2D PVKs possess longer carrier lifetimes and lower defect densities.^[198, 199] Chen et al.^[192] prepared a versatile ultrathin 2D PVK (5-AVA)₂PbI₄ layer by spin-coating 5-AVAI solution on the

Cite this paper as: F. Cheng, J. Zhu, Th. Pauporté, Chlorides, other Halides and Pseudohalides as Additives for the Fabrication of Efficient and Stable Perovskite Solar Cells. ChemSusChem 14 (2021) 3665–3692. DOI: 10.1002/cssc.202101089

(FAPbI₃)_{0.88}(CsPbBr₃)_{0.12}, which suppressed ion migration and improved interfacial charge extraction efficiency. Meanwhile, 5-AVA-modified devices showed enhanced moisture stability and photostability due to the excellent moisture stability of hydrophobic nature of interfacial 2D layer. So far, many ammonium halide salts such as n-hexyl trimethyl ammoniumbromide,^[200] n-hexylammonium bromide,^[201] cyclopropylammonium iodide,^[202] alkyl ammonium bromides,^[203] diethylenetriamine^[204] have been employed to construct 2D PVK layer between PVK and HTL interface for improving performances of PSCs.

4.4 HTL surface engineering

HTLs play a key role in extracting and transporting the holes in the photoconversion process of PSCs. Among a variety of HTMs, organic poly(bis(4-phenyl)-(2,4,6-trimethylphenyl)amine) (PTAA), 2,2',7,7'-tetrakis(N,N-di(4-methoxyphenyl)amino)-9,9'-spirobifluorene (Spiro-MeOTAD) and inorganic NiO_x, CuSCN are the most common. In order to achieve high performance of PSCs, considerable efforts, *i.e.* additives, interface treatment, new materials have been successfully made to enhance energy alignment at HTL interface, thermal/photochemical stability, hole mobility and electrical conductivity of HTLs.

Modified HTLs materials with organo-halogen molecular doping is an efficient strategy to increase the performances of PSCs. Chen et al.^[205] reported a doping approach to tailor the optoelectronic properties of HTL by spin-coating an acetonitrile solution of 2,2'-(perfluoronaphthalene-2,6-diylidene)dimalononitrile (F6TCNNQ) onto the NiO_x. The F6TCNNQ doping increased Fermi level of NiO_x HTLs from -4.63 eV to -5.07 eV, and reduced the valence band maximum from 0.58 eV to 0.29 eV, leading to an increase in champion PCE of CsFAMA mixed cations and MAPbI₃-based devices to 20.86% and 19.75%, respectively. Alkali halide were introduced as interlayer between HTL/PVK to manipulate the properties of PVK and improve the performance of inverted PSCs. Chen et al.^[206] reported a facial strategy for suppressing interfacial recombination by alkali chloride interface modification of NiO_x HTL surface. They revealed that alkali chloride interface modification results in improved properties of CsFAMA-based PVK and reduced interfacial recombination owing to the interface contact healing by halide elements. Finally, this KCl-doping strategy led to a significant improvement in the V_{oc} from 1.07 eV for pristine NiO_x to 1.15 eV for KCl-treated NiO_x, resulting in a

Cite this paper as: F. Cheng, J. Zhu, Th. Pauporté, Chlorides, other Halides and Pseudohalides as Additives for the Fabrication of Efficient and Stable Perovskite Solar Cells. ChemSusChem 14 (2021) 3665–3692. DOI: 10.1002/cssc.202101089

power conversion efficiency approaching 21%. Moreover, the PVK deposited on the alkali halide modified NiO_x layer exhibited lower rates of ion migration, showing improved device stability.

In conclusion, we have shown that halides compounds are also employed at the interface of ETL/PVK and PVK/HTL, suppressing the defects of ETL and PVK, improving the charge transfer and reducing the charge recombination. Meanwhile, modification of interfaces of PSCs improves the PVK crystallinity, energy-level alignment and the stabilization of the PSCs against UV-light, humidity and oxygen degrading agents.

Conclusion and Outlook

PSCs have attracted special attentions due to their excellent power conversion efficiency, low cost and great promise for the future of solar energy. The best PSC has already achieved a certified PCE of 25.5% after an unprecedented rapid performance rise. However, high requirement with respect to large area high efficiency devices and stability are still the challenge and focuses major efforts on the PSC research. The primary requirement to achieve high efficiency and stable devices is to understand in great depth the optoelectronic loss mechanism for the devices and the degradation mechanism of individual layers in PSCs. Although various mechanisms still need to be explored, the bulk and surface trap states and large numbers of grain boundaries are the main reasons reported up to now affecting the performances of PSCs. To overcome the bulk and surface trap states, one of the ways is additive/compositional engineering in the PVK bulk. On the other hand, interfacial modifications to form proper capping/buffer layer or charge transport layer are considered as effective strategies to improve stability and efficiency of PSCs.

Herein, we have given an in-depth review of the various strategies and halide/pseudo-halide compounds employed as additives for films and interfaces quality improvements. If many experimental works have been implemented and analyzed throughout the paper, the exact role of these additive should be rationalized. Developing modelling and theoretical works could help the understanding.

Halide additives-engineered PVKs have been proved as an effective approach to passivate the defects in the PVK bulk and interfaces, reducing energy loss and improving the performance of PSCs. However, complete understanding of passivation mechanism and PVK crystallization process has yet to be totally resolved, due to the limited characterization technique for the defect types and density in different PVK

Cite this paper as: F. Cheng, J. Zhu, Th. Pauporté, Chlorides, other Halides and Pseudohalides as Additives for the Fabrication of Efficient and Stable Perovskite Solar Cells. *ChemSusChem* 14 (2021) 3665–3692. DOI: 10.1002/cssc.202101089

materials. It renders difficult to guide the design of efficient additives and achieve universal efficient passivation strategy. Thus, a further understanding of passivation mechanism through characterizing the traps types and concentration at the PVK surface and grain boundaries, as well as revealing the role of additives on the PVK crystallization process will be crucial for highly efficient and stable PSCs. New techniques to understand the crystallization mechanism and growth direction of the crystals in the layer must be developed. Developing double (or more) mixed halide additive is of high interest and must be developed to achieve multiple and synergistic beneficial effects (phase purity, better crystallinity, grain boundaries reduction, defect passivation, monolithic morphology...).

Concerning the PVK surface treatment by halide compounds, it will be necessary to better control the properties of the produced interfacial layers including their thickness and their chemical composition. An in-depth understanding of why the treatment with a halide compound is beneficial with a PVK and not with another is required and give an important research direction for future works. Halide additives in charge carrier layers have mainly been used in inorganic materials. A further understanding if their effects are bulk or near-interface related is still necessary and give another important research direction for the future. For the testing of the device stability, standardized aging tests should be implemented on the perovskites and devices implementing halide/pseudo-halide additives. The objective should be to meet stability standards of IEC61215:2016 qualification tests, for instance, a target that would necessitate to encapsulate tightly and efficiently the solar cells.

Acknowledgements

Dr. Jie Zhang acknowledges the program for the Guangdong Basic and Applied Basic Research Foundation (2020A1515010378), the Science and Technology Program of Guangzhou (201804010176), the Fundamental Research Funds for the Central Universities (2019MS049) and the NSFC (21703070) for financial support. Prof. Thierry Pauporté acknowledges the French research Agency (ANR) for financial support via the Moreless project ANR-18-CE05-0026.

References:

- [1] J. H. Im, C. R. Lee, J. W. Lee, S. W. Park, N. G. Park, *Nanoscale* **2011**, 3, 4088-4093.

Cite this paper as: F. Cheng, J. Zhu, Th. Pauporté, Chlorides, other Halides and Pseudohalides as Additives for the Fabrication of Efficient and Stable Perovskite Solar Cells. ChemSusChem 14 (2021) 3665–3692. DOI: 10.1002/cssc.202101089

- [2] H. P. Zhou, Q. Chen, G. Li, S. Luo, T. B. Song, H. S. Duan, Z. R. Hong, J. B. You, Y. S. Liu, Y. Yang, *Science* **2014**, *345*, 542-546.
- [3] A. Mei, X. Li, L. Liu, Z. Ku, T. Liu, Y. Rong, M. Xu, M. Hu, J. Chen, Y. Yang, M. Graetzel, H. Han, *Science* **2014**, *345*, 295-298.
- [4] W.-J. Yin, J.-H. Yang, J. Kang, Y. Yan, S.-H. Wei, *J. Mater. Chem. A* **2015**, *3*, 8926-8942.
- [5] N.-G. Park, *Mater. Today* **2015**, *18*, 65-72.
- [6] M. A. Green, A. Ho-Baillie, H. J. Snaith, *Nat. Photonics* **2014**, *8*, 506-514.
- [7] W. J. Yin, T. Shi, Y. Yan, *Adv. Mater.* **2014**, *26*, 4653-4658.
- [8] C. C. Stoumpos, C. D. Malliakas, M. G. Kanatzidis, *Inorg. Chem.* **2013**, *52*, 9019-9038.
- [9] S. D. Stranks, G. E. Eperon, G. Grancini, C. Menelaou, M. J. P. Alcocer, T. Leijtens, L. M. Herz, A. Petrozza, H. J. Snaith, *Science* **2013**, *342*, 341-344.
- [10] R. J. Sutton, G. E. Eperon, L. Miranda, E. S. Parrott, B. A. Kamino, J. B. Patel, M. T. Hrantner, M. B. Johnston, A. A. Haghighirad, D. T. Moore, *Adv. Energy Mater.* **2016**, *6*, 1502458.
- [11] J. Zhang, P. Barboux, T. Pauporté, *Adv. Energy Mater.* **2014**, *4*, 1400932.
- [12] J. Zhang, E. J. Juárez-Pérez, I. Mora-Seró, B. Viana, T. Pauporté, *J. Mater. Chem. A* **2015**, *3*, 4909-4915.
- [13] J. Zhang, T. Pauporté, *J. Phys. Chem. C* **2015**, *119*, 14919–14928.
- [14] M. Ulfa, P. Wang, J. Zhang, J. Liu, W. D. de Marcillac, L. Coolen, S. Peralta, T. Pauporté, *ACS Appl. Mater. Inter.* **2018**, *10*, 35118-35128.
- [15] J. Qian, M. Ernst, N. Wu, A. Blakers, *Sustainable Energy Fuels* **2019**, *3*, 1439-1447.
- [16] P. Roy, N. K. Sinha, S. Tiwari, A. Khare, *Solar Energy* **2020**, *198*, 665-688.
- [17] B. Li, D. Binks, G. Cao, J. Tian, *Small* **2019**, *15*, 1903613.
- [18] D. Zheng, T. Zhu, T. Pauporté, *ACS Appl. Energy Mater.* **2020**, *3*, 10349-10361.
- [19] M. Ulfa, P. Wang, Z. Shao, B. Viana, T. Pauporte, in *Oxide-Based Materials And Devices Ix*, Vol. 10533 (Eds: D. J. Rogers, D. C. Look, F. H. Teherani) **2018**.
- [20] P.J. Wang, Z.P. Shao, M. Ulfa, T. Pauporté, *J. Phys. Chem. C*, **2017**, *121*, 9131-9141.
- [21] M. Ulfa, T. Zhu, F. Goubard, T. Pauporté, *J. Mater. Chem. A* **2018**, *6*, 13350-13358.
- [22] M. Ulfa, T. Pauporté, B. Thanh-Tuan, F. Goubard, *J. Phys. Chem. C* **2018**, *122*, 11651-11658.
- [23] L. Gollino, T. Pauporté, *Solar RRL* **2021**, *5*, 2000616.

Cite this paper as: F. Cheng, J. Zhu, Th. Pauporté, Chlorides, other Halides and Pseudohalides as Additives for the Fabrication of Efficient and Stable Perovskite Solar Cells. ChemSusChem 14 (2021) 3665–3692. DOI: 10.1002/cssc.202101089

- [24] <https://www.nrel.gov/pv/cell-efficiency.html>, accessed May 23rd, 2021.
- [25] S. Ruhle, *Solar Energy* **2016**, *130*, 139-147.
- [26] N. G. Park, H. Segawa, *ACS Photonics* **2018**, *5*.
- [27] C. Ma, N. G. Park, *Chem* **2020**, *6*, 1254-1264.
- [28] M. Stolterfoht, C. M. Wolff, Y. Amir, A. Paulke, L. Perdigon-Toro, P. Caprioglio, D. Neher, *Energy Environ. Sci.* **2017**, *10*, 1530-1539.
- [29] Z. Ni, C. Bao, Y. Liu, Q. Jiang, W.-Q. Wu, S. Chen, X. Dai, B. Chen, B. Hartweg, Z. Yu, Z. Holman, J. Huang, *Science* **2020**, *367*, 1352-1358.
- [30] Q. Fu, X. Tang, B. Huang, T. Hu, L. Tan, L. Chen, Y. Chen, *Adv. Sci.* **2018**, *5*, 1700387;
- [31] F. Bella, G. Griffini, J.-P. Correa-Baena, G. Saracco, M. Gratzel, A. Hagfeldt, S. Turri, C. Gerbaldi, *Science* **2016**, *354*, 203-206.
- [32] A. Mahapatra, D. Prochowicz, M. M. Tavakoli, S. Trivedi, P. Kumar, P. Yadav, *J. Mater. Chem. A* **2020**, *8*, 27-54.
- [33] K. O. Kosmatos, L. Theofylaktos, E. Giannakaki, D. Deligiannis, T. Stergiopoulos, *Energy Environ. Mater.* **2019**, *2*, 79-92.
- [34] S. Liu, Y. Guan, Y. Sheng, Y. Hu, H. Han, *Adv. Energy Mater.* **2019**, *10*, 1902492.
- [35] S. Ghosh, T. Singh, *Nano Energy* **2019**, *63*, 103828.
- [36] T. Zhu, D. Zheng, M.-N. Rager, T. Pauporté, *Solar RRL* **2020**, *4*, 2000348.
- [37] Q. Jiang, Y. Zhao, X. Zhang, X. Yang, Y. Chen, Z. Chu, Q. Ye, X. Li, Z. Yin, J. You, *Nat. Photonics* **2019**, *13*, 460-466.
- [38] M. Kim, G.-H. Kim, T. K. Lee, I. W. Choi, H. W. Choi, Y. Jo, Y. J. Yoon, J. W. Kim, J. Lee, D. Huh, H. Lee, S. K. Kwak, J. Y. Kim, D. S. Kim, *Joule* **2019**, *3*, 2179-2192.
- [39] G. Kim, H. Min, K. S. Lee, D. Y. Lee, S. I. Seok, *Science* **2020**, *370*, 108-112.
- [40] M. Lyu, N. G. Park, *Solar RRL* **2020**, *4*, 2000331.
- [41] Q. Chen, C. R. Jack, D. Wang, Z. Mokhtar, Z. Liu, *Appl. Surf. Sci.* **2020**, *536*, 147949.
- [42] S. You, X. Xi, X. Zhang, H. Wang, P. Gao, X. Ma, S. Bi, J. Zhang, H. Zhou, Z. Wei, *J. Mater. Chem. A* **2020**, *8*, 17756-17764;
- [43] N. Pant, A. Kulkarni, M. Yanagida, Y. Shirai, T. Miyasaka, K. Miyano, *Adv. Mater. Inter.* **2020**, *7*, 1901748;

Cite this paper as: F. Cheng, J. Zhu, Th. Pauporté, Chlorides, other Halides and Pseudohalides as Additives for the Fabrication of Efficient and Stable Perovskite Solar Cells. ChemSusChem 14 (2021) 3665–3692. DOI: 10.1002/cssc.202101089

- [44] P. Singh, P. J. S. Rana, P. Dhingra, P. Kar, *J. Mater. Chem. C* **2016**, *4*, 3101-3105;
- [45] C. Mu, J. Pan, S. Feng, Q. Li, D. Xu, *Adv. Energy Mater.* **2016**, *7*, 1601297.
- [46] H.-S. Kim, C.-R. Lee, J.-H. Im, K.-B. Lee, T. Moehl, A. Marchioro, S.-J. Moon, R. Humphry-Baker, J.-H. Yum, J. E. Moser, M. Graetzel, N.-G. Park, *Scientific reports* **2012**, *2*, 591.
- [47] J. M. Ball, M. M. Lee, A. Hey, H. J. Snaith, *Energy Environ. Sci.* **2013**, *6*, 1739-1743.
- [48] W. Zhang, S. Pathak, N. Sakai, T. Stergiopoulos, P. K. Nayak, N. K. Noel, A. A. Haghighirad, V. M. Burlakov, D. W. deQuilettes, A. Sadhanala, W. Li, L. Wang, D. S. Ginger, R. H. Friend, H. J. Snaith, *Nat. Commun.* **2015**, *6*, 10030.
- [49] J. Xu, C. C. Boyd, Z. J. Yu, A. F. Palmstrom, D. J. Witter, B. W. Larson, R. M. France, J. Werner, S. P. Harvey, E. J. Wolf, W. Weigand, S. Manzoor, M. F. A. M. van Hest, J. J. Berry, J. M. Luther, Z. C. Holman, M. D. McGehee, *Science* **2020**, *367*, 1097-1104.
- [50] D. Zheng, T. Zhu, T. Pauporté, *Solar RRL* **2021**, DOI : 10.1002/solr.202100010.
- [51] M. M. Lee, J. Teuscher, T. Miyasaka, T. N. Murakami, H. J. Snaith, *Science* **2012**, *338*, 643-647.
- [52] P. Ngoc Duy, V. T. Tiong, P. Chen, L. Wang, G. J. Wilson, J. Bell, H. Wang, *J. Mater. Chem. A* **2017**, *5*, 5195-5203.
- [53] X. Cao, L. Zhi, Y. Jia, Y. Li, K. Zhao, X. Cui, L. Ci, K. Ding, J. Wei, *Electrochim. Acta* **2018**, *275*, 1-7.
- [54] K. M. Boopathi, R. Mohan, T.-Y. Huang, W. Budiawan, M.-Y. Lin, C.-H. Lee, K.-C. Ho, C.-W. Chu, *J. Mater. Chem. A* **2016**, *4*, 1591-1597.
- [55] M. Murata, T. Oizumi, M. Gi, R. Tsuji, M. Arita, A. Fujii, M. Ozaki, *Sol. Energy Mater. Sol. Cells* **2020**, *208*, 110409.
- [56] B. Zong, W. Fu, Z.-a. Guo, S. Wang, L. Huang, B. Zhang, H. Bala, J. Cao, X. Wang, G. Sun, Z. Zhang, *J. Colloid Interface Sci.* **2019**, *540*, 315-321.
- [57] D. Zheng, C. Tong, T. Zhu, Y. Rong, T. Pauporte, *Nanomaterials* **2020**, *10*, 2512.
- [58] F. X. Xie, H. Su, J. Mao, K. S. Wong, W. C. H. Choy, *J. Phys. Chem. C* **2016**, *120*, 21248-21253.
- [59] Z. Li, C. Kolodziej, C. McCleese, L. Wang, A. Kovalsky, A. C. Samia, Y. Zhao, C. Burda, *Nanoscale Adv.* **2019**, *1*, 827-833.
- [60] L. Mao, C. C. Stoumpos, M. G. Kanatzidis, *J. Am. Chem. Soc.* **2019**, *141*, 1171-1190;
- [61] Y. Fu, H. Zhu, J. Chen, M. P. Hautzinger, X. Y. Zhu, S. Jin, *Nat. Rev. Mater.* **2019**, *4*, 169-188;

Cite this paper as: F. Cheng, J. Zhu, Th. Pauporté, Chlorides, other Halides and Pseudohalides as Additives for the Fabrication of Efficient and Stable Perovskite Solar Cells. *ChemSusChem* 14 (2021) 3665–3692. DOI: 10.1002/cssc.202101089

- [62] H. Tsai, W. Nie, J.-C. Blancon, C. C. S. Toumpos, R. Asadpour, B. Harutyunyan, A. J. Neukirch, R. Verduzco, J. J. Crochet, S. Tretiak, L. Pedesseau, J. Even, M. A. Alam, G. Gupta, J. Lou, P. M. Ajayan, M. J. Bedzyk, M. G. Kanatzidis, A. D. Mohite, *Nature* **2016**, *536*, 312-316;
- [63] X. Zhang, R. Munir, Z. Xu, Y. Liu, H. Tsai, W. Nie, J. Li, T. Niu, D.-M. Smilgies, M. G. Kanatzidis, A. D. Mohite, K. Zhao, A. Amassian, S. Liu, *Adv. Mater.* **2018**, *30*, 1707166.
- [64] T. Luo, Y. Zhang, Z. Xu, T. Niu, J. Wen, J. Lu, S. Jin, S. Liu, K. Zhao, *Adv. Mater.* **2019**, *31*, 1903848.
- [65] Y. Wang, W. Li, T. Zhang, D. Li, M. Kan, X. Wang, X. Liu, T. Wang, Y. Zhao, *Small Methods* **2020**, *4*, 1900511.
- [66] M. M. Tavakoli, M. Saliba, P. Yadav, P. Holzhey, A. Hagfeldt, S. M. Zakeeruddin, M. Graetzel, *Adv. Energy Mater.* **2019**, *9*, 1802646.
- [67] T. Zhu, D. Zheng, J. Liu, L. Coolen, T. Pauporte, *ACS Appl. Mater. Inter.* **2020**, *12*, 37197-37207.
- [68] G. M. Kim, A. Ishii, S. Oz, T. Miyasaka, *Adv. Energy Mater.* **2020**, *10*, 1903299.
- [69] M. M. Tavakoli, P. Yadav, D. Prochowicz, M. Sponseller, A. Osherov, V. Bulović, J. Kong, *Adv. Energy Mater.* **2019**, *9*, 1803587.
- [70] A. Suzuki, M. Kato, N. Ueoka, T. Oku, *J. Electron. Mater.* **2019**, *48*, 3900-3907.
- [71] Y. Wu, X. Li, S. Fu, L. Wan, J. Fang, *J. Mater. Chem. A* **2019**, *7*, 8078–8084
- [72] H. Min, M. Kim, S.-U. Lee, H. Kim, G. Kim, K. Choi, J. H. Lee, S. I. Seok, *Science* **2019**, *366*, 749-753.
- [73] M. I. Dar, N. Arora, P. Gao, S. Ahmad, M. Graetzel, M. K. Nazeeruddin, *Nano Lett.* **2014**, *14*, 6991-6996.
- [74] B. Yang, J. Keum, O. S. Ovchinnikova, A. Belianinov, S. Chen, M.-H. Du, I. N. Ivanov, C. M. Rouleau, D. B. Geohegan, K. Xiao, *J. Am. Chem. Soc.* **2016**, *138*, 5028-5035.
- [75] M. Mateen, Z. Arain, Y. Yang, X. Liu, S. Ma, C. Liu, Y. Ding, X. Ding, M. Cai, S. Dai, *ACS Appl. Mater. Inter.* **2020**, *12*, 10535-10543.
- [76] H. Chen, Y. Xia, B. Wu, F. Liu, T. Niu, L. Chao, G. Xing, T. Sum, Y. Chen, W. Huang, *Nano Energy* **2019**, *56*, 373-381.
- [77] L. Cojocar, S. Uchida, A. K. Jena, T. Miyasaka, J. Nakazaki, T. Kubo, H. Segawa, *Chem. Lett.* **2015**, *44*, 1089-1091.

Cite this paper as: F. Cheng, J. Zhu, Th. Pauporté, Chlorides, other Halides and Pseudohalides as Additives for the Fabrication of Efficient and Stable Perovskite Solar Cells. *ChemSusChem* 14 (2021) 3665–3692. DOI: 10.1002/cssc.202101089

- [78] S. Colella, E. Mosconi, P. Fedeli, A. Listorti, F. Gazza, F. Orlandi, P. Ferro, T. Besagni, A. Rizzo, G. Calestani, G. Gigli, F. De Angelis, R. Mosca, *Chem. Mater.* **2013**, 25, 4613-4618.
- [79] F. Xie, C. C. Chen, Y. Wu, X. Li, M. Cai, X. Liu, X. Yang, L. Han, *Energy Environ. Sci.* **2017**, 10, 1942-1949;
- [80] T. Leijtens, R. Prasanna, K. A. Bush, G. E. Eperon, J. A. Raiford, A. Gold-Parker, E. J. Wolf, S. A. Swifter, C. C. Boyd, H.-P. Wang, M. F. Toney, S. F. Bent, M. D. McGehee, *Sustainable Energy Fuels* **2018**, 2, 2450-2459;
- [81] B. Chen, Z. Yu, K. Liu, X. Zheng, Y. Liu, J. Shi, D. Spronk, P. N. Rudd, Z. Holman, J. Huang, *Joule* **2019**, 3, 177-190.
- [82] J. Jin, H. Li, C. Chen, B. Zhang, L. Xu, B. Dong, H. Song, Q. Dai, *ACS Appl. Mater. Inter.* **2017**, 9, 42875-42882.
- [83] C.-M. Tsai, H.-P. Wu, S.-T. Chang, C.-F. Huang, C.-H. Wang, S. Narra, Y.-W. Yang, C.-L. Wang, C.-H. Hung, E. W.-G. Diau, *ACS Energy Lett.* **2016**, 1, 1086-1093.
- [84] N. Ali, X. Wang, S. Rauf, S. Attique, A. Khesro, S. Ali, N. Mushtaq, H. Xiao, C. P. Yang, H. Wu, *Solar Energy* **2019**, 189, 325-332.
- [85] D. Ma, P. Todorovic, S. Meshkat, M. I. Saidaminov, Y.-K. Wang, B. Chen, P. Li, B. Scheffel, R. Quintero-Bermudez, J. Z. Fan, Y. Dong, B. Sun, C. Xu, C. Zhou, Y. Hou, X. Li, Y. Kang, O. Voznyy, Z.-H. Lu, D. Ban, E. H. Sargent, *J. Am. Chem. Soc.* **2020**, 142, 5126-5134;
- [86] Q. Wang, X. Wang, Z. Yang, N. Zhou, Y. Deng, J. Zhao, X. Xiao, P. Rudd, A. Moran, Y. Yan, J. Huang, *Nat. Commun.* **2019**, 10, 5633.
- [87] Y. Wu, X. Li, S. Fu, L. Wan, J. Fang, *J. Mater. Chem. A* **2019**, 7, 8078-8084.
- [88] X. Dai, Y. Deng, C. H. Van Brackle, S. Chen, P. N. Rudd, X. Xiao, Y. Lin, B. Chen, J. Huang, *Adv. Energy Mater.* **2020**, 10, 1903108.
- [89] B. Lee, T. Hwang, S. Lee, B. Shin, B. Park, *Scientific reports* **2019**, 9, 4803.
- [90] K. Yan, M. Long, T. Zhang, Z. Wei, H. Chen, S. Yang, J. Xu, *J. Am. Chem. Soc.* **2015**, 137, 4460-4468.
- [91] G. E. Eperon, S. D. Stranks, C. Menelaou, M. B. Johnston, L. M. Herz, H. J. Snaith, *Energy Environ. Sci.* **2014**, 7, 982-988.
- [92] D. P. McMeekin, Z. Wang, W. Rehman, F. Pulvirenti, J. B. Patel, N. K. Noel, M. B. Johnston,

Cite this paper as: F. Cheng, J. Zhu, Th. Pauporté, Chlorides, other Halides and Pseudohalides as Additives for the Fabrication of Efficient and Stable Perovskite Solar Cells. *ChemSusChem* 14 (2021) 3665–3692. DOI: 10.1002/cssc.202101089

- S. R. Marder, L. M. Herz, H. J. Snaith, *Adv. Mater.* **2017**, *29*, 1607039.
- [93] J. H. Heo, D. H. Song, S. H. Im, *Adv. Mater.* **2014**, *26*, 8179-8183.
- [94] F. Wang, H. Yu, H. Xu, N. Zhao, *Adv. Funct. Mater.* **2015**, *25*, 1120-1126.
- [95] S. Pang, Y. Zhou, Z. Wang, M. Yang, A. R. Krause, Z. Zhou, K. Zhu, N. P. Padture, G. Cui, *J. Am. Chem. Soc.* **2016**, *138*, 750-753.
- [96] G. E. Eperon, G. M. Paternò, R. J. Sutton, A. Zampetti, A. A. Haghighirad, F. Cacialli, H. J. Snaith, *J. Mater. Chem. A* **2015**, *3*, 19688-19695.
- [97] S. Xiang, Z. Fu, W. Li, Y. Wei, J. Liu, H. Liu, L. Zhu, R. Zhang, H. Chen, *ACS Energy Lett.* **2018**, *3*, 1824-1831.
- [98] L. Ma, F. Hao, C. C. Stoumpos, B. T. Phelan, M. R. Wasielewski, M. G. Kanatzidis, *J. Am. Chem. Soc.* **2016**, *138*, 14750-14755;
- [99] M. H. Kumar, S. Dharani, W. L. Leong, P. P. Boix, R. R. Prabhakar, T. Baikie, C. Shi, H. Ding, R. Ramesh, M. Asta, *Adv. Mater.* **2014**, *26*, 7122-7127.
- [100] T. Handa, T. Yamada, H. Kubota, S. Ise, Y. Miyamoto, Y. Kanemitsu, *J. Phys. Chem. C* **2017**, *121*, 16158-16165.
- [101] L. Ma, F. Hao, C.C. Stoumpos, B.T. Phelan, M.R. Wasielewski, M.G. Kanatzidis, *J. Am. Chem. Soc.* **2016**, *138*, 14750–14755.
- [102] W. Liao, D. Zhao, Y. Yu, C. R. Grice, C. Wang, A. J. Cimaroli, P. Schulz, W. Meng, K. Zhu, R. G. Xiong, Y. Yan, *Adv. Mater.* **2016**, *28*, 9333-9340.
- [103] S. J. Lee, S. S. Shin, Y. C. Kim, D. Kim, T. K. Ahn, J. H. Noh, J. Seo, S. I. Seok, *J. Am. Chem. Soc.* **2016**, *138*, 3974-3977.
- [104] S. Yuan, F. Qian, S. Yang, Y. Cai, Q. Wang, J. Sun, Z. Liu, S. Liu, *Adv. Funct. Mater.* **2019**, *29*, 1807850.
- [105] N. Li, S. Tao, Y. Chen, X. Niu, C. K. Onwudinanti, C. Hu, Z. Qiu, Z. Xu, G. Zheng, L. Wang, Y. Zhang, L. Li, H. Liu, Y. Lun, J. Hong, X. Wang, Y. Liu, H. Xie, Y. Gao, Y. Bai, S. Yang, G. Brocks, Q. Chen, H. Zhou, *Nat. Energy* **2019**, *4*, 408-415.
- [106] C. Li, Z. Song, D. Zhao, C. Xiao, B. Subedi, N. Shrestha, M. M. Junda, C. Wang, C.-S. Jiang, M. Al-Jassim, R. J. Ellingson, N. J. Podraza, K. Zhu, Y. Yan, *Adv. Energy Mater.* **2019**, *9*, 1803135.

Cite this paper as: F. Cheng, J. Zhu, Th. Pauporté, Chlorides, other Halides and Pseudohalides as Additives for the Fabrication of Efficient and Stable Perovskite Solar Cells. ChemSusChem 14 (2021) 3665–3692. DOI: 10.1002/cssc.202101089

- [107] Y. Ogomi, A. Morita, S. Tsukamoto, T. Saitho, N. Fujikawa, Q. Shen, T. Toyoda, K. Yoshino, S. S. Pandey, T. Ma, S. Hayase, *J. Phys. Chem. Lett.* **2014**, *5*, 1004-1011.
- [108] J. Wu, F. Fang, Z. Zhao, T. Li, R. Ullah, Z. Lv, Y. Zhou, D. Sawtell, *RSC Adv.* **2019**, *9*, 37119-37126.
- [109] L. Deying, Y. Wenqiang, W. Zhiping, S. Aditya, H. Qin, S. Rui, S. Ravichandran, G. F. Trindade, J. F. Watts, X. Zhaojian, *Science* **2018**, *360*, 1442-1446.
- [110] A. Aziz, N. Aristidou, X. Bu, R. J. E. Westbrook, S. A. Haque, M. S. Islam, *Chem. Mater.* **2019**, *32*, 400-409.
- [111] J. H. Noh, S. H. Im, J. H. Heo, T. N. Mandal, S. I. Seok, *Nano Lett.* **2013**, *13*, 1764-1769.
- [112] J. Huang, S. Xiang, J. Yu, C.-Z. Li, *Energy Environ. Sci.* **2019**, *12*, 929-937.
- [113] Z. B. Yang, A. Rajagopal, A. K. Y. Jen, *Adv. Mater.* **2017**, *29*, 1704418.
- [114] G. E. Eperon, H. J. Snaith, M. T. Hrantner, *Nat. Rev. Chem.* **2017**, *1*, 0095;
- [115] M. Anaya, G. Lozano, M. E. Calvo, H. Míguez, *Joule* **2017**, *1*, 769-793.
- [116] W. S. Yang, B. W. Park, E. H. Jung, N. J. Jeon, Y. C. Kim, D. U. Lee, S. S. Shin, J. Seo, E. K. Kim, J. H. Noh, *Science* **2017**, *356*, 1376-1379.
- [117] R. Prasanna, A. Gold-Parker, T. Leijtens, B. Conings, A. Babayigit, H. G. Boyen, M. F. Toney, M. D. McGehee, *J. Am. Chem. Soc.* **2017**, *139*, 11117-11124.
- [118] J. Tong, Z. Song, D. H. Kim, X. Chen, C. Chen, A. F. Palmstrom, P. F. Ndione, M. O. Reese, S. P. Dunfield, O. G. Reid, J. Liu, F. Zhang, S. P. Harvey, Z. Li, S. T. Christensen, G. Teeter, D. Zhao, M. M. Al-Jassim, M. F. A. M. van Hest, M. C. Beard, S. E. Shaheen, J. J. Berry, Y. Yan, K. Zhu, *Science* **2019**, *364*, 475-479.
- [119] X. Zhou, L. Zhang, X. Wang, C. Liu, S. Chen, M. Zhang, X. Li, W. Yi, B. Xu, *Adv. Mater.* **2020**, *32*, 1908107.
- [120] F. Zhang, D. Bi, N. Pellet, C. Xiao, Z. Li, J. J. Berry, S. M. Zakeeruddin, K. Zhu, M. Grätzel, *Energy Environ. Sci.* **2018**, *11*, 3480-3490.
- [121] F. Zhang, H. Lu, J. Tong, J. J. Berry, M. C. Beard, K. Zhu, *Energy Environ. Sci.* **2020**, *13*, 1154-1186.
- [122] G. Grancini, C. Roldán-Carmona, I. Zimmermann, E. Mosconi, X. Lee, D. Martineau, S. Narbey, F. Oswald, F. De Angelis, M. Graetzel, M. K. Nazeeruddin, *Nat. Commun.* **2017**, *8*, 15684;

Cite this paper as: F. Cheng, J. Zhu, Th. Pauporté, Chlorides, other Halides and Pseudohalides as Additives for the Fabrication of Efficient and Stable Perovskite Solar Cells. *ChemSusChem* 14 (2021) 3665–3692. DOI: 10.1002/cssc.202101089

- [123] M. Xu, W. Ji, Y. Sheng, Y. Wu, H. Han, *Nano Energy* **2020**, *74*, 104842.
- [124] A. Mei, Y. Sheng, Y. Ming, Y. Hu, Y. Rong, W. Zhang, S. Luo, G. Na, C. Tian, X. Hou, Y. Xiong, Z. Zhang, S. Liu, S. Uchida, T.-W. Kim, Y. Yuan, L. Zhang, Y. Zhou, H. Han, *Joule* **2020**, *4*, 2646-2660.
- [125] Y. Hu, Z. Zhang, A. Mei, Y. Jiang, X. Hou, Q. Wang, K. Du, Y. Rong, Y. Zhou, G. Xu, H. Han, *Adv. Mater.* **2018**, *30*, 1705786.
- [126] W. S. Yang, B. W. Park, E. H. Jung, N. J. Jeon, Y. C. Kim, D. U. Lee, S. S. Shin, J. Seo, E. K. Kim, J. H. Noh, *Science* **2017**, *356*, 1376-1379.
- [127] Y. C. Kim, N. J. Jeon, J. H. Noh, W. S. Yang, J. Seo, J. S. Yun, A. Ho-Baillie, S. Huang, M. A. Green, J. Seidel, T. K. Ahn, S. I. Seok, *Adv. Energy Mater.* **2016**, *6*, 1502104.
- [128] T. Supasai, N. Rujisamphan, K. Ullrich, A. Chemseddine, T. Dittrich, *Appl. Phys. Lett.* **2013**, *103*, 183906.
- [129] A. Calloni, A. Abate, G. Bussetti, G. Berti, R. Yivlialin, F. Ciccacci, L. Duò, *J. Phys. Chem. C* **2015**;
- [130] Q. Chen, H. Zhou, T. B. Song, S. Luo, Z. Hong, H. S. Duan, L. Dou, Y. Liu, Y. Yang, *Nano Lett.* **2014**, *14*, 4158-4163.
- [131] L. Wang, C. McCleese, A. Kovalsky, Y. Zhao, C. Burda, *J. Am. Chem. Soc.* **2014**, *136*, 12205-12208.
- [132] T. Zhang, N. Guo, G. Li, X. Qian, Y. Zhao, *Nano Energy* **2016**, *26*, 50-56.
- [133] C. Roldán-Carmona, P. Gratia, I. Zimmermann, G. Grancini, P. Gao, M. Graetzel, M. K. Nazeeruddin, *Energy Environ. Sci.* **2015**, *8*, 3550-3556;
- [134] F. Jiang, Y. Rong, H. Liu, T. Liu, L. Mao, W. Meng, F. Qin, Y. Jiang, B. Luo, S. Xiong, J. Tong, Y. Liu, Z. Li, H. Han, Y. Zhou, *Adv. Funct. Mater.* **2016**, *26*, 8119-8127.
- [135] E. J. Juarez-Perez, L. K. Ono, M. Maeda, Y. Jiang, Z. Hawash, Y. Qi, *J. Mater. Chem. A* **2018**, *6*, 9604-9612.
- [136] M. Abdi-Jalebi, Z. Andaji-Garmaroudi, S. Cacovich, C. Stavrakas, B. Philippe, J. M. Richter, M. Alsari, E. P. Booker, E. M. Hutter, A. J. Pearson, S. Lilliu, T. J. Savenije, H. Rensmo, G. Divitini, C. Ducati, R. H. Friend, S. D. Stranks, *Nature* **2018**, *555*, 497-501.
- [137] D. Y. Son, S. G. Kim, J. Y. Seo, S. H. Lee, H. Shin, D. Lee, N. G. Park, *J. Am. Chem. Soc.* **2018**,

Cite this paper as: F. Cheng, J. Zhu, Th. Pauporté, Chlorides, other Halides and Pseudohalides as Additives for the Fabrication of Efficient and Stable Perovskite Solar Cells. *ChemSusChem* 14 (2021) 3665–3692. DOI: 10.1002/cssc.202101089

140, 1358-1364.

- [138] Y. H. Lee, J. Luo, R. Humphry-Baker, P. Gao, M. Grätzel, M. K. Nazeeruddin, *Adv. Funct. Mater.* **2015**, 25, 3925-3933;
- [139] D. Bi, A. M. El-Zohry, A. Hagfeldt, G. Boschloo, *Acs Photonics* **2015**, 2, 589-594.
- [140] F. Liu, Q. Dong, M. K. Wong, A. B. Djurišić, A. Ng, Z. Ren, Q. Shen, C. Surya, W. K. Chan, J. Wang, A. M. C. Ng, C. Liao, H. Li, K. Shih, C. Wei, H. Su, J. Dai, *Adv. Energy Mater.* **2016**, 6, 1502206.
- [141] G. Tumen-Ulzii, C. Qin, D. Klotz, M. R. Leyden, P. Wang, M. Auffray, T. Fujihara, T. Matsushima, J. W. Lee, S. J. Lee, Y. Yang, C. Adachi, *Adv. Mater.* **2020**, 32, 1905035.
- [142] Z. Tang, T. Bessho, F. Awai, T. Kinoshita, M. M. Maitani, R. Jono, T. N. Murakami, H. Wang, T. Kubo, S. Uchida, H. Segawa, *Scientific reports* **2017**, 7, 12183.
- [143] J. Cao, S. X. Tao, P. A. Bobbert, C. P. Wong, N. Zhao, *Adv. Mater.* **2018**, 30, 1707350.
- [144] M. Abdi-Jalebi, M. I. Dar, A. Sadhanala, S. P. Senanayak, M. Franckevičius, N. Arora, Y. Hu, M. K. Nazeeruddin, S. M. Zakeeruddin, M. Grätzel, R. H. Friend, *Adv. Energy Mater.* **2016**, 6, 1502472.
- [145] J.-P. Correa-Baena, *Science* **2019**.
- [146] A. Halder, R. Chulliyil, A. S. Subbiah, T. Khan, S. Chattoraj, A. Chowdhury, S. K. Sarkar, *J. Phys. Chem. Lett.* **2015**, 6, 3483-3489;
- [147] Y. Yu, C. Wang, C. R. Grice, N. Shrestha, J. Chen, D. Zhao, W. Liao, A. J. Cimaroli, P. J. Roland, R. J. Ellingson, Y. Yan, *Chemsuschem* **2016**, 9, 3288-3297;
- [148] B. Walker, G. H. Kim, J. Y. Kim, *Adv. Mater.* **2019**, 31, 1807029.
- [149] C. Wang, D. Zhao, Y. Yu, N. Shrestha, C. R. Grice, W. Liao, A. J. Cimaroli, J. Chen, R. J. Ellingson, X. Zhao, Y. Yan, *Nano Energy* **2017**, 35, 223-232.
- [150] Y. Chen, B. Li, W. Huang, D. Gao, Z. Liang, *Chem. Commun.* **2015**, 51, 11997-11999.
- [151] Y. Zhou, Y.-H. Jia, H.-H. Fang, M. A. Loi, F.-Y. Xie, L. Gong, M.-C. Qin, X.-H. Lu, C.-P. Wong, N. Zhao, *Adv. Funct. Mater.* **2018**, 28, 1803130.
- [152] Y. Yu, C. Wang, C. R. Grice, N. Shrestha, D. Zhao, W. Liao, L. Guan, R. A. Awni, W. Meng, A. J. Cimaroli, K. Zhu, R. J. Ellingson, Y. Yan, *ACS Energy Lett.* **2017**, 2, 1177-1182.
- [153] D. H. Kim, C. P. Muzzillo, J. Tong, A. F. Palmstrom, B. W. Larson, C. Choi, S. P. Harvey, S.

Cite this paper as: F. Cheng, J. Zhu, Th. Pauporté, Chlorides, other Halides and Pseudohalides as Additives for the Fabrication of Efficient and Stable Perovskite Solar Cells. ChemSusChem 14 (2021) 3665–3692. DOI: 10.1002/cssc.202101089

- Glynn, J. B. Whitaker, F. Zhang, Z. Li, H. Lu, M. F. A. M. van Hest, J. J. Berry, L. M. Mansfield, Y. Huang, Y. Yan, K. Zhu, *Joule* **2019**, *3*, 1734-1745.
- [154] H. Dong, Z. Wu, J. Xi, X. Xu, L. Zuo, T. Lei, X. Zhao, L. Zhang, X. Hou, A. K. Y. Jen, *Adv. Funct. Mater.* **2018**, *28*, 1704836.
- [155] Q. Han, Y. Bai, J. Liu, K.-z. Du, T. Li, D. Ji, Y. Zhou, C. Cao, D. Shin, J. Ding, A. D. Franklin, J. T. Glass, J. Hu, M. J. Therien, J. Liu, D. B. Mitzi, *Energy Environ. Sci.* **2017**, *10*, 2365-2371.
- [156] D. Wang, W. Li, Z. Du, G. Li, W. Sun, J. Wu, Z. Lan, *ACS Appl Mater Interfaces* **2020**, *12*, 10579-10587;
- [157] F. Wang, X. Jiang, H. Chen, Y. Shang, H. Liu, J. Wei, W. Zhou, H. He, W. Liu, Z. Ning, *Joule* **2018**, *2*, 2732-2743.
- [158] H. Zhang, M. Hou, Y. Xia, Q. Wei, Z. Wang, Y. Cheng, Y. Chen, W. Huang, *J. Mater. Chem. A.* **2018**, *6*, 9264–9270.
- [159] E. Jokar, C.-H. Chien, A. Fathi, M. Rameez, Y.-H. Chang, E. W.-G. Diau, *Energy Environ. Sci.* **2018**, *11*, 2353-2362.
- [160] H. Kim, Y. H. Lee, T. Lyu, J. H. Yoo, T. Park, J. H. Oh, *J. Mater. Chem. A* **2018**, *6*, 18173-18182.
- [161] C. Wang, Z. Song, Y. Yu, D. Zhao, R. A. Awni, C. R. Grice, N. Shrestha, R. J. Ellingson, X. Zhao, Y. Yan, *Sustainable Energy Fuels* **2018**, *2*, 2435-2441.
- [162] Z. Yao, Z. Jin, X. Zhang, Q. Wang, H. Zhang, Z. Xu, L. Ding, S. Liu, *J. Mater. Chem. C* **2019**, *7*, 13736-13742.
- [163] H. Tan, A. Jain, O. Voznyy, X. Lan, F. P. G. de Arquer, J. Z. Fan, R. Quintero-Bermudez, M. Yuan, B. Zhang, Y. Zhao, F. Fan, P. Li, L. N. Quan, Y. Zhao, Z.-H. Lu, Z. Yang, S. Hoogland, E. H. Sargent, *Science* **2017**, *355*, 722-726.
- [164] X. Gong, Q. Sun, S. Liu, P. Liao, Y. Shen, C. Gratzel, S. M. Zakeeruddin, M. Gratzel, M. Wang, *Nano Lett.* **2018**, *18*, 3969-3977.
- [165] L. F. Zhu, Y. Z. Xu, J. J. Shi, H. Y. Zhang, X. Xu, Y. H. Zhao, Y. H. Luo, Q. B. Meng, D. M. Li, *RSC Adv.* **2016**, *6*, 82282-82288.
- [166] T. Zhu, J. Su, F. Labat, I. Ciofini, T. Pauporte, *ACS Appl. Mater. Inter.* **2020**, *12*, 744-752.
- [167] J. Su, T. Zhu, T. Pauporte, I. Ciofini, F. Labat, *J. Comput. Chem.* **2020**, *41*, 1740-1747.
- [168] M. M. Byranvand, T. Kim, S. Song, G. Kang, S. U. Ryu, T. Park, *Adv. Energy Mater.* **2018**, *8*,

Cite this paper as: F. Cheng, J. Zhu, Th. Pauporté, Chlorides, other Halides and Pseudohalides as Additives for the Fabrication of Efficient and Stable Perovskite Solar Cells. *ChemSusChem* 14 (2021) 3665–3692. DOI: 10.1002/cssc.202101089

1702235.

- [169] W. Li, W. Zhang, S. Van Reenen, R. J. Sutton, J. Fan, A. A. Haghghirad, M. B. Johnston, L. Wang, H. J. Snaith, *Energy Environ. Sci.* **2016**, *9*, 490-498.
- [170] S. Yuan, J. Wang, K. Yang, P. Wang, X. Zhang, Y. Zhan, L. Zheng, *Nanoscale* **2018**, *10*, 18909-18914.
- [171] J. Ma, X. Guo, L. Zhou, Z. Lin, C. Zhang, Z. Yang, G. Lu, J. Chang, Y. Hao, *ACS Appl. Energy Mater.* **2018**, *1*, 3826-3834.
- [172] R. Azmi, N. Nurrosyid, S.-H. Lee, M. Al Mubarak, W. Lee, S. Hwang, W. Yin, A. Tae Kyu, T.-W. Kim, D. Y. Ryu, Y. R. Do, S.-Y. Jang, *ACS Energy Lett.* **2020**, *5*, 1396-1403.
- [173] M. V. Khenkin, E. A. Katz, A. Abate, G. Bardizza, J. J. Berry, C. Brabec, F. Brunetti, V. Bulovic, Q. Burlingame, A. Di Carlo, R. Cheacharoen, Y.-B. Cheng, A. Colmann, S. Cros, K. Domanski, M. Dusza, C. J. Fell, S. R. Forrest, Y. Galagan, D. Di Girolamo, M. Graetzel, A. Hagfeldt, E. von Hauff, H. Hoppe, J. Kettle, H. Koebler, M. S. Leite, S. Liu, Y.-L. Loo, J. M. Luther, C.-Q. Ma, M. Madsen, M. Manceau, M. Matheron, M. McGehee, R. Meitzner, M. K. Nazeeruddin, A. F. Nogueira, C. Odabasi, A. Osherov, N.-G. Park, M. O. Reese, F. De Rossi, M. Saliba, U. S. Schubert, H. J. Snaith, S. D. Stranks, W. Tress, P. A. Troshin, V. Turkovic, S. Veenstra, I. Visoly-Fisher, A. Walsh, T. Watson, H. Xie, R. Yildirim, S. M. Zakeeruddin, K. Zhu, M. Lira-Cantu, *Nat. Energy* **2020**, *5*, 35-49.
- [174] X. Liu, Y. Zhang, L. Shi, Z. Liu, J. Huang, J. S. Yun, Y. Zeng, A. Pu, K. Sun, Z. Hameiri, J. A. Stride, J. Seidel, M. A. Green, X. Hao, *Adv. Energy Mater.* **2018**, *8*, 1800138.
- [175] Q. Wang, Q. Dong, T. Li, A. Gruverman, J. Huang, *Adv. Mater.* **2016**, *28*, 6734-6739.
- [176] J. Yang, C. Liu, C. Cai, X. Hu, Z. Huang, X. Duan, X. Meng, Z. Yuan, L. Tan, Y. Chen, *Adv. Energy Mater.* **2019**, *9*, 1900198.
- [177] C. Wu, K. Wang, X. Feng, Y. Jiang, D. Yang, Y. Hou, Y. Yan, M. Sanghadasa, S. Priya, *Nano letters* **2019**, *19*, 1251-1259.
- [178] Y. Liu, S. Akin, L. Pan, R. Uchida, N. Arora, J. V. Milic, A. Hinderhofer, F. Schreiber, A. R. Uhl, S. M. Zakeeruddin, A. Hagfeldt, M. I. Dar, M. Gratzel, *Sci. Adv.* **2019**, *5*, eaaw2543.
- [179] Y. Wang, T. Zhang, M. Kan, Y. Li, T. Wang, Y. Zhao, *Joule* **2018**, *2*, 2065-2075.
- [180] A. Buin, R. Comin, J. Xu, A.H. Ip, E.H. Sargent, *Chem. Mater.* **2015**, *27*, 4405–4412.

Cite this paper as: F. Cheng, J. Zhu, Th. Pauporté, Chlorides, other Halides and Pseudohalides as Additives for the Fabrication of Efficient and Stable Perovskite Solar Cells. *ChemSusChem* 14 (2021) 3665–3692. DOI: 10.1002/cssc.202101089

- [181] M.H. Du, *J. Mater. Chem. A* **2014**, 2, 9091–9098.
- [182] C. Liu, J. Tu, X. Hu, Z. Huang, X. Meng, J. Yang, X. Duan, L. Tan, Z. Li, Y. Chen, *Adv. Funct. Mater.* **2019**, 29, 1808059.
- [183] Z. Hawash, S. R. Raga, D.-Y. Son, L. K. Ono, N.-G. Park, Y. Qi, *J. Phys. Chem. Lett.* **2017**, 8, 3947-3953.
- [184] K. T. Cho, S. Paek, G. Grancini, C. Roldán-Carmona, P. Gao, Y. Lee, M. K. Nazeeruddin, *Energy Environ. Sci.* **2017**, 10, 621-627.
- [185] Y. Wang, T. Zhang, M. Kan, Y. Zhao, *J. Am. Chem. Soc.* **2018**, 140, 12345-12348.
- [186] M. Salado, A. D. Jodlowski, C. Roldan-Carmona, G. de Miguel, S. Kazim, M. K. Nazeeruddin, S. Ahmad, *Nano Energy* **2018**, 50, 220-228.
- [187] E. A. Alharbi, A. Y. Alyamani, D. J. Kubicki, A. R. Uhl, B. J. Walder, A. Q. Alanazi, J. Luo, A. Burgos-Caminal, A. Albadri, H. Albrithen, M. H. Alotaibi, J.-E. Moser, S. M. Zakeeruddin, F. Giordano, L. Emsley, M. Grätzel, *Nat. Commun.* **2019**, 10, 3008.
- [188] D. J. Kubicki, D. Prochowicz, A. Hofstetter, M. Saski, P. Yadav, D. Bi, N. Pellet, J. Lewiński, S. M. Zakeeruddin, M. Grätzel, L. Emsley, *J. Am. Chem. Soc.* **2018**, 140, 3345-3351.
- [189] Z. Ren, N. Wang, M. Zhu, X. Li, J. Qi, *Electrochim. Acta* **2018**, 282, 653-661.
- [190] M. A. R. Laskar, W. Luo, N. Ghimire, A. H. Chowdhury, B. Bahrami, A. Gurung, K. M. Reza, R. Pathak, R. S. Bobba, B. S. Lamsal, K. Chen, M. T. Rahman, S. I. Rahman, K. Emshadi, T. Xu, M. Liang, W.-H. Zhang, Q. Qiao, *Adv. Funct. Mater.* **2020**, 30, 2000778.
- [191] J. Zhang, J. Liu, A. Tan, J. Piao, Z. Fu, *Chem. Commun.* **2020**, 56, 13816-13819.
- [192] J. Chen, J.-Y. Seo, N.-G. Park, *Adv. Energy Mater.* **2018**, 8, 1702714.
- [193] Y. Wang, M. I. Dar, L. K. Ono, T. Zhang, M. Kan, Y. Li, L. Zhang, X. Wang, Y. Yang, X. Gao, Y. Qi, M. Gratzel, Y. Zhao, *Science* **2019**, 365, 591-595.
- [194] X. Zheng, B. Chen, J. Dai, Y. Fang, Y. Bai, Y. Lin, H. Wei, Xiao C. Zeng, J. Huang, *Nat. Energy* **2017**, 2, 17102.
- [195] J.-W. Lee, Z. Dai, T.-H. Han, C. Choi, S.-Y. Chang, S.-J. Lee, N. De Marco, H. Zhao, P. Sun, Y. Huang, Y. Yang, *Nat. Commun.* **2018**, 9, 3021.
- [196] L. N. Quan, M. Yuan, R. Comin, O. Voznyy, E. M. Beauregard, S. Hoogland, A. Buin, A. R. Kirmani, K. Zhao, A. Amassian, D. H. Kim, E. H. Sargent, *J. Am. Chem. Soc.* **2016**, 138, 2649-

Cite this paper as: F. Cheng, J. Zhu, Th. Pauporté, Chlorides, other Halides and Pseudohalides as Additives for the Fabrication of Efficient and Stable Perovskite Solar Cells. ChemSusChem 14 (2021) 3665–3692. DOI: 10.1002/cssc.202101089

2655.

- [197] S. Li, Z. Liu, Z. Qiao, X. Wang, L. Cheng, Y. Zhai, Q. Xu, Z. Li, K. Meng, G. Chen, *Adv. Funct. Mater.* **2020**, *30*, 2005846.
- [198] T. M. Koh, V. Shanmugam, X. Guo, S. S. Lim, O. Filonik, E. M. Herzig, P. Müller-Buschbaum, V. Swamy, S. T. Chien, S. G. Mhaisalkar, N. Mathews, *J. Mater. Chem. A* **2018**, *6*, 2122-2128;
- [199] K. T. Cho, G. Grancini, Y. Lee, E. Oveisi, J. Ryu, O. Almora, M. Tschumi, P. A. Schouwink, G. Seo, S. Heo, *Energy Environ. Sci.* **2018**, *11*, 952-959.
- [200] E. H. Jung, N. J. Jeon, E. Y. Park, C. S. Moon, T. J. Shin, T.-Y. Yang, J. H. Noh, J. Seo, *Nature* **2019**, *567*, 511-515.
- [201] J. J. Yoo, S. Wieghold, M. C. Sponseller, M. R. Chua, S. N. Bertram, N. T. P. Hartono, J. S. Tresback, E. C. Hansen, J.-P. Correa-Baena, V. Bulović, T. Buonassisi, S. S. Shin, M. G. Bawendi, *Energy Environ. Sci.* **2019**, *12*, 2192-2199.
- [202] C. Ma, C. Leng, Y. Ji, X. Wei, K. Sun, L. Tang, J. Yang, W. Luo, C. Li, Y. Deng, S. Feng, J. Shen, S. Lu, C. Du, H. Shi, *Nanoscale* **2016**, *8*, 18309-18314.
- [203] J. J. Yoo, S. Wieghold, M. C. Sponseller, M. R. Chua, S. N. Bertram, N. T. P. Hartono, J. S. Tresback, E. C. Hansen, J.-P. Correa-Baena, V. Bulovic, T. Buonassisi, S. S. Shin, M. G. Bawendi, *Energy Environ. Sci.* **2019**, *12*, 2192-2199.
- [204] H. Zhang, X. Ren, X. Chen, J. Mao, J. Cheng, Y. Zhao, Y. Liu, J. Milic, W.-J. Yin, M. Grätzel, W. C. H. Choy, *Energy Environ. Sci.* **2018**, *11*, 2253-2262.
- [205] W. Chen, Y. Zhou, L. Wang, Y. Wu, B. Tu, B. Yu, F. Liu, H. W. Tam, G. Wang, A. B. Djurisić, L. Huang, Z. He, *Adv. Mater.* **2018**, *30*, 1800515.
- [206] W. Chen, Y. Zhou, G. Chen, Y. Wu, B. Tu, F. Z. Liu, L. Huang, A. M. C. Ng, A. B. Djurišić, Z. He, *Adv. Energy Mater.* **2019**, *9*, 1803872.

Cite this paper as: F. Cheng, J. Zhu, Th. Pauporté, Chlorides, other Halides and Pseudohalides as Additives for the Fabrication of Efficient and Stable Perovskite Solar Cells. ChemSusChem 14 (2021) 3665–3692. DOI: 10.1002/cssc.202101089



Fei Cheng received her master's degree from Guangzhou Institute of Chemistry, University of Chinese Academy of Sciences in 2019. She is a current Ph.D. student under the supervision of Prof. Thierry Pauporté in Chimie ParisTech-PSL University. Her research interests are focused on development of efficient and stable perovskite solar cells.



Dr. Jie Zhang is currently an assistant professor in the School of Chemistry and Chemical Engineering at the South China University of Technology. She received her M. Sc. and Ph. D. degree at the South China University of Technology and Chimie ParisTech in 2012 and 2015, respectively. Her interests concentrate on the synthesis of novel photo-functional materials and perovskite solar cells, including photochromic materials, low-dimensional perovskites and device engineering for perovskite solar cells.



Prof. Thierry Pauporté is director of research at the Centre National de la Recherche Scientifique (CNRS) in France and works at Chimie-Paristech-PSL University. He is graduated in Chemistry from the École Normale Supérieure de Lyon. He received his Ph.D. in physical chemistry from Montpellier II University, France, in 1995. He works on the synthesis, characterization and understanding of fundamental chemical and physical properties of oxide and halide perovskite films and nanostructures. The applications of these materials and structures include light emitting diodes, perovskite solar cells, dye-sensitized solar cells, nanosensors,

Cite this paper as: F. Cheng, J. Zhu, Th. Pauporté, Chlorides, other Halides and Pseudohalides as Additives for the Fabrication of Efficient and Stable Perovskite Solar Cells.

ChemSusChem 14 (2021) 3665–3692. DOI: 10.1002/cssc.202101089

photodetectors, photocatalysis, wettability and fouling. More information at : www.pauportegroup.com

Table of Content

Progresses made on the employment of halide and pseudo-halide additives in organo-metal perovskite solar cells are reviewed. Their function in morphology adjusting, phase stabilizing, energy-level adjusting, trap state passivation and hysteresis elimination are detailed. A deep understanding of the relationship between halide/pseudohalide additive and the improved properties of perovskite solar cell is presented.

